UNIVERSITY
OF TASMANIA

Interneuron dysfunction in amyotrophic lateral sclerosis

by

Rosemary Maree Clark, BMedRes (Hons)

Submitted in fulfilment of the requirement for the
Degree of Doctor of Philosophy

Menzies Institute for Medical Research
University of Tasmania

3rd July 2017

COPYRIGHT STATEMENT

Rosemary Maree Clark

University of Tasmania, Hobart

3rd July 2017

STATEMENT OF AUTHORITY OF ACCESS

This thesis may be made available for loan and limited copying and communication in accordance with the *Copyright Act 1968*.

Rosemary Maree Clark

STATEMENT OF CO-AUTHORSHIP

The following people and institutions contributed to the publication of work undertaken as part of this thesis:

Rosemary M Clark, Menzies Institute for Medical Research = **Candidate**

Catherine A Blizzard, Menzies Institute for Medical Research = **Author 1**

Kaylene M Young, Menzies Institute for Medical Research = **Author 2**

Anna E King, Wicking Dementia Research and Education Centre = **Author 3**

Tracey C Dickson, Menzies Institute for Medical Research = **Author 4**

***Paper 1,* 'Calretinin and Neuropeptide Y interneurons are differentially altered in the motor cortex of SOD1^{G93A} mouse model of ALS'.**

Located in Chapter 2

Candidate was first author. Authors 1, 2, 3 and 4 contributed to the idea, its formalisation and development.

***Paper 2,* 'Inhibitory dysfunction in amyotrophic lateral sclerosis: future therapeutic opportunities'.**

Located in Chapter 1

Candidate was the primary author. Authors 2 and 4 contributed to the idea, its formalisation and development. Author 4 assisted in refinement and revision.

We the undersigned agree with the above stated “proportion of work undertaken” for each of the above published (or submitted) peer-reviewed manuscripts contributing to this thesis:

Signed:

Candidate: _____

Author 1: _____

Author 2: _____

Author 3: _____

Author 4: _____

Date: 03.07.17

This thesis contains work either published or submitted for publication as follows:

I. **Rosemary Clark**, Catherine Blizzard, Kaylene Young, Anna King and Tracey Dickson. 2017. Calretinin and Neuropeptide Y interneurons are differentially altered in the motor cortex of SOD1^{G93A} mouse model of ALS. Scientific Reports. Accepted.

II. **Rosemary Clark**, Catherine Blizzard and Tracey Dickson. 2015. Inhibitory dysfunction in amyotrophic lateral sclerosis: future therapeutic opportunities. Neurodegenerative disease management 5:511-525.

III. **Rosemary Clark**, Mariana Brizuela, Catherine Blizzard and Tracey Dickson. 2017. Altered intrinsic electrical properties and morphological development of cortical interneurons in the SOD1^{G93A} mouse model of ALS [*manuscript in preparation*].

Publications not included in the thesis:

I. **Rosemary Clark***, Shiwei Wang*, Marta Bolos*, Carlie Cullen, Katherine Southam, Tracey Dickson and Kaylene Young. 2016. Amyloid beta precursor protein regulates neuron survival and maturation in the adult mouse brain. Molecular Cellular Neuroscience. 77, 21-33. *co-first authors.

II. Emily Handley, Kimberley Pitman, Edgar Dawkins, Kaylene Young, **Rosemary Clark**, Tonqcui Jiang, Brad Turner, Tracey Dickson, Catherine Blizzard. 2016. Synapse dysfunction of layer V pyramidal neurons precedes neurodegeneration in a mouse model of TDP-43 proteinopathies. Cerebral Cortex. doi:10.1093/cercor/bhw185.

This thesis contained work presented at the following conferences:

I. **Rosemary Clark**, Mariana Brizuela, Catherine Blizzard, Anna King, Kaylene Young and Tracey Dickson. 2016. Subtype-specific alteration of inhibitory circuits in the primary motor cortex in motor neuron disease: a cellular basis for cortical pathophysiology. Australasian Neuroscience Society Meeting, Tasmania, Australia. Invited Talk, Symposia "Motor Cortex Excitability in Health and Disease."

II. **Rosemary Clark**, Mariana Brizuela, Catherine Blizzard, Anna King, Kaylene Young and Tracey Dickson. 2015. Regional- and lamina-specific alterations in Calretinin and NPY interneuron populations in SOD1 mice and amyotrophic lateral sclerosis patients: A potential source of cortical hyperexcitability. Poster at the 26th International Symposium on ALS/MND, Orlando, Florida, USA. **Winner of the International ALS/MND Symposium Scientific Poster Prize.**

III. **Rosemary Clark**, Mariana Brizuela, Catherine Blizzard and Tracey Dickson. 2015. Intrinsic interneuronal vulnerabilities in the GAD67.SOD1 mouse cortex. Poster at the Motor Neuron Disease Australia Research Meeting, Sydney, Australia. **Runner up Scientific Poster Prize.**

IV. **Rosemary Clark**, Anna King and Tracey Dickson. 2014. Interneuron loss and dysfunction in amyotrophic lateral sclerosis. Oral presentation at GABAergic Signaling in Health and Disease, 24th: Neuropharmacology Conference - Satellite to the 2014 Meeting of the Society for Neuroscience, Washington DC, USA.

V. **Rosemary Clark**, Timothy Fielder, Anna King and Tracey Dickson. 2013. Inhibitory loss or dysfunction: A primary mechanism in ALS? Poster at the International Symposium on ALS/MND, Milan, Italy.

VI. **Rosemary Clark**, Timothy Fielder, Anna King and Tracey Dickson. 2013. Inhibitory loss or dysfunction: A primary mechanism in ALS? Symposium Presented by T. Dickson at the International Symposium on ALS/MND, Milan, Italy.

VII. **Rosemary Clark**, Anna King, Catherine Blizzard and Tracey Dickson. 2013. A role for interneurons in ALS? Oral at Australian Neuroscience Symposium, Melbourne, Australia.

SUMMARY

Despite more than a century of research, there is still no cure for amyotrophic lateral sclerosis (ALS) and the only available therapeutic extends survival by mere months. The most common motor neuron (MN) disease, ALS is traditionally characterised by selective degeneration of MNs and the systematic destruction of the motor system. However, in the last decade the classification of ALS is evolving from a pure MN disease to be considered instead a multi-system, non-cell autonomous and complex neurodegenerative disease. With new insights into the pathological mechanisms underlying ALS there is increased interest in the regulatory mechanisms that may compromise MN function, in particular those that may contribute to an excitatory and inhibitory imbalance in the disease. Indeed, there is great interest in determining the biological basis for increased cortical hyperexcitability and impaired inhibition identified in the motor cortex of both familial and sporadic ALS patients. It is proposed that altered motor network excitability may be a central pathogenic mechanism in the disease, possibly initiating the final progressive decline of motor neuron function. While intrinsic regulation of the MN is likely implicated in this pathophysiology, loss of inhibitory network function is presumably mediated by intra-cortical inhibitory interneurons; however, the exact cell types responsible are yet to be identified. As such, the intent of this thesis was to examine the role of key inhibitory neuronal populations in the cortex, as they are crucial for normal brain functioning and the balance of excitatory neurotransmission. The current thesis is based upon the hypothesis that the "ALS pathogenesis involves cortical interneuron dysfunction".

The current thesis examined the role of cortical interneurons in disease by first establishing a timeline of cortical interneuron involvement in the motor circuitry of the $SOD1^{G93A}$ mouse model of ALS. The intent of this initial study was to determine which interneurons are involved in disease, and the time frame of their alteration relative to symptom-onset and motor neuron deficits. Subsequently, the validity of interneuron pathology was established in post-mortem ALS cases. An additional aim of this secondary study was to determine the relationship between interneuron pathology, cortical pathology and clinical characteristics. The final study investigated the potential vulnerability of interneuron populations using an *in vitro* approach, with electrophysiological techniques designed to explore the innate susceptibility of interneurons in the presence of the $SOD1^{G93A}$ mutation.

This thesis determined that specific interneuron populations were altered within the motor cortex of the $SOD1^{G93A}$ mouse model of ALS. Moreover, a novel timeline of interneuron involvement was identified that included dynamic changes in the density of NPY- and CR-expressing interneuron populations throughout the disease course. Changes originated in the upper cortical layers of the

motor cortex from early symptom onset, and progressed to involve the entire motor cortex by end-stage. Interneurons were unaltered in the somatosensory cortex, nor other interneuron populations altered in either region, suggesting NPY and CR-interneurons represent a motor-specific inhibitory phenotype early in disease. Interestingly, pathology is found to change throughout disease, suggesting inhibitory involvement may not be a static phenomenon.

The validity of interneuron involvement was subsequently investigated using post-mortem ALS cases. Comparing ALS cases and controls revealed changes in CR and NPY interneurons that largely recapitulated the interneuron pathology observed in the $SOD1^{G93A}$ mouse model. NPY-pathology was clearly increased in all ALS cases examined, supporting a similar pathogenic process in the motor cortex of ALS patients and the $SOD1^{G93A}$ mouse model. However, CR-interneuron pathology was recapitulated in a proportion of ALS cases, suggesting innate differences in the extent of interneuron involvement in individual cases. While no clear link was observed between interneuron pathology and clinical case characteristics, a positive correlation was demonstrated between heterogeneous CR-interneuron pathology, NPY-pathology and pyramidal pathology, which may provide a novel perspective on the neuronal basis of circuit dysfunction in the ALS motor cortex. In support of a role for inhibitory dysfunction in ALS, the examination of cortical interneurons *in vitro* identified that populations were innately susceptible to the SOD1 mutation, as demonstrated by the alteration of intrinsic electrophysiological properties and morphological development.

Collectively, these studies provide strong evidence in support of the hypothesis that the "ALS pathogenesis involves cortical interneuron dysfunction." Herein, evidence is provided for a dynamic and continual influence of interneurons throughout disease, which may include subtype specific dysfunction, initiated during early development, influencing disease-associated circuitry until the final stages of disease. These results highlight the non-cell autonomous nature of ALS, and suggest that further efforts should be made to understand the biological basis of inhibitory deficits in the disease. This will be essential for future efforts aimed at the restoration of normal excitability for the treatment and prevention of ALS, as the efficacy of treatment regimes will likely depend on the extent, type and timing of underlying dysfunction, and therefore pathophysiology, in the disease. Equally, it may also be of great therapeutic benefit to investigate the potential compensatory processes initiated, or contributed to, by these diverse cortical interneuron populations.

ACKNOWLEDGEMENTS

I would first like to thank my primary supervisor Associate Professor Tracey Dickson for her continued support and guidance throughout my PhD. Your attitude to science and life has made the past few years incredibly meaningful and fun, who without, this thesis would not have been possible. To my other supervisors, Dr Catherine Blizzard your enthusiasm is catching, Dr Kaylene Young and Associate Professor Anna King, you know what your support has meant to me and I thank you for always having an open door whenever I needed help.

I would like to thank my fellow friends and colleagues of the Dickson Lab, in particular Jayden Clark, who really should be my unofficial twin and has stuck with me on this journey from day one class one, to day two-thousand nine-hundred and nineteen. Special thanks to past members of the Dickson group Dr Katherine Southam, Dr Kate Lewis, Dr Edgar Dawkins, Dr Stan Mitew and in particular Dr Mariana Brizuela for representing team interneuron. I would also like my fellow peers at the Menzies Institute for Medical Research for their continual support and friendly faces.

I would also like to thank our collaborators, Professor Catriona McLean for her technical expertise, and Professor John Bekkers for providing the transgenic mouse line with the Gad67-GFP expression.

I would also like to acknowledge Ron and Jo Statham for their continual support and friendship over the last few years; you have both been great role models for an aspiring scientist.

Finally, I would like to thank my family, my brother Nic, parents Adrian and Jenny and my literal twin Melissa, for their understanding and constant support, cheeky cheerful Noah and Tess, and grandpa John for always encouraging me to aim high in life. I would also like to thank my fiancé William Borthwick, for his constant support, understanding and fine tea-brewing skills.

I would like to dedicate this work to the loving memory of my beautiful grandma, a most kind-hearted, gentle, funny and brave soul. For always seeing and believing the best in everyone.

ABBREVIATIONS

ALS	amyotrophic lateral sclerosis
ANOVA	analysis of variance
AMPA	α-amino-3-hydroxyl-5-methylisoxazole-4-propionic acid
C9orf72	Chromosome 9 Open Reading Frame 72
CB	calbindin
CNS	central nervous system
CO_2	carbon dioxide
CR	calretinin
DIV	days *in vitro*
FALS	familial amyotrophic lateral sclerosis
FTD	frontotemporal dementia
FUS	fused in sarcoma
Gad67	Glutamic acid decarboxylase 67
GABA	Gamma aminobutyric acid
GFP	green fluorescent protein
Hz	hertz
IgG	Immunoglobulin G
L	Litre
LMN	lower motor neuron
M	Molar
mg	milligram
ml	milli litre
mM	milli molar
mm	milli metre
mV	milli volts
MN	motor neuron disease
MND	motor neuron
ms	milli seconds
mOsm	milli osmoles

nA	nano amps
nM	nano molar
nm	nano metre
NPY	neuropeptide y
PBS	phosphate buffered saline
pA	pico amps
PCR	polymerase chain reaction
pF	pico farad
PV	parvalbumin
PSD-95	post-synaptic density 95
s	seconds
SALS	sporadic amyotrophic lateral sclerosis
SD	standard deviation
SEM	standard error of the mean
SMI32	neurofilament h non phosphorylated
SOD1	superoxide dismutase 1
SOM	somatostatin
TDP-43	transactive response DNA binding protein 43
UMN	upper motor neuron
VGAT	vesicular GABA transporter
VIP	vasoactive intestinal peptide
VGLUT-1	vesicular glutamate transporter 1
qPCR	quantitative polymerase chain reaction
µL	micro litre
µm	micro metre
µM	micro molar
^{o}C	degrees Celsius
Ω	ohms

Chapter 1

1 INTRODUCTION

First described by Jean-Martin Charcot in 1869 (Charcot & Joffroy 1869), amyotrophic lateral sclerosis is a progressive neurodegenerative disorder that has become synonymous with the systematic destruction of the motor system. Characterised by the loss of upper motor neurons within the brain and lower motor neurons within the spinal cord (**Figure 1.1**), it is the most common form of motor neuron disease (Cleveland & Rothstein 2001, Bruijn et al 2004, Talbot 2014). An incurable and ultimately fatal disease, it has an annual incidence of 2/100,000 individuals and a mean onset of 55-60 years (Chio et al 2013). The loss of motor neurons rapidly destroys the motor system and the ability to control voluntary muscles required for walking, talking, swallowing and breathing (Hardiman et al 2011).

Clinically heterogeneous, ALS often begins focally with patients typically experiencing fatigue, cramp, muscle weakness and wasting of one or more limbs (defined as limb onset), or fasciculation of the tongue (bulbar onset) (Turner & Swash 2015). Approximately 35% of cases begin in a lower limb, 30% in an upper limb and 30% in the muscles involved in speech and swallowing, while a smaller percentage is initiated in the respiratory muscles (**Figure 1.1**) (Chio et al 2011, Swinnen & Robberecht 2014). In classical ALS this is followed by a diffuse and ordered spread of pathology throughout motor networks that culminates in progressive muscle weakness, atrophy and eventual paralysis, resulting in respiratory failure and death within 2 – 5 years of symptom onset (Ravits & La Spada 2009, Verstraete et al 2014). The systematic spread of pathology from a specific anatomical site raises a number of fundamental questions - what causes the initial onset of disease in a particular region? How does it spread? And what underlies the vulnerability of both the network and neurons implicated in the disease?

At the system level the disease has been suggested to be propagated through defined anatomical networks by a cell-to-cell mediated 'prion like' mechanism involving the spread of pathogenic proteins (Lee & Kim 2015, Maniecka & Polymenidou 2015), or by degeneration passing though specific synaptic networks (Casas et al 2016). While either scenario is plausible, the complexity of such a biological basis is added to by the finding of subtle cognitive abnormalities in up to 50% of ALS patients, and pure frontotemporal dementia (FTD) symptoms such as behavioural, personality and language dysfunction in 15% of ALS patients (Ferrari et al 2011). Consequently, ALS is now considered a multi-system disorder in which patients can present with predominate motor symptoms, mixed motor and cognitive dysfunction, or cognitive predominance with minor motor involvement (**Figure 1.2**) (Ling et al 2013, Guerreiro et al 2015). Intriguingly, in either

Figure 1.1. Site of onset in ALS.

In the field there remains a number of points of contention that are of clear therapeutic and clinical consequence, including the site of disease origination and the primary process of spread. **a**, In particular, it is unclear whether the disease begins independently in lower motor neurons and upper motor neurons, or whether it is initiated primarily in the motor cortex, subsequently spreading to lower motor neurons (green arrow) in a process termed the "dying forward hypothesis." The contrasting theory suggests ALS results from a dying-back change at the neuromuscular junction associated (blue arrow) with axonal degeneration retrogradely propagated throughout the motor system. **b**, This controversy is supported by the seemingly disparate onset of symptoms, where patients can present with a range of key symptoms including the most common limb onset, and the less frequent bulbar or respiratory onset. Patient phenotype is strongly influenced by the degree of lower motor neuron (orange) and upper motor neuron involvement (blue), but also by the severity of involvement in distinct anatomical regions (grey shading). However, the spread of pathology through adjacent anatomical regions, to encompass the entire motor system, suggests a common final neurodegenerative pathway in the disease.

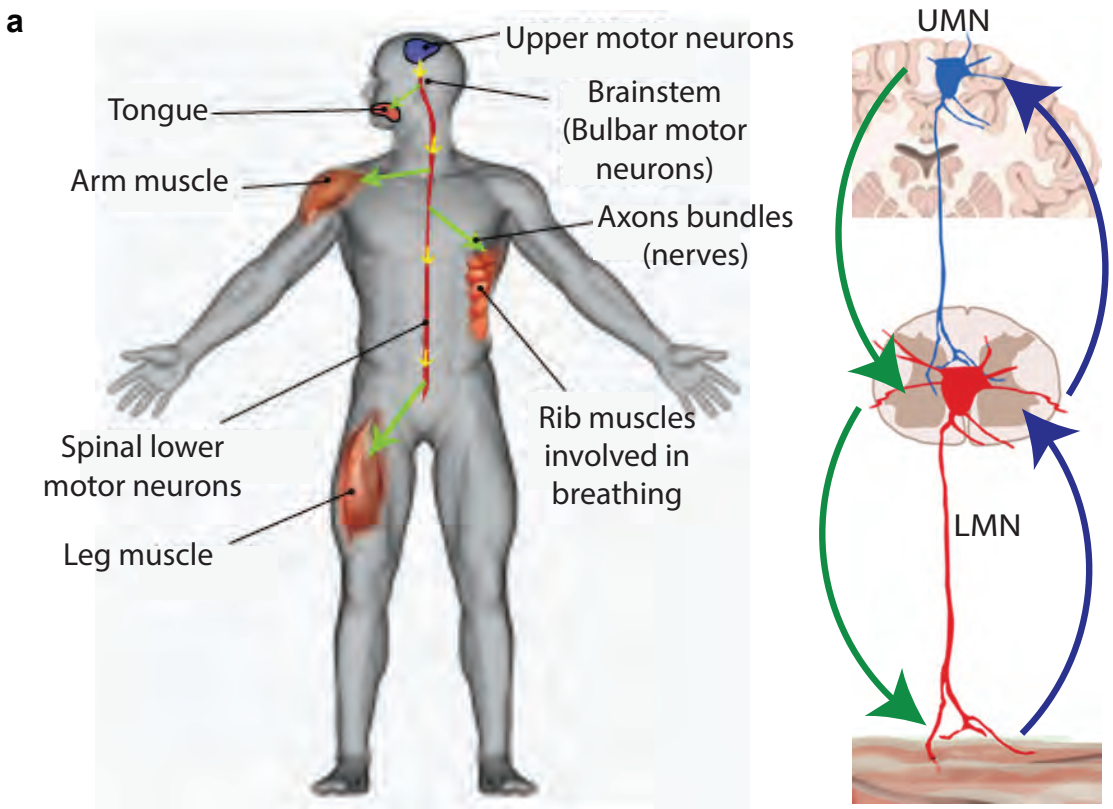

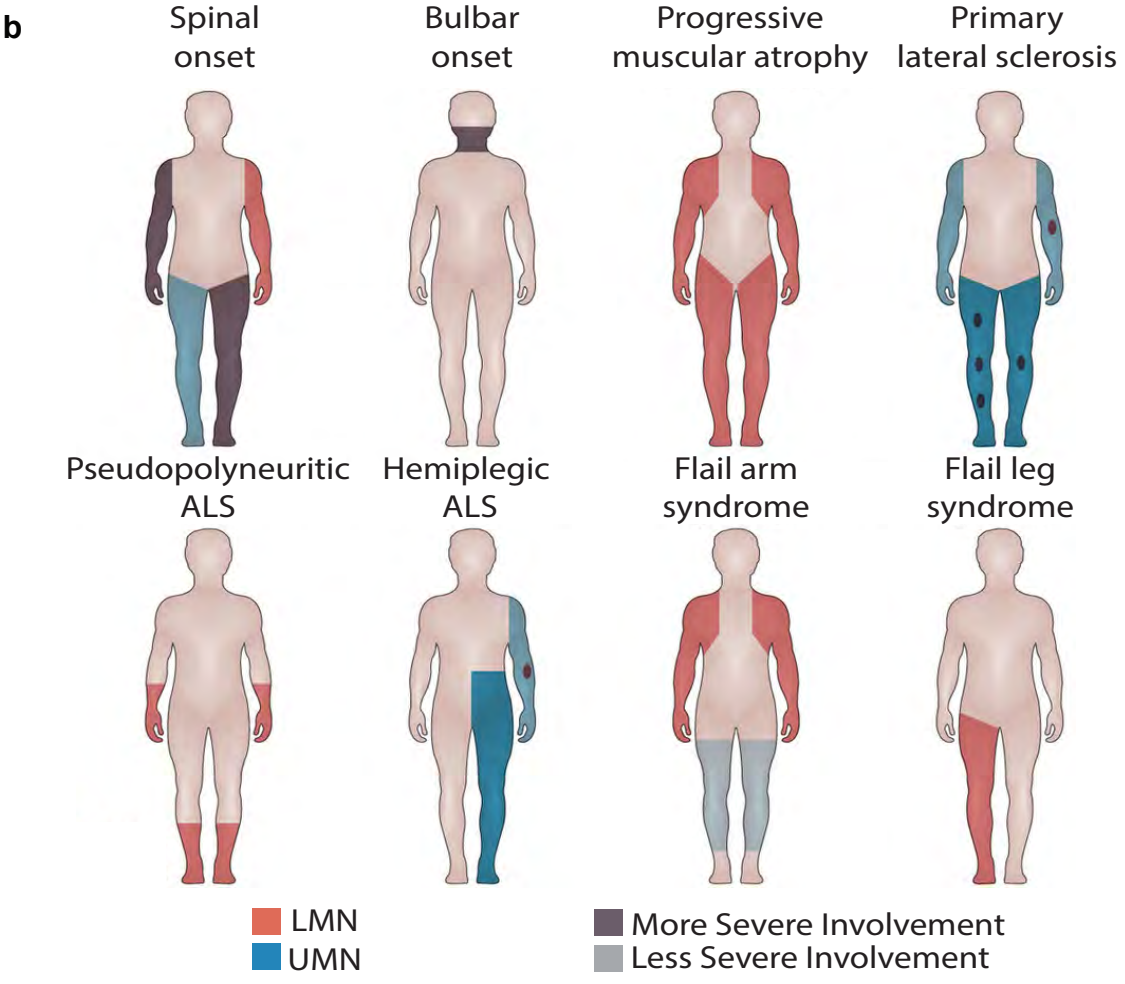

"The phenotypic variability of amyotrophic lateral sclerosis, Swinnen & Robberecht, 2014"

presentation higher order cognitive functions such as memory, problem solving and spatial orientation are spared (Strong et al 2009). Likewise, not all motor neuron populations degenerate, as eye movement and bladder control are unaffected by disease progression (Bruijn et al 2004). Therefore, it is essential to understand the interaction between system level vulnerability and cellular degeneration in order to understand the pathogenesis of disease.

At the cellular level a number of molecular and biochemical pathways have been implicated in the dysfunction of motor neurons and allow for insight into the potential pathogenicity underlying the disease. These include oxidative and proteasome stress (Karademir et al 2015), excitotoxicity caused by aberrant glutamate signalling (Van Den Bosch et al 2006), mitochondrial dysfunction (Carrì et al 2016), cytoskeletal dysfunction and axonal transport deficits (Clark et al 2016b), neuroinflammation (Hooten et al 2015), endoplasmic reticulum and protein folding stress (Matus et al 2013). While it remains to be determined which are primary disease mechanisms involved in the initiation of the disease, it is quite likely that mechanisms are not mutually exclusive, but instead are interconnected pathological processes, reflected by the non-cell autonomous nature of the disease (**Figure 1.3**)(Ilieva et al 2009). This is supported by the incredible spectrum of genetic factors now associated with the disease, which implicate a range of factors including RNA toxicity, maintenance of protein homeostasis and axonal transport (Renton et al 2014). Furthermore, while the majority of ALS cases are sporadic, with only ten percent of cases implicating genetic mutations (Al-Chalabi et al 2012), similarities in the clinical presentation of both the genetic and non-genetic forms of the disease have led to the suggestion of a commonality in the final neurodegenerative pathway (Byrne et al 2012). While several cellular, genetic and molecular mechanisms are likely involved in these common pathways, as a system-wide disorder, it is increasingly apparent that overactivation and abnormal excitability of circuitry may be of central importance in the disease (Eisen et al 1993, Vucic et al 2011, Bae et al 2013, De Carvalho et al 2014).

Excitation and inhibition are critically balanced in the central nervous system, such that alterations in one should be counteracted by alterations in the other (Lehmann et al 2012, Kepecs & Fishell 2014, Kubota 2014). In ALS, this homeostatic regulation appears to fail, with the manifestation of altered excitability evident in circuitry at critical stages in disease (Kuo et al 2004, Vucic & Kiernan 2006a, Vucic & Kiernan 2006b, Pambo-Pambo et al 2009, Bae et al 2013, Vucic et al 2013, Menon et al 2014, Fogarty et al 2015). This typically presents as a ‘hyperexcitability’, whereby MNs generate a greater number of action potentials per unit of input (Neumann & Nachmansohn 1975). The outcome of this overstimulation was first proposed by Eisen in 1992

Figure 1.2. ALS a multi-system disorder on a spectrum with FTD.

Advances in gene wide association studies have led to considerable breakthroughs in our understanding of ALS. **a**, Most prominently the identification of the C9orf72 repeat expansion in both ALS and frontotemporal dementia (FTD)(**a**), which has placed these two seemingly distinct diseases on a continuum that may represent a broader category of neurodegenerative disease. **b**, Neuropathological studies have provided further credence to this notion, as TDP-43 is identified as the major protein constitute of inclusions in both ALS and FTD, reflecting pathological overlap in the diseases. The identification of clinical symptom overlap in $_{\text{patients}}$, alongside potential monogenic and polygenic involvement of overlapping genes, suggests genetic penetrance may have a important role in the disease and highlights their may be a greater genetic component to the disease than previously appreciated.

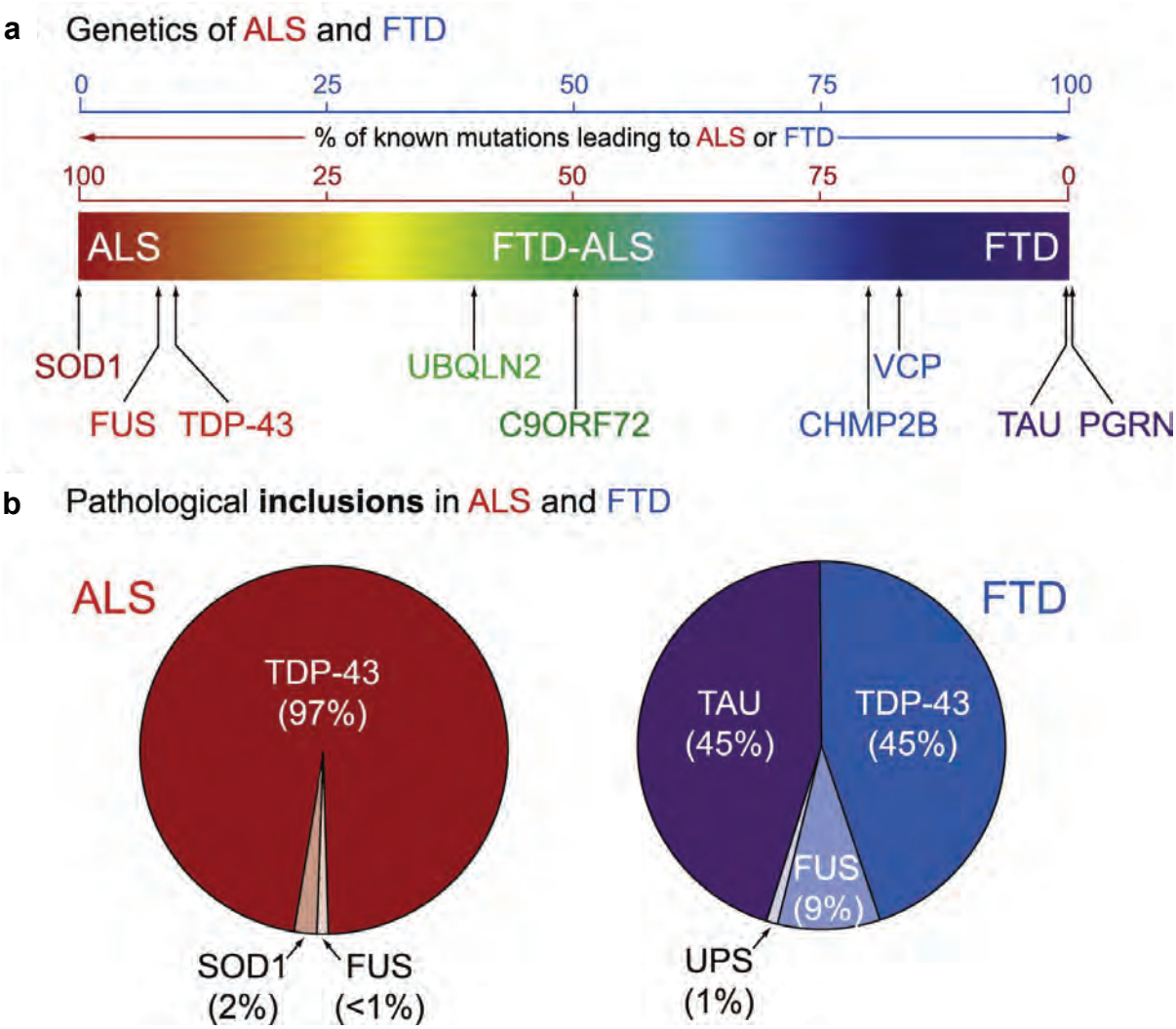

"Converging mechanisms in ALS and FTD: Disrupted RNA and protein homeostasis, Ling et. al. , 2013"

(Eisen et al 1992), suggesting that hyperexcitability drives MN degeneration through a mechanism of glutamate-mediated excitotoxicity, driven by excessive calcium overload, leading to cell death.

Although several molecular mechanisms may be implicated in this pathophysiology, this introductory thesis chapter will focus on the regulation of MN excitability. In particular, the extrinsic control of MNs is considered in relation to motor neuron hyperexcitability, highlighting inhibitory control of excitability and the potential contribution of altered inhibition to ALS disease processes and vulnerabilities.

1.1 A GENETIC CONVERGENCE ON ALTERED EXCITABILITY

In ALS the majority of cases are deemed sporadic (SALS) with no known cause, however, ten percent of cases are familiarly inherited (FALS) and have led to the identification of over 16 different genes and genetic loci associated with the disease. The most common genes implicated include a hexanucleotide repeat expansion in the C9orf72 gene (39.3%) (DeJesus-Hernandez et al 2011, Renton et al 2011), and mutation of the genes Superoxide Dismutase (SOD1) (12-23.5%) (Rosen et al 1993), TAR DNA Binding Protein (TARDBP) (5%) (Sreedharan et al 2008, Vance et al 2009) and Fused in Sarcoma (FUS) (4.1%) [reviewed in (Renton et al 2014)]. With the identification of the C9orf72 expansion also in 8% of SALS (Majounie et al 2012), there is increased interest in pathogenic mechanisms that may represent a point of genic convergence in the disease, such as altered excitability.

Several clinical and experimental studies suggest a genetic convergence on altered motor neuron excitability in both sporadic ALS and familial forms of the disease with mutations in C9orf72, SOD1, TDP-43 and FUS (Delestree et al 2014, Wainger et al 2014, Devlin et al 2015). Altered excitability has predominantly been associated with spinal pathology in ALS, due to the suggested relationship of fasciculation with LMN populations (De Carvalho & Swash 1998, Kleine et al 2008). However, more recently hyperexcitability has been shown to develop in both UMN (Eisen et al 1993, Vucic & Kiernan 2006b, Vucic et al 2013, Fogarty et al 2015) and LMN compartments (Kuo et al 2004, Kanai et al 2006, Vucic & Kiernan 2006a, Pambo-Pambo et al 2009).

Indeed, a number of clinical studies support a central role for cortical hyperexcitability in ALS (Eisen et al 1993, Zanette et al 2002b, Vucic & Kiernan 2006b, Vucic et al 2008). Traditionally UMN excitability measures were clinically evasive (Swash 2012), however more recent transcranial magnetic stimulation (TMS) studies have allowed for the earliest changes in excitability to be studied (Vucic et al 2013). Intriguingly, cortical hyperexcitability has been

Figure 1.3. ALS as a non-cell autonomous disease

While ALS has been traditionally viewed as a disease of pure motor neuron dysfunction, there are now several molecular and cellular mechanisms recognised to impede the function of other neuronal and non-neuronal populations in the disease. Considered as a non-cell autonomous disease, there is increasing interest in the supportive and regulatory cell populations required for normal motor neuron health and function. It is increasingly thought that the convergence of these supportive cell types may underlie major aspects of disease pathogenesis.

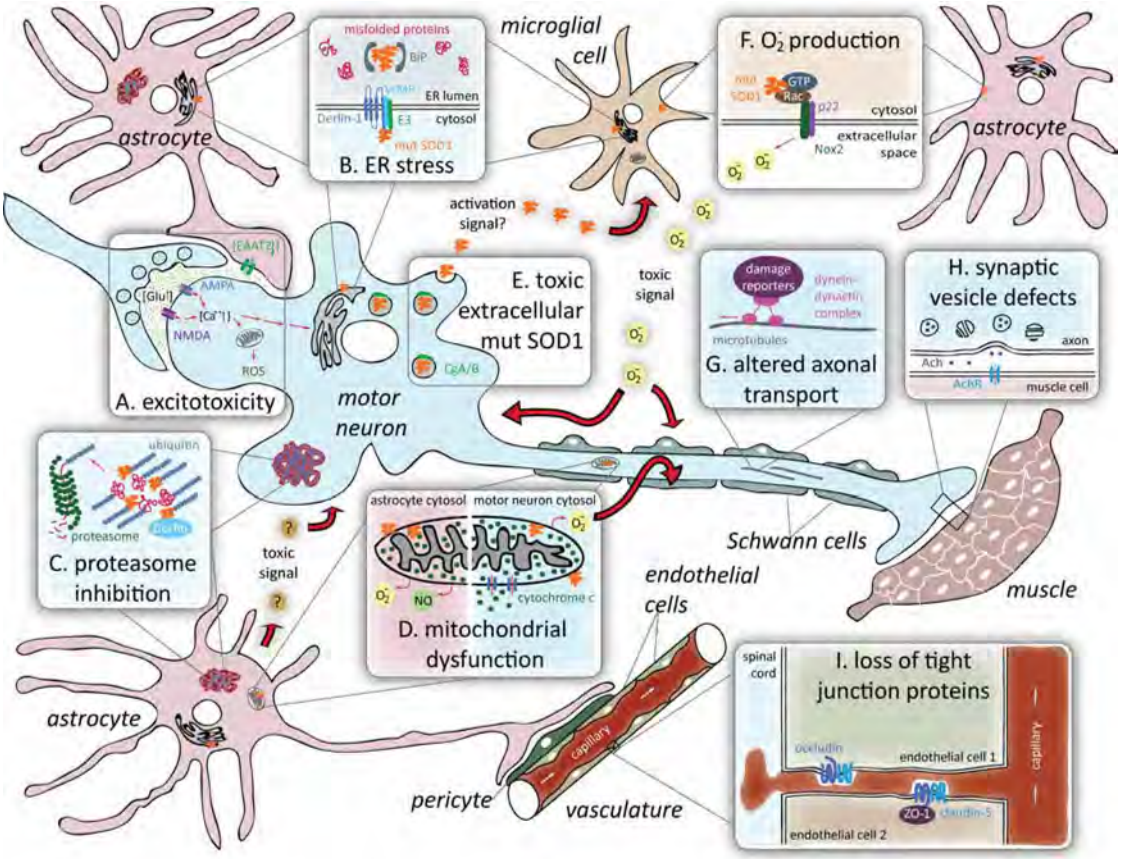

"Non-cell autonomous toxicity in neurodegenerative disorders: ALS and beyond, Ilieva, 2009"

identified in sporadic and familial forms of disease and precedes both the onset of clinical symptoms and measurable LMN dysfunction (Vucic & Kiernan 2006b, Vucic et al 2008, Menon et al 2014). This indicates that imbalances in motor cortex excitation may be a pathological event occurring upstream of LMN dysfunction. In line with this, cortical hyperexcitability has been linked to the anterograde trans synaptic propagation of glutamate toxicity (Menon et al 2014), leading to LMN degeneration (Vucic et al 2013), an adaption of the dying forward theory of ALS pathogenesis first proposed by Eisen (Eisen et al 1992). While it still cannot be discounted that perhaps cortical hyperexcitability may occur independent (Ravits et al 2007, Ravits & La Spada 2009) of, or secondary to (Pamphlett et al 1995), LMN dysfunction and degeneration, a relative loss of corticomotoneurons will have a greater clinical effect than loss of other MNs (Eisen & Weber 2001). Despite this controversy, as this chapter will emphasise, many studies in cellular and transgenic models of ALS highlight a primary role for altered excitability in both UMN and LMNs (Sareen et al 2013, Wainger et al 2014, Devlin et al 2015).

1.1.1 Temporal dynamics of excitability – protective or pathogenic?

Measures of excitability in transgenic animal models have suggested that a continuum of dynamic alteration is present throughout disease, which may represent, not only responsive compensatory mechanisms, but also initiating factors. Complimenting clinical studies, hyperexcitability is established in the G93A-hSOD1 mouse at embryonic (Pieri et al 2003, Kuo et al 2004, Martin et al 2013), neonatal (van Zundert et al 2008, Fogarty et al 2015, Saba et al 2015) and adult stages (Carunchio et al 2010) in both spinal and cortical cultures and acute cortical slices. However, transient states of both hyperexcitability, and hypoexcitability, are present throughout the disease course. In G93A-hSOD1 mice between postnatal day 34 and 82 at a presymptomatic stage, a third of spinal MNs have been reported to transition to hypoexcitability (Delestree et al 2014) and at end-stage hyperexcitability is absent (Fuchs et al 2013). The importance of varying excitability states is further confirmed by recent studies that demonstrate excitability is a disease-modifying factor capable of determining the fate of MNs. Disease-resistant MN populations are hyperexcitable, while vulnerable populations are unaltered (Leroy et al 2014). Additionally, generation of excitability in a vulnerable MN population has been shown to be capable of reversing disease pathology (Saxena et al 2013).

While a wide range of evidence has implicated early intrinsic spinal MN hyperexcitability, and pre-symptomatic cortical hyperexcitability, more recent studies in pluripotent patient stem cell lines (iPSCs) suggest a genetic divergence in excitability. For example, neurons with the C9orf72

expansion demonstrate a decreased capacity for action potential initiation (Sareen et al 2013), while hyperexcitability is also reported in neurons with the SOD1, C9orf72 and FUS mutations (Wainger et al 2014). These studies highlight a common pathway of altered excitability alterations, however they also highlight an apparent contradiction of hypoexcitability and hyperexcitability in iPSC neurons with the C9orf72 expansion. This conflict is explained by a recent study that followed both TDP-43 mutation and C9orf72 expansion iPSCs over a 10-week period, finding an initial phase of hyperexcitability, which was followed by a progressive loss of both action potential output and synaptic activity (Devlin et al 2015). This suggests key disease-related genes may be involved in a progressive alteration of excitability throughout the life of a neuron. Indeed, it is theorised that this transition from hyper to hypoexcitability may represent the pathogenic decline of the MN, whereby chronic over-excitation initiates more spikes in response to a synaptic input and subsequent intracellular calcium overload leads to neuronal death. This theory is further substantiated by *in vivo* recordings from G93A-hSOD1 mice that demonstrate a proportion of spinal MNs become hypoexcitable at a stage just prior to neuromuscular denervation (Delestree et al 2014). Thus, a progression from hyperexcitability to hypoexcitability may represent a common final pathway in vulnerable MN populations (Figure 1).

Supporting this hypothesis in the context of ALS, aberrant electrical activity of MNs has been linked to dysfunction, degeneration and the accumulation of misfolded proteins (Kiskinis et al 2014). In pluripotent stem cell-derived MNs activation of voltage-gated potassium channels reversed hyperexcitability and improved MN survival *in vitro* (Wainger et al 2014). Intriguingly, voltage-activated Na^+ and K^+ currents are reduced with advanced disease and the onset of hypoexcitability (Devlin et al 2015), indicating dysfunction or loss of ion channels may also have an important role to play in the disease, influencing the probability for normal neuronal activity and cell excitability. However, in contrast to this pathogenic view of hyperexcitability, in transgenic SOD1 mice increased excitability is demonstrated to protect vulnerable fast fatiguing spinal MNs normally lost in this model. The neuroprotective effect of enhanced excitability reversed misfolded SOD1 accumulation and MN pathology via activation of the mammalian target of rapamycin pathway (mTOR) (Saxena et al 2013). Importantly, further reduction of excitability in these populations enhanced misfolded SOD1 accumulation and accelerated disease. Hence the role of excitability in disease remains controversial, with both a pathogenic and neuroprotective role indicated. However, as a switch from hyperexcitability to hypoexcitability appears central to motor neuron decline, it may suggest that hyperexcitability is pivotal in a pathogenic switch, where resultant hypoexcitability ultimately defines the failure of motor neurons. Taken together,

these findings indicate that maintaining balanced neuronal excitability throughout disease could be of therapeutic benefit.

1.1.2 Glutamate-mediated excitotoxicity

Excitotoxicity is caused by over-stimulation of neuronal glutamate receptors, leading to neuronal dysfunction and ultimately to cellular death through activation of Ca^{2+}-dependent enzymatic pathways (Arundine & Tymianski 2003). A glutamate-mediated pathogenic process was first proposed in ALS due to elevated levels of glutamate observed in the cerebrospinal fluid (CSF) of patients (Rothstein et al 1990). A follow up study involving one of the largest investigations of patients with sporadic ALS, found increased CSF glutamate levels in nearly 40% of patients which correlated with disease severity (Spreux-Varoquaux et al 2002). Anti-glutamate drugs subsequently entered clinical trials, producing riluzole, the only drug currently approved for ALS treatment (Cheah et al 2010). With advances in clinical screening of patients, it is now apparent that enhanced glutamate release may also be a central pathophysiological process involved in hyperexcitability in both familial and sporadic forms of the disease (Vucic et al 2013).

The release of glutamate during normal neurotransmission is a tightly regulated process (**Figure 1.4 a**). Glutamate exerts its effects through both ligand-gated ionotropic receptors, including N-methyl-D-asparate (NMDA), ∝-amino-3-hydroxyl-5-methyl-4-isoxazoleproprionic acid (AMPA) and kainate receptors, and G-protein-coupled (metabotropic) receptors, allowing calcium influx and action potential propagation (Seeburg 1993). The excitatory signal is terminated by active removal of glutamate via transporters (EAAT1 and EAAT2) predominately found on astrocytes surrounding the synapse (Vandenberg 1998). Astrocytes then convert glutamate to glutamine, which is recycled back to glutamate at presynaptic neurons via glutaminase and packaged into functional vesicles, ready to be released again (Danbolt 2001).

In ALS evidence for a glutamate-mediated excitotoxic process has been provided in both human and animal studies (**Figure 1.4 b**). The glutamate transporters on astrocytes required for the rapid binding and clearance of synaptic glutamate (EAAT-2) have been reported to be dysfunctional in both the spinal cord and motor cortex of ALS patients (Lin et al 1998), and in the transgenic SOD1 mouse (Trotti et al 1999). Overexpression of EAAT-2 appears to be neuroprotective (Rothstein et al 2005), whereas downregulation accelerated disease progression (Pardo et al 2006). However, the loss of EAAT-2 does not appear to be a primary event in ALS, as abnormal glutamate transport is not unique to ALS and appears in several other neurodegenerative diseases, such as Alzheimer's disease and Parkinson's disease (Martin et al 1997, Hinoi et al 2005). Despite

Figure 1.4 Glutamatergic neurotransmission (adapted from Heath & Shaw, 2002). **a**, Normal glutamatergic neurotransmission is highly regulated process in the central nervous system, which relies on regulatory mechanisms involving extrinsic synaptic influences and intrinsic cell properties. Inhibitory interneurons help regulate pre- and post-synaptic excitability and levels of glutamate released. Combinations of glutamate transporters effectively terminate glutamatergic effects on receptors by re-uptake and recycling of this excitatory neurotransmitter. **b**, When these regulatory mechanisms fail an excitotoxic calcium-mediated pathogenic process can damage neurons by the overactivation of receptors by increased extracellular glutamate. In ALS, excitotoxicity is thought to be a central pathogenic mechanism that may result from reduced astrocytic glutamate uptake, increased AMPA receptor permeability and increased excitability, potentially mediated by aberrant inhibition.

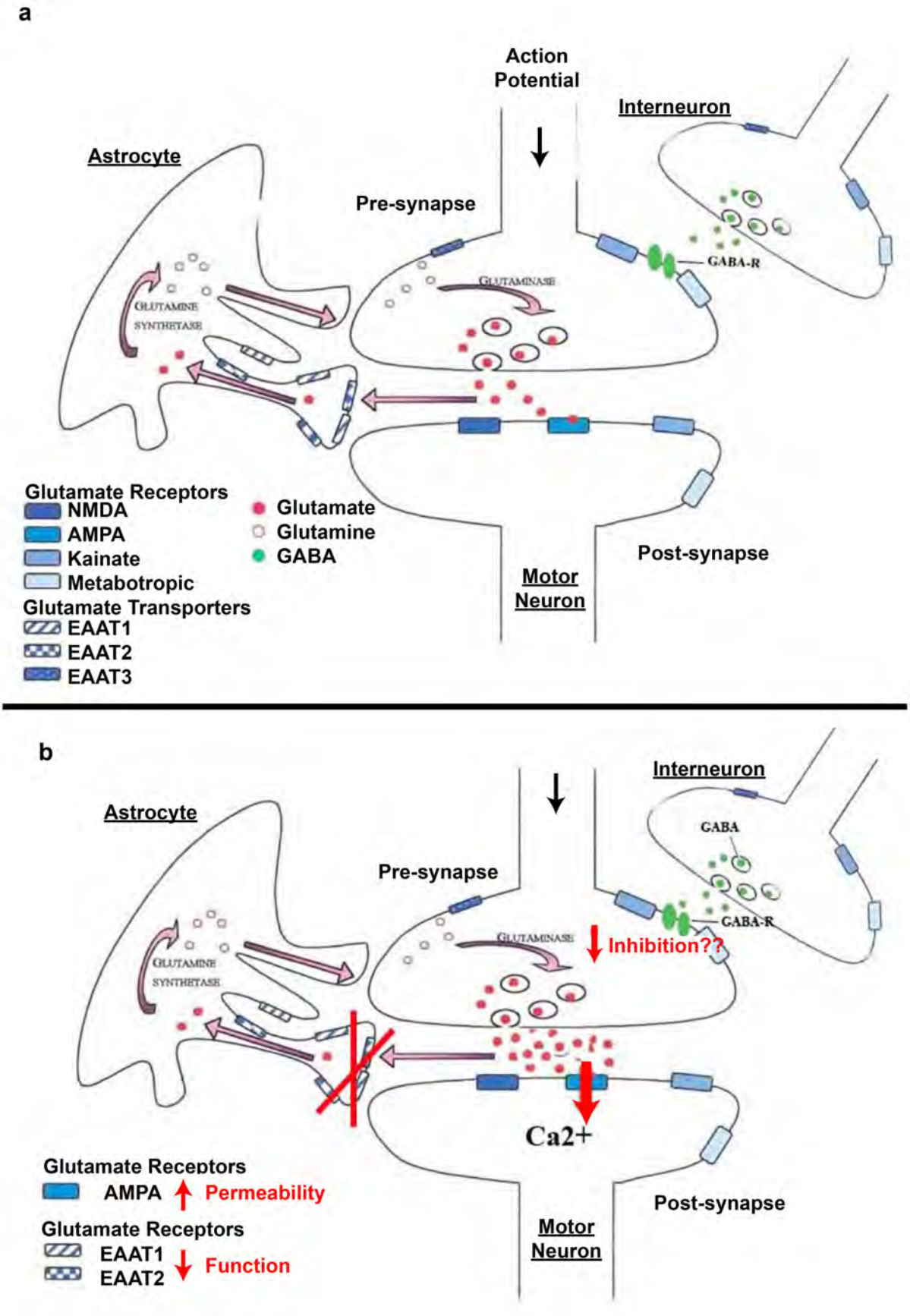
a
Action Potential
Interneuron
Astrocyte
Pre-synapse
GABA-R
GLUTAMINASE
GLUTAMINE SYNTHETASE
Glutamate Receptors
NMDA
AMPA
Kainate
Metabotropic
Glutamate Transporters
EAAT1
EAAT2
EAAT3
Glutamate
Glutamine
GABA
Post-synapse
Motor Neuron
b
Interneuron
Astrocyte
GABA
Pre-synapse
GABA-R
GLUTAMINASE
Inhibition??
GLUTAMINE SYNTHETASE
Ca2+
Glutamate Receptors
AMPA
Permeability
Glutamate Receptors
EAAT1
EAAT2
Function
Post-synapse
Motor Neuron

this, several studies have indicated that motor neurons are particularly vulnerable to excitotoxic insults (Bar-Peled et al 1999, Sun et al 2006, King et al 2007, Mitra et al 2013), with a most recent study supporting a die forward mechanism of excitotoxicity, chronic excitotoxin exposure of the lower motor neuron soma initiated neuromuscular denervation (Blizzard et al 2015). Motor neurons are known to have an innately low calcium-buffering capacity that may render them more susceptible to excitotoxic insults (Alexianu et al 1994). Adding to this, in the ALS disease setting patients have been found to have deficits in RNA-editing of the GluR2 glutamatergic AMPA receptor subunit (Kawahara et al 2004), which appears specific to motor neurons, rendering them highly permeable to calcium (Williams et al 1997).

In combination such factors may explain innate vulnerability to normal glutamate levels, however calcium enters motor neurons not only through glutamate receptors during neurotransmission, but also through voltage-gated Ca^{2+} channels during each action potential (Powers & Binder 2001). Thus, the more excitable a cell is, the greater the calcium influx it may experience and the greater the likelihood of vulnerability to excitotoxicity. In the context of hyperexcitability, excessive glutamate release may therefore prime susceptible motor neurons towards excitotoxic degeneration. Hence there is great interest in the underlying factors that may be contributing to hyperexcitability in ALS.

1.2 THE EXCITING PROSPECT OF INHIBITION IN ALS

While intrinsic regulation of the MN is likely implicated in the pathophysiological basis of excitability changes in ALS (Williams et al 1997, Zanette et al 2002b, Zanette et al 2002a, Kawahara et al 2004, Kuo et al 2005, Kanai et al 2006), recent advances highlight the many facets of the inhibitory circuitry that are associated with extrinsic control of this selectively vulnerable population and may also contribute to disease (Andersen et al 1996, Weber et al 2000, Lorenzo et al 2006, Vucic et al 2008, Brockington et al 2013, Menon et al 2014).

1.2.1 Inhibitory control of excitability

In order to generate harmony in circuits, excitation must be balanced with an equally effective inhibition. In the central nervous system this balance is achieved through the regulatory actions of interneurons, a key inhibitory neuronal population that modulates the excitatory functions of pyramidal neuron populations throughout the brain and the spinal cord (Markram et al 2004). While the excitatory pyramidal neurons constitute the majority of neurons in the central nervous system, it is the incredible heterogeneity and diversity afforded by the remaining 20-30% of cells,

the interneurons, that allows for the fine-tuning of network excitability (Markram et al 2004). Typically classified by morphology, axonal targets, or by the expression of calcium binding proteins and neuropeptides (DeFelipe 2002, Markram et al 2004, Ascoli et al 2008, Suzuki & Bekkers 2010b), it is their differing intrinsic biophysical properties, connectivity and placement in networks that determines their functionality (**Figure 1.5**) (Buzsaki et al 2004, Wonders & Anderson 2006, Kubota 2014). In essence, as interneurons usually project locally they can modulate circuitry and affect output via either the presynaptic recruitment that drives the interneuron itself to fire, and/or by the post-synaptic targets of their inhibitory influence. These actions subsequently determine circuit activity and the output frequency of local pyramidal, or MN, populations (Kepecs & Fishell 2014). While interneurons receive both excitatory and inhibitory synapses themselves (Douglas et al 2004), it is the distinct axonal arborisation patterns exhibited by specific interneuron subsets that allow them to selectively control the input, integration and output of target cells (Buzsaki et al 2004). Interneurons can innervate the dendrite, soma or axon of neurons in different columns, or laminar, with great precision (DeFelipe 1997, Somogyi et al 1998). This elaborate diversity of connections can be thought of as divisive (axo-axonic innervation) or subtractive (axo-somatodendritic) in nature and reflects the overarching complexity with which interneurons function to correctly apply balanced inhibition (Holt & Koch 1997, Silver 2010).

1.2.2 The motor cortex and its inhibitory cells

Interneuron populations in the cortex have a role in the regulation of layer V corticomotoneurons, which are the major source of descending motor commands for voluntary muscle movement (Jara et al 2014). Fast spiking interneurons within the same cortical layer, directly synapse onto the corticomotoneurons and are thought to provide feedback or lateral inhibition (Tanaka et al 2011). Interestingly, interneurons located in layer II/III of the motor cortex, may also have a large impact on corticomotoneurons by disynaptic feedforward inhibition – a pathway from layer II/III to layer V is thought to represent the major excitatory input to corticomotoneurons (Thomson & Lamy 2007), and the major synaptic output of the motor cortex (Yu et al 2008). Receiving descending inputs from the corticospinal tract system, spinal MNs (LMNs) focus motor activity, and also receive descending connections from other key motor structures, such as the basal ganglia and thalamus, many of them interneuronal (Miri et al 2013). The interneurons within the spinal cord, such as Renshaw cells, exhibit recurrent inhibition, in which they receive excitation from LMNs and in turn inhibit the same population of MNs (Renshaw 1941, Eccles et al 1954). They have actions upon α MNs initiating muscle contraction, γ MNs controlling muscle spindle length, 1a

Figure 1.5 Cortical interneuron heterogeneity and classification

a, Interneurons of the neocortex are localised to specific lamina in which they display substantial phenotypic diversity and can be classified by differences in cell morphology and molecular markers including but not restricted to: calbindin (CB), calretinin (CR), parvalbumin (PV), neuropeptide (NPY), somatostatin (SOM) and vasoactive intestinal peptide (VIP). Functional diversity can also be used to classify interneurons due to varying postsynaptic targets and projection patterns. **b**, The location of embryonic generation can also be used to classify interneurons, with differences in molecular markers, functional intrinsic properties and receptor profiles demonstrated in cells arising from caudal/lateral eminence (CGE) or medial ganglionic eminence (MGE).

a

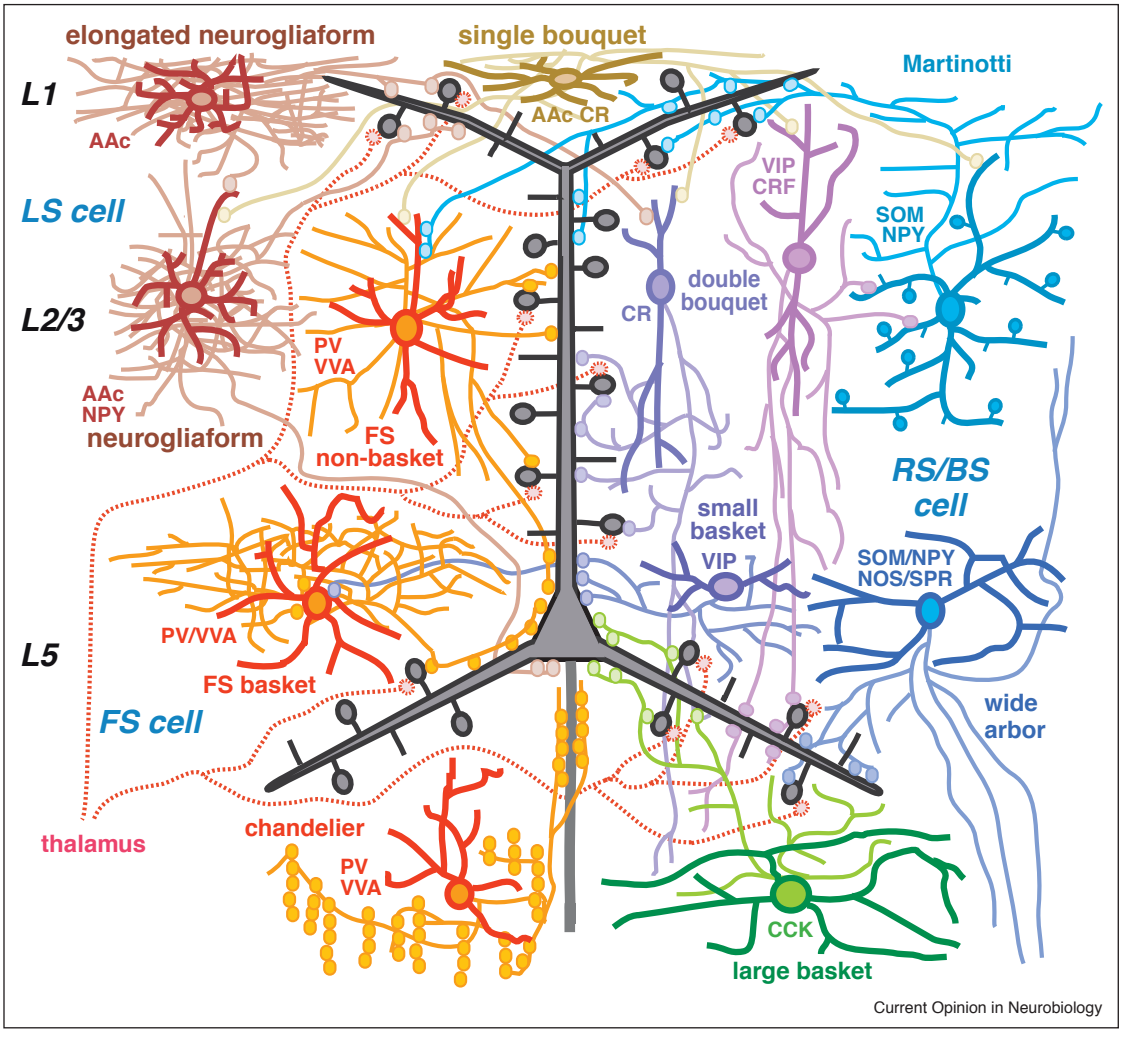

"Untangling GABAergic wiring in the cortical microcircuit, Kubota, 2014"

b

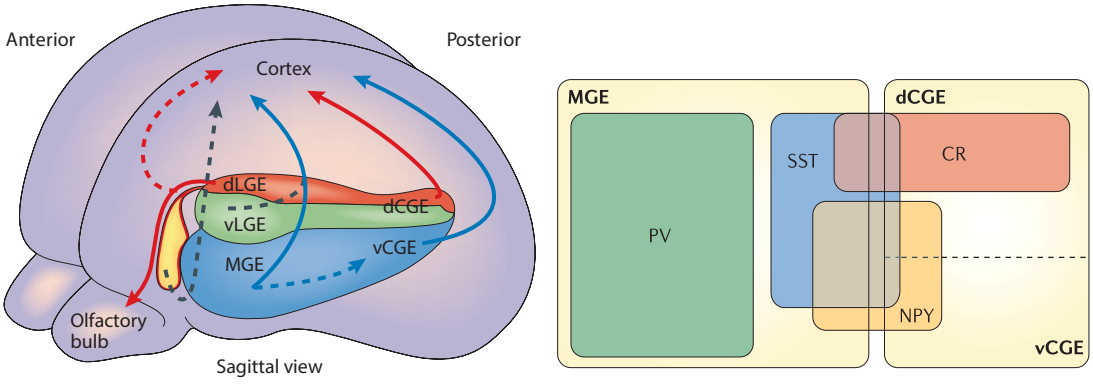

"The origin and specification of cortical interneurons, Wonders & Anderson, 2006"

interneurons mediating reciprocal inhibition of antagonistic muscles and other Renshaw cells (Alvarez & Fyffe 2007). Therefore, interneuronal control is important for many facets of motor system function, from the initiation of motor movements to the facilitation of firing in functional motor units.

1.3 FUNCTIONAL CORRELATES OF INHIBITORY DYSFUNCTION IN ALS

Over the last few decades a wealth of evidence has pointed towards an excitatory dysfunction in ALS motor circuitry (Caramia et al 1991, Eisen et al 1993, Prout & Eisen 1994, Mills & Nithi 1998, Desiato et al 2002, Vucic & Kiernan 2006b, Vucic et al 2008), however it has remained unclear to what extent inhibitory alterations, or indeed interneuronal alteration, may underlie this pathophysiology. With the advent of transcranial magnetic stimulation (TMS) studies examining intracortical circuitry, it is has become evident that multiple measures of inhibitory regulation are pre-symptomatically disrupted.

In ALS patients concurrent reductions in the short interval intracortical inhibition (SICI) (Hanajima et al 1996, Yokota et al 1996, Ziemann et al 1997, Sommer et al 1999, Zanette et al 2002b), predominantly seen in patients with limb-onset disease, the cortical silent period (CSP) duration, predominantly seen in patients with bulbar-onset disease (Desiato et al 2002) and the resting membrane potential are documented (Menon et al 2014). Indeed, many of these TMS measures are now identified prior to LMN dysfunction and are associated with excitability in the cortex (Menon et al 2014). While some debate exists regarding the varying cortical components that are represented by these measures (Roshan et al 2003), it is a commonly held view that SICI is mediated by GABA-secreting inhibitory cortical interneurons via $GABA_A$ receptors (Ziemann et al 1996, Ziemann 2004). Although, perturbations that move neurons closer to their action potential threshold, such as alterations to voltage gated sodium (Na+) and potassium (K) channels may also contribute to reductions of SICI in ALS (Kuo et al 2005, Kanai et al 2006, Stafstrom 2007). Nonetheless, CSP duration is thought to reflect both inhibition of anterior horn cells from the spinal cord and cortical influences via $GABA_B$ receptors (Cantello et al 1992, Inghilleri et al 1993, Chen et al 1999, Werhahn et al 1999, Sanger et al 2001). Thus, the reduced CSP duration observed in ALS patients is likely in keeping with previous studies that have documented both disinhibition of anterior horn cells (Raynor & Shefner 1994, Drory et al 2001) and dysfunction of cortical inhibitory interneurons acting via $GABA_B$ receptors (Zanette et al 2002b).

Further, evidence for interneuronal dysfunction is found in the motor cortex, where levels of the inhibitory neurotransmitter GABA is reduced (Foerster et al 2012), $GABA_A$ receptor subunit

alpha-1 mRNA is reduced (Petri et al 2003) and Flumazenil, a GABA receptor ligand shows reduced binding (Lloyd et al 2000). In this key-disease affected region concurrent losses of GABAergic activity is observed alongside elevated levels of glutamate (Foerster et al 2013). Therefore, a loss of cortical inhibitory influence (via $GABA_A$ and $GABA_B$ receptors dysfunction) and occurrence of ion conductance alterations (via Na+ and K channels) may concurrently facilitate increased motor network excitability. Together, these measures suggest a wider interneuronal phenotype that may underlie alterations in excitability and ultimately confer motor system vulnerability.

1.4 PATHOLOGICAL EVIDENCE FOR INTERNEURON DYSFUNCTION

In ALS a progressive destruction of motor control is emphasised by loss of UMNs (Betz cells) in the motor cortices (Udaka et al 1986), alpha and gamma MN losses in the spinal cord (Swash & Fox 1974, Swash et al 1986) and corticospinal degeneration (Swash et al 1988, Ellis et al 2001, Yin et al 2008). The functional deficit in ALS has therefore been assumed to result from motoneuronal death. However, a complex neuronal network controls the motor system, including interneurons that pervade these neuronal compartments (Jara et al 2014), and several histological studies support clinical findings and also suggest that inhibitory populations may be equally involved in pathology.

1.4.1 The cortex

In the ALS cortex a range of inhibitory populations have been implicated in pathology, however, evidence is fragmentary and there is a need for systematic investigations. In post-mortem ALS tissue, parvalbumin positive cells and neuropeptide Y positive neurites are decreased in the motor cortex (Nihei & Kowall 1993, Nihei et al 1993). Calbindin positive neurons have been reported to be unaltered in the motor cortex (Ince et al 1993), and to be reduced specifically in cortical layers V and VI (Maekawa et al 2004). A trend towards reduced calretinin positive cells is also demonstrated (Maekawa et al 2004). In the cortex of the G93A-hSOD1 transgenic mouse model of ALS, qualitative assessments suggest reduced calretinin cells in the motor cortex, but also in the hippocampus (Chung et al 2005). However, in contrast to findings in human cortical tissue, another study in G93A-hSOD1 mice found increased parvalbumin containing cortical interneurons in motor and somatosensory cortices (Minciacchi et al 2009). Thus, there appears a certain disconnect between human studies and animal studies, and while this may reflect clinical heterogeneity in patients or the divergent complexity of interneuronal circuitry between species

(DeFelipe 2002, DeFelipe 2011), it highlights the need for further histological studies aimed at determining interneuronal alterations.

1.4.2 The spinal cord

In the ALS spinal cord, a loss of anterior horn interneurons occurs in parallel, and to a similar extent, with MN losses in this region (Stephens et al 2006). Likewise, in the G86R-mSOD1 mouse model the temporal onset of degeneration in MNs and interneurons is reportedly the same (Morrison et al 1996, Morrison et al 1998). This suggests that the greater motor circuitry may be equally vulnerable in the ventral horn. In line with this theory, human spinal interneurons display similar pathology to degenerative MNs, with ubiquitinated cytoplasmic inclusions observed in some patients (Stephens et al 2001). However, also in the G93A-hSOD1 model, it has been reported that reduced glycinergic interneuron populations precede degeneration of MNs (Martin et al 2007, Chang & Martin 2009). Therefore, there may be differential vulnerability of glycinergic and GABAergic populations in this region.

1.5 SELECTIVE MOTOR NEURON VULNERABILITY TO INHIBITORY DISTURBANCES

Despite heterogeneity in the potential mechanisms of ALS (Bruijn et al 2004, Goodall & Morrison 2006, Rothstein 2009), current studies lend support to differences in excitatory and inhibitory receptor profiles as key determinants of MN vulnerability and potential for survival.

In ALS, not all MNs degenerate, rather there is spectrum of vulnerability in MN subtypes. Specific MNs are spared, such as the oculomotor and abducens populations responsible for preservation of eye movements in patients (Mannen et al 1977). Recent gene expression studies have explored the normal gene profiles of the subpopulations of MNs known to be either vulnerable or resilient to ALS (Brockington et al 2013). These studies have identified a number of factors that may contribute to differential vulnerability, including differences in genes implicated in ubiquitin-dependent proteolysis, mitochondrial function, immune system function and the extracellular matrix. However, the most striking differences were present in genes associated with functions in synaptic transmission, in particular genes responsible for the GABA and glutamate receptor subunits. In disease-resistant oculomotor neurons an upregulation of six different $GABA_A$ receptor units was identified compared to vulnerable spinal MNs (Brockington et al 2013). AMPA receptor subunits were also differentially altered with upregulation of GluR1 and GluR2 subunits. Indeed, the expression of $GABA_A$ receptor density ratios and synaptic and extrasynaptic $GABA_A$ receptors were altered in a separate gene study assessing differential features of ALS resistant

MNs (oculomotor, trochlear and abducens) compared with vulnerable MNs (facial, hypoglossal and trigeminal nerve) (Lorenzo et al 2006, Wijesekera & Leigh 2009). There are a number of reasons why these differing receptor profiles may produce differential vulnerability in the ALS disease setting, as discussed below.

A baseline increase in GluR2 subunits in resilient MNs may maintain vital AMPA receptor calcium impermeability. The loss of the GluR2 subunit (Burnashev et al 1992, Lomeli et al 1994), causes AMPA receptors to become permeable to calcium (Van Damme et al 2002, Isaac et al 2007), resulting in increased burden on downstream cell signaling cascades (Rothstein 2009). In ALS, defects in the RNA-editing of the GluR2 subunit are identified in sporadic patients (Kawahara et al 2004) and genetically engineered mice lacking ADAR, the enzyme responsible for normal GluR2 editing, develop symptoms suggestive of MN degeneration (Hideyama et al 2010). Interestingly, ADAR2 has been identified as a site of TDP-43 misprocessing in sporadic ALS patient MNs (Yamashita & Kwak 2014), which may suggest a pathological convergence of the proposed RNA-editing dysfunction in ALS on this GluR2 subunit.

$GABA_A$ receptors subunit composition determines the localisation of the receptor as well as its distinct pharmacological and electrophysiological properties thus differential $GABA_A$ subunit expression will alter GABAergic receptor function (Sieghart & Sperk 2002, Sigel & Steinmann 2012, Labrakakis et al 2014). Furthermore an increase in $GABA_A$ receptors may allow for a greater extent of GABAergic influence and protection from altered neuronal activity such as excessive glutamate. This is supported by observations of reduced levels of the neurotransmitter GABA in ALS patients (Foerster et al 2012) and of the $GABA_A$ receptors alpha1-subunit in the motor cortex of patients (Petri et al 2003). Indeed, the hyperexcitability that develops in ALS (Eisen et al 1993) can be reversed by Diazepam, a prominent $GABA_A$ receptor agonist (Caramia et al 2000), indicating that loss of inhibitory input may be driving the hyperexcitability in this disease.

THESIS HYPOTHESIS AND AIMS

Hyperexcitability and excitotoxicity are increasingly implicated in the pathogenesis of ALS, yet studies to investigate the pathological alterations to interneurons, a key regulator of excitability, are fragmentary. The great diversity of interneurons in the CNS has likely contributed to the failure to fully explore the role of this cell type in disease processes, with most studies focusing on pyramidal and motor neuron populations. There is accumulating evidence for a role of interneurons in ALS, however, this evidence is limited and a systematic investigation is required. This thesis aims to establish the role of cortical interneurons in ALS by firstly establishing a time course of interneuron pathology in the motor neuron circuitry of a well-established ALS mouse model. The validity of interneuron pathology is subsequently determined in human post-mortem ALS cases, examining neuronal pathology in key disease-associated cortical regions. Finally, the vulnerability of interneuronal populations is assessed *in vitro* in order to develop insight into the pathogenicity of interneurons in disease.

Aim 1: Determine cortical interneuron involvement in the SOD1^{G93A} mouse model of ALS. *Hypothesis 1: The inhibitory motor neuronal circuit is central to disease in ALS, evidenced by specific interneuronal pathology in the motor cortex.*

Investigations focusing on interneuronal populations in the cortex are few and incomplete, despite increasing evidence of aberrant excitation in ALS. The first aim of this thesis will be to investigate if specific interneuron populations are altered in the cortex of the SOD1^{G93A} mouse model of ALS. In addition, interneuron populations will be assessed at defined stages relative to disease progression, as less is known about the potential timing of inhibitory involvement in the disease. This will be completed by systematic assessment of specific interneuronal markers in cortical lamina utilising immunohistochemical and confocal microscopy techniques.

Aim 2: Establish if specific interneuron pathology is recapitulated in human post-mortem ALS cortical tissue. *Hypothesis 2: Specific interneuron populations affected in the SOD1^{G93A} mouse are affected in ALS patients and are associated with the extent of cortical pathology.*

Inhibitory circuit dysfunction during early hyperexcitability is an increasingly recognised event in the ALS patient cortex. Further, GABAergic dysfunction and glutamatergic overload occur concurrently in the ALS motor cortex. Hence the inhibitory circuit is likely implicated in hyperexcitability and excitotoxicity in ALS. However, a cellular basis for inhibitory alterations in the ALS cortex remains to be determined. Therefore, Aim 2 will determine if interneuron

pathology identified in Aim 1 is present in post-mortem ALS cortical tissue. The extent of interneuron pathology will be established in individual cases and compared to cortical pathology after optimisation of relevant immunohistochemical markers.

Aim 3: Identify the effect of the SOD1^{G93A} mutation on interneuron development *in vitro*. *Hypothesis 3: The SOD1 mutation will affect the intrinsic function of interneurons and their normal development in vitro.*

In ALS there is potential for early interneuron dysfunction to initiate, or respond to, changes in excitability. However, as interneurons are primarily considered an adaptive cell type, little is known about their innate vulnerability in disease. Despite studies that demonstrate motor neurons on an ALS genetic background have altered excitability and neurite development *in vitro*, it is unknown if interneurons are affected similarly. Therefore, using an *in vitro* primary culture model, Aim 3 will investigate the affect of the SOD1 mutation on normal interneuron function and neurite development, by examining intrinsic electrophysiological properties and neurite arborisation patterns.

Chapter 2

2 A TIME COURSE OF DIFFERENTIAL INTERNEURON VULNERABILITY IN THE CORTEX OF THE SOD1^{G93A} MOUSE MODEL OF ALS

2.1 INTRODUCTION

Clinical TMS studies have given incredible insight into the time frame and regional involvement of inhibitory/excitatory disturbance in the cortex (Eisen et al 1993, Zanette et al 2002b, Vucic & Kiernan 2006b, Vucic et al 2008, Menon et al 2014, Geevasinga et al 2015). In ALS, TMS critically identifies concurrent hyperexcitability and reduced inhibitory function in the motor cortex of both familial and sporadic ALS patients (Menon et al 2014, Geevasinga et al 2015). This is thought to contribute to an imbalance between inhibitory and excitatory synaptic drive to UMNs, which occurs prior to measurable lower motor neuron involvement and is linked to anterograde transynaptic propagation of glutamatergic toxicity. TMS studies suggest inhibitory dysfunction is mediated by intra-cortical inhibitory interneurons, however the parameters of TMS are such that it is difficult to identify the specific neuronal populations associated with pathophysiology (Menon et al 2014). This is particularly evident when investigating complex inhibitory cortical circuits, as a diverse range of interneurons comprise these networks, making it difficult to differentiate between individual populations (Ziemann 2004). Hence, there is relatively little known about the underlying architecture that may initiate inhibitory dysfunction in ALS, in particular the specific inhibitory populations involved and therefore interneuronal networks implicated in disease. Adding to this, it is difficult to establish a time course of alteration in ALS with either functional imaging studies or post-mortem histopathological studies, as patients are typically followed from symptom onset due to a lack of early biomarkers (Turner et al 2013, Benatar et al 2016). Moreover, investigation of other neurodegenerative diseases and cognitive disorders suggest that not all interneuron populations are equally vulnerable in disease with specific inhibitory populations susceptible in key disease-affected regions and neuronal layers (Kowall et al 1987, Baglietto-Vargas et al 2010, Lewis et al 2012). Therefore, despite increasing evidence that interneurons are likely of central importance in ALS pathophysiology, it is poorly understood which interneuron populations are involved in disease, and the time frame of their alteration relative to symptom-onset and motor neuron deficits.

To address these gaps in our knowledge, this study aimed to determine the extent and timing of interneuron involvement in the cortex of the SOD1^{G93A} mouse model of ALS (Gurney et al 1994). The transgenic SOD1 mouse has a substitution of glycine by alanine at residue 93 and is the most widely studied model of ALS (Kaur et al 2016). These mice are phenotypically normal at birth,

but begin to develop MN dysfunction at 8 weeks of age that progresses from hindlimbs to forelimbs presenting as weakness, tremors, reduced extension reflex, total paralysis and finally death (Azzouz et al 1997, Bendotti & Carri 2004, Wooley et al 2005).

Traditionally this model has been used to investigate distal pathology, such as lower motor neuron dysfunction and loss (Gurney et al 1994, van Zundert et al 2008, Vinsant et al 2013, Delestree et al 2014), it is only in recent years that the potential contribution of cortical pathology has begun to be investigated (Ozdinler et al 2011, Jara et al 2014). Recent studies show that corticospinal motor neurons mirror some of the earliest signs of degeneration that occur in lower motor neurons (Pieri et al 2009), including early electrophysiological changes, dendritic regression and cell loss (Pieri et al 2003, Kuo et al 2004, Kuo et al 2005). Additionally, dysfunctional astrocytes, microglia and oligodendrocytes have been shown to contribute to disease progression and motor neuron degeneration in SOD1 mice (Clement et al 2003, Beers et al 2006, Boillee et al 2006a, Wang et al 2009, Lasiene & Yamanaka 2011, Nonneman et al 2014), increasing interest in the role of cortical neuronal and non-neuronal populations in these models (Boillee et al 2006a, Ilieva et al 2009).

Importantly, alongside evidence of early cortical motor dysfunction (Ozdinler et al 2011), there are reports of increased excitability of layer V pyramidal cells in the motor cortex (Fogarty et al 2015), which precede lower motor neuron symptoms (Vinsant et al 2013) and degeneration of cortico-spinal motor neuron pathways (Jara et al 2012). Furthermore, numerous studies have established hyperexcitability in this mouse model followed by hypoexcitability in a proportion of vulnerable motor neuron populations as the disease progresses (discussed in Chapter 1.1). However, the potential for an underlying interneuronal phenotype has not yet been fully explored in this ALS model. Therefore, the first aim of this thesis was to investigate a region-dependent vulnerability of specific interneuron populations in the cortex of the $SOD1^{G93A}$ mouse, and to investigate their fate at defined time points to establish a time course of disease-induced alteration. Immunohistochemical classification of interneurons is used to assess changes in numbers of key interneuron populations within the primary motor and secondary somatosensory cortices. Cell tracing software is used to assess changes in the morphology of key interneuron populations. The current investigation aims to determine the biological basis for inhibitory alteration in the $SOD1^{G93A}$ model to better understand the potential for therapeutic intervention aimed at the restoration of excitability in ALS.

2.2 METHODS

2.2.1 Animals

Male transgenic mice carrying a high copy number of the human SOD1^{G93A} mutation on the human SOD1 promoter (Gurney et al 1994) [strain 004435 B6.Cg-Tg(SOD1^{G93A})1Gur.J - backcrossed for more than 10 generations on a C57BL/6 background] [Jackson Laboratory (USA) (http://www.jax.org/strain/004435)], and their wild-type littermates, were used for histological analyses. Animals were housed in individually ventilated cages at 20^{o}C, on a 12 hour light-dark cycle, with access to food and water *ad libitum*. All procedures were approved by the Animal Ethics Committee of the University of Tasmania and conducted in accordance with the Australian Code of Practice for the Care and Use of Animals for Scientific Purposes, 2013.

2.2.2 Genotyping

Mice were genotyped at the time of weaning (28 days post-natal) using a clipping from the end portion of the tail, which was removed and stored at -20°C until DNA extraction was undertaken. DNA was extracted using an Extract-N-Amp Tissue PCR tissue kit (Sigma-Aldrich) according to the manufacturer's instructions and stored at -4°C. A multiplexed quantitative polymerase chain reaction was used to assess all mice for the presence of the SOD1^{G93A} transgene and copy number determined according to standard protocols (25 ± 2) (Leitner et al 2009).

Briefly, qPCR was performed as a 12.5µl reaction containing 50-100ng DNA (~1µl), 0.625µl ApoB F+R primer mix (500nmol, GeneWorks), 0.19µl SOD1 F+R primer mix (150nmol, GeneWorks), 1µl Tmol ApoB (0.15µmol, HEX TaqMan probe, GeneWorks), 1µl Tmol SOD1 (0.15µmol, 6-FAM TaqMan probe, GeneWorks), 6.25ul 2xSensiFAST SYBR no-ROX kit (Bioline, USA), 2.5µl milliQ water. The PCR amplification was carried out using the following primers: SOD1^{G93A} transgene forward, 5'-GGG AAG CTG TTG TCC CAA G-3'; SOD1 transgene reverse, 5'-CAA GGG GAG GTA AAA GAG AGC-3'; ApoB forward, 5'-CAC GTG GGC TCC AGC AT-3'; ApoB reverse, 5'-TCA CCA GTC ATT TCT GCC TTT G-3' under the following conditions: 95^{o}C for 5min, followed by 45 cycles of 95^{o}C for 15sec, 45 cycles of 60^{o}C for 15sec, 90sec preconditioning, 60-95^{o}C, 5sec per step, on a Rotor-Gene Q (Qiagen, Germany). The apolipoprotein B (*ApoB*) gene was used as an internal positive control.

2.2.3 Preparation of time-series cortical tissue from SOD1^{G93A} and WT mice

SOD1^{G93A} transgenic mice and age-matched wild-type controls were sacrificed from symptom onset in the *SOD1*^{G93A} mouse (Ozdinler et al 2011) and assessed at defined time points until end-stage in the disease course: 8 weeks (symptom-onset), 12 weeks, 16 weeks and 20 weeks of age (end-stage). The final time point was determined as an ethical stage preceding the 157-day typical life span in this *SOD1*^{G93A} mouse model (Wooley et al 2005), and the earliest time point investigated when distal pathology has been previously described in our laboratory (Clark et al 2016a). Mice were terminally anaesthetised (sodium pentobarbitone, 140mg/kg, i.p) and transcardially perfused with 4% paraformaldehyde (PFA; w/v) [(in 0.01M phosphate buffered saline (PBS)]. For each of the above time points, the cortex was obtained from six animals per genotype per time point. The brains were post-fixed in 4% PFA overnight at 4^{o}C, then stored at 4^{o}C in 0.01M PBS containing 0.1% w/v sodium azide (Sigma Aldrich, Australia).

Tissue processing. The brain was cut at Bregma -4.00mm, and the anterior portion cryoprotected with increasing concentrations sucrose (4%, 16%, 30%) dissolved in 0.01M PBS. Serial coronal cryostat sections (40μm) were generated using a Leica CM 1850 cryostat (Biosystems, Australia) and collected as free-floating sections into 24 well plates (Corning Life Sciences, USA) containing sodium azide, kept in sequential order and stored at 4^{o}C until processed for immunohistochemistry.

2.2.4 Immunolabeling for interneuron markers in SOD1^{G93A} and WT cortex

For analysis of cortical interneuron pathology, free-floating sections were processed using standard immunohistochemical methods (Blizzard et al 2016, Handley et al 2016). Cortical interneurons were identified by the expression of calcium binding proteins: calbindin (CB), calretinin (CR) and parvalbumin (PV), or by neuropeptides: neuropeptide Y (NPY), vasoactive intestinal peptide (VIP) and somatostatin (SOM)(Markram et al 2004). Every tenth serial sections (400μm apart) was incubated with antibodies recognizing cell-type specific interneuron markers diluted in 0.01M PBS containing 0.3% Triton-X-100 (see **Table 2.1** for antibody dilutions). Following washes (3 x 0.01M PBS, 10min) to remove excess unbound antibodies, sections were incubated with alexa-fluor conjugated secondary antibodies (1:1000, Thermo-Fisher Scientific, Australia) diluted in 0.01M PBS at room temperature for 2hrs, followed by DAPI staining (4',6-diamidino-2-phenylindole, 1/50000, Thermo-Fisher Scientific, Australia). After further washes (3 x 0.01M PBS, 10min), sections were mounted onto glass slides and coverslipped using fluorescent PermaFluor™ aqueous mounting medium (Thermo-Fisher Scientific Australia Pty Ltd, Australia).

Table 2.1. Primary Antibodies used for immunohistochemistry in mouse cortex

Antigen	Description of Immunogen	Source, Host Species, Cat#, Clone or Lot#, RRID	Concentration Used
Calbindin D-28k	Calcium-binding protein of the EF-hand family related to calmodulin and troponin-C	Millipore, rabbit polyclonal, Cat#AB1778 Lot# RRID:AB_2068336	1:1000µl
Calretinin	Calcium-binding protein of the EF-hand family related to calbindin D-28k and calmodulin	Swant, mouse monoclonal, Cat#6B3 Lot#010399 RRID:AB_1000330	1:1000µl
Parvalbumin	Calcium-binding protein of the EF-hand family related to calmodulin and troponin-C	Swant, mouse monoclonal, Cat#235 Lot#10-11 (F) RRID:AB_10000343	1:1000µl
Neuropeptide Y	Neuropeptide Y conjugated to bovine thyroglobulin (BTg) with glutaraldehyde	Immunostar, rabbit polycloncal, Cat#22940 Lot#1112001 RRID:AB_572253	1:500µl
Somatostatin	Synthetic peptide coupled to keyhole limpet hemocyanin (KLH) with carbodiimide (CDI) linker	Immunostar, rabbit polyclonal, Cat#20067 Lot#216002 RRID:AB_572264	1:1000µl
Vasoactive Intestinal Peptide	Porcine VIP coupled to bovine thyroglobulin (BTg) with carbodiimide (CDI) linker	Immunostar, rabbit polyclonal, Cat#20077 Lot#1339001 RRID:AB_572270	1:1000µl

Specificity of all antibodies was verified by incubating sections with the corresponding secondary antibody without pre-incubation of primary antibody.

2.2.5 Imaging and quantification

Immunofluorescence was captured using a Zeiss LSM 510 DuoScan confocal microscope (Carl Zeiss Microscopy, Germany), running Zen software (V3.2, 2008) equipped with Ar488 and HeNe543 lasers. Cell bodies were quantified blind to genotype in the supragranular (layers I-IV) and infragranular lamina (layers V-VI) of the primary motor and secondary somatosensory cortices (**Figure 2.1**), comparable coronal sections were selected from 1.18mm to -0.58mm relative to bregma. Sections 21-36 according to the Paxinos and Franklin Mouse Brain Atlas (Paxinos & Franklin 2007). A plan-apochromat 20x objective (N.A. 0.8, Zeiss) was used to generate z-plane images with 2μm intervals through 16μm of tissue depth. Primary motor and secondary somatosensory cortices were identified by anatomical landmarks referring to the appearance of the lateral ventricles, the shape of the third ventricle and the appearance of the anterior commissure and corpus callosum, as visualized with DAPI staining and according to the Allen Mouse Brain Atlas (© Allen Institute for Brain Science: http://mouse.brain-map.org) (**Figure 2.1**). Immunopositive neurons (cells with positive labeling in cell soma) were counted using Image J software (National Institutes of Health, USA) with the integrated Cell Counter plugin utilising Nissl staining to identify cortical layers. To compare densities of immunopositive neurons in $SOD1^{G93A}$ and wild-type mice, all neurons within the regions of interest (ROI) were manually marked, counted and the density calculated using the area of the ROI (values are given in cells/mm^2). The densities were then averaged across animals with 4 sections per cortical region per mouse included in analyses.

2.2.6 Morphological analyses

For analysis of neurite labelling patterns, 40μm coronal tissue sections were used to generate Z-stack images of neurons with 1μm intervals through 16μm of tissue depth within the motor cortex. Neurons with full arbours within z-stack were analysed using the cell tracing software Neurolucida™ (MBF Bioscience, USA) with the z-stack margins set to include one complete cell layer. For quantification of neurites immunoreactive for calretinin (CR), neurons were traced through stacks with processes marked, and images then exported to Neurolucida™ Explorer II (MBF Bioscience, USA). Branched structure analysis was used to analyse the number, area and

Figure 2.1. Representative images of sections used for quantitative analysis in WT and SOD1^{G93A} mice.

a, Coronal sections, each 40μm thick, from bregma 1.18 to -0.58 were used for quantitative analysis at four stages of disease progression in each cohort of mice. Arrows highlight anatomical landmarks used to identify primary motor (M1) and secondary somatosensory (S2) regions of interest in an example section used in the study (Interaural 4.06mm, Bregma 0.26mm), as identified in the Allen Mouse Brain Atlas and visualised by DAPI staining: namely the third (3V) and lateral ventricles (LV), shape and appearance of the corpus callosum (cc) and anterior commissure (aca). **b**, The motor cortex imaging site as validated in the Thy1-eYFP-H mouse, which has particularly prominent yellow fluorescent protein expression in large layer V corticospinal neurons (green) within the motor cortex[57,80]. **c**, A representative image of a calretinin (green), Nissl (red), DAPI (blue) cortical coronal section used for analyses. In each section, the motor (**i**) and somatosensory (**ii**) regions of interest (boxed areas enlarged to the right) were used for quantitative analyses, with cortical layers I-VI visualised by Nissl staining (**iii**).

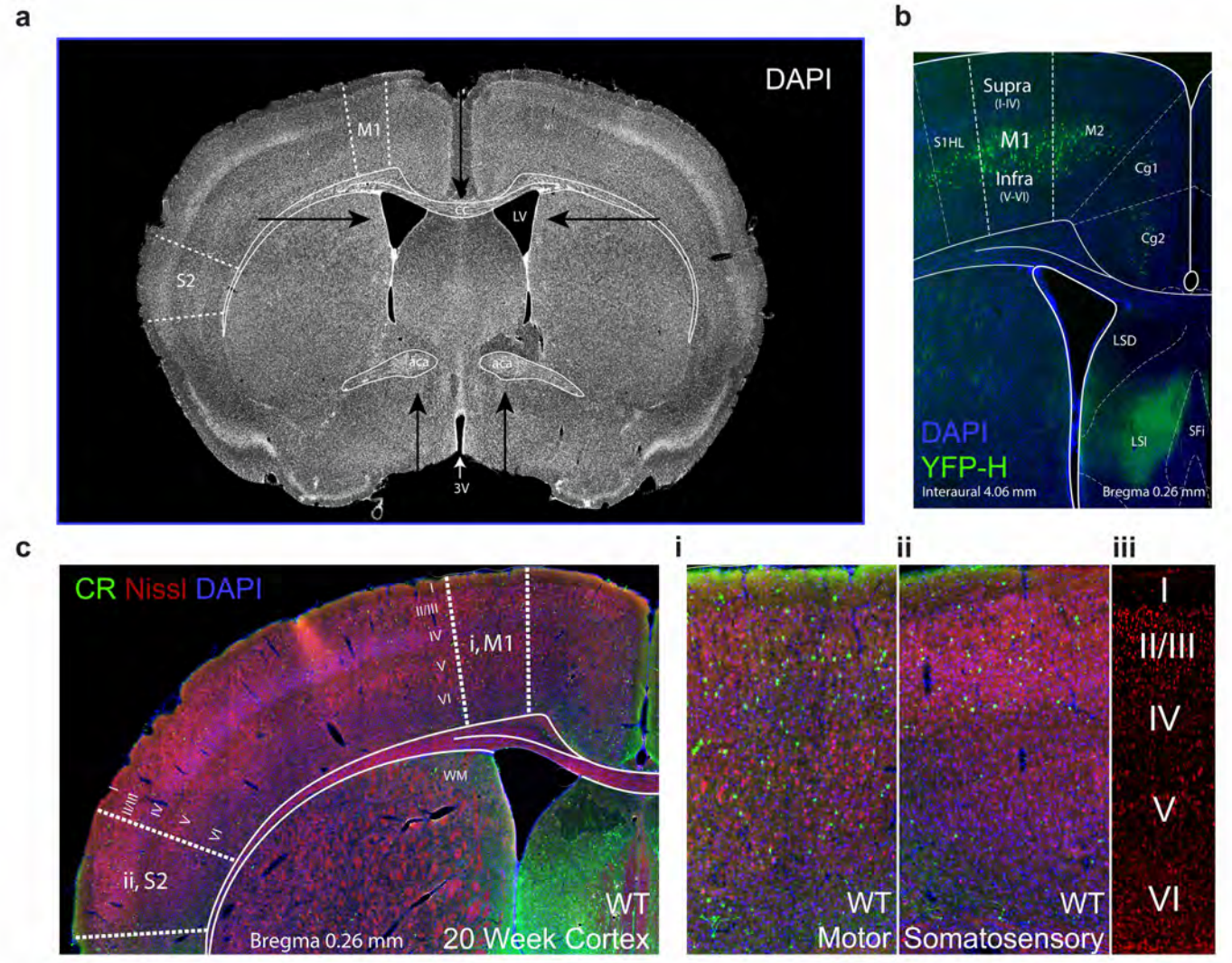
a
DAPI
M1
cc
LV
S2
aca
aca
3V
b
Supra
(I-IV)
S1HL
M1
M2
Infra
(V-VI)
Cg1
Cg2
LSD
DAPI
YFP-H
LSI
SFi
Interaural 4.06 mm
Bregma 0.26 mm
c
CR Nissl DAPI
I
II/III
IV
V
VI
i, M1
WM
ii, S2
WT
Bregma 0.26 mm
20 Week Cortex
i
ii
iii
WT
Motor
WT
Somatosensory
I
II/III
IV
V
VI

length of primary, secondary, tertiary and quaternary order neurite processes, encompassing both axons and dendrites, of CR-labelled neurons.

2.2.7 Statistical analyses

Neuronal density was analysed using a two-way analysis of variance followed by Bonferroni post hoc tests (GraphPad Prism, Version 6.0) for group and regional comparisons. Overall group differences (main effects of genotype) were identified using non-parametric two-tailed *t*-tests. To assess neuronal densities across the disease course, three-way analysis of variance was used for comparisons of group and cortical regions between different time points (SPSS, Version 20). All variables were tested for statistical interaction, with any significant interactions included in the model. Statistical significance was set at $P < 0.05$. Average values were expressed as means ± standard error of mean.

2.3 RESULTS

2.3.1 A subtype-specific interneuron alteration after symptom onset in the SOD1^{G93A} motor cortex

Within the cortex, inhibitory microcircuits are comprised of a wide variety of interneuron populations that target specific neuronal domains to facilitate the fine-tuning of cortical neuronal activity (Holt & Koch 1997, Silver 2010). These cell types are arranged in well-ordered wiring patterns that maintain the complex functions of cortical regions by their unique placement, connections and firing properties (Kubota 2014). Changes in specific interneuron populations are therefore likely to affect synaptic transmission in the motor cortex and compromise the regulation of network excitability, including motor output from layer V corticomotoneurons. To determine if specific interneuron populations were altered in the SOD1 cortex, we used immunohistochemistry to assess the potential for changes in the density of interneuron populations in the motor and somatosensory cortex of late-symptomatic (20 week) SOD1 mice, and in age and litter-matched wild type (WT) controls. Interneuron density was quantified (cells per mm^2) in both the supragranular and infragranular lamina of motor (Ms, Mi) and somatosensory cortices (Ss, Si) to determine if cell position in cortical regions influenced pathology (**Figure 2.1 a-c**). GABAergic interneuron subtypes were differentiated according to the selective expression of calcium binding proteins [calbindin (CB), calretinin (CR), parvalbumin (PV)] and neuropeptides [neuropeptide Y (NPY), somatostatin (SOM), vasoactive intestinal peptide (VIP)](Markram et al 2004) (**Figure 2.2 a-f**). Analysis revealed that of the interneuron populations expressing calcium-binding proteins, the density of CR-expressing neurons was significantly decreased in the supragranular lamina of the motor cortex (layers I-IV) (**Figure 2.2 g-h**). In this region, CR-neurons were reduced by up to 37% of WT controls (55 ± 6 p/mm^2 WT Ms, 35 ± 6 p/mm^2 SOD1^{G93A} Ms) ($P < 0.05$, two-way ANOVA, Bonferroni post-hoc) (**Figure 2.2 j**), while the density of this population remained unaltered in the infragranular motor cortex (32 ± 5 p/mm^2 WT Mi, 19 ± 1.9 p/mm^2 SOD1^{G93A} Mi), and unaltered in both lamina of the somatosensory cortex relative to WT controls (43 ± 6 p/mm^2 WT Ss, 44 ± 4 p/mm^2 SOD1^{G93A} Ss; 12 ± 1 p/mm^2 WT Si, 10 ± 1 p/mm^2 SOD1^{G93A} Si). No significant differences were detected in either of the other calcium binding populations, CB- or PV-expressing neurons in SOD1^{G93A} mice and WT controls (**Figure 2.2 i, k**).

In direct contrast, the density of NPY-expressing neurons was significantly increased by 29% in the supragranular motor cortex (41 ± 1 p/mm^2 WT Ms, 54 ± 2 p/mm^2 SOD1^{G93A} Ms) and by 30% in the infragranular motor cortex of SOD1^{G93A} mice compared with WT (35 ± 1 p/mm^2 WT Mi, 46

Figure 2.2. Calretinin and Neuropeptide Y interneuron subtypes are differentially altered in specific lamina of the SOD1^{G93A} motor cortex.

a-f, Calcium binding proteins and neuropeptides (green) were used to visualise specific interneuron populations in the cortex, showing labelling patterns of calbindin (CB; **a**), calretinin (CR; **b**), parvalbumin (PV; **c**) and neuropeptide Y (NPY; **d**), somatostatin (SOM; **e**) and vasoactive intestinal peptide (VIP; **f**) populations in 20 week WT cortex stained with DAPI (blue) and Nissl (red). The boxed areas (**a-f**) in the high magnification images show co-localisation of interneuron labels with Nissl stain. **g-h**, At 20 weeks, analysis of motor cortex, reveals the normal distribution of CR-expressing interneurons in WT motor cortex (**g**), but a striking reduction in particular in layers I-IV of SOD1^{G93A} motor cortex (**h**). Analysis of immunopositive neurons within the SOD1^{G93A} motor (M) and somatosensory (S) cortex showed that the density of calretinin-expressing interneurons was significantly decreased specifically within the supragranular (Ms, layers I-IV) lamina of the motor cortex (**j**) and the density of Neuropeptide Y-expressing interneurons was significantly increased in both the supragranular (Ms, layers I-IV) and infragranular lamina (Mi, layers V-VI) of the motor cortex (**l**) (*$P < 0.05$, two-way ANOVA, Bonferonni's multiple-comparison test). No other interneuron populations were significantly altered in either motor or somatosensory cortex (**i**, **k**, **m**, **n**). Values in graphs represent means ± SEM, n = 6 mice per group. Scale bar in (**a-f**) 20μm, (**g-h**) 100μm.

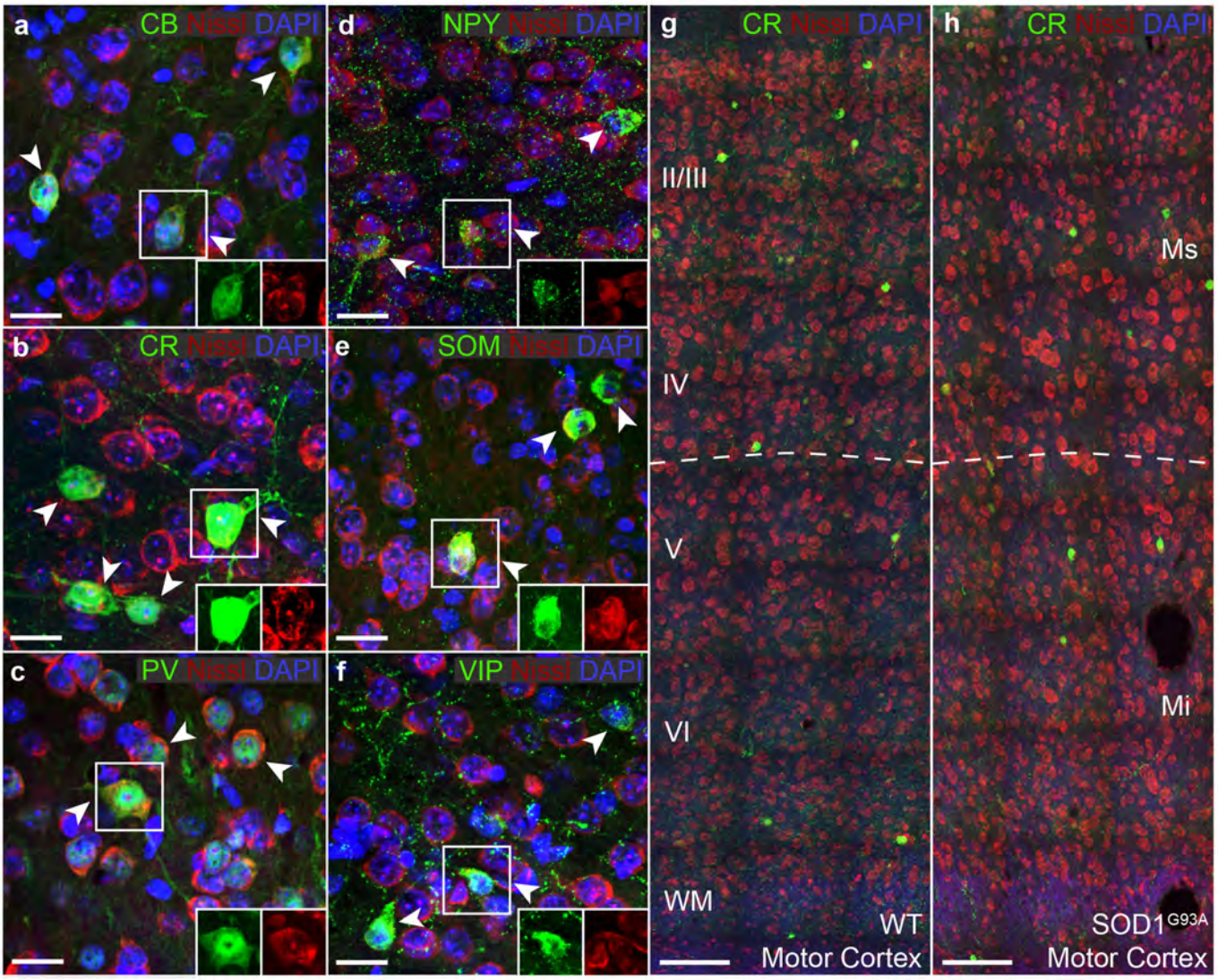
a CB Nissl DAPI
b CR Nissl DAPI
c PV Nissl DAPI
d NPY Nissl DAPI
e SOM Nissl DAPI
f VIP Nissl DAPI
g CR Nissl DAPI
h CR Nissl DAPI
II/III
IV
V
VI
WM
WT
Motor Cortex
Ms
Mi
SOD1G93A
Motor Cortex

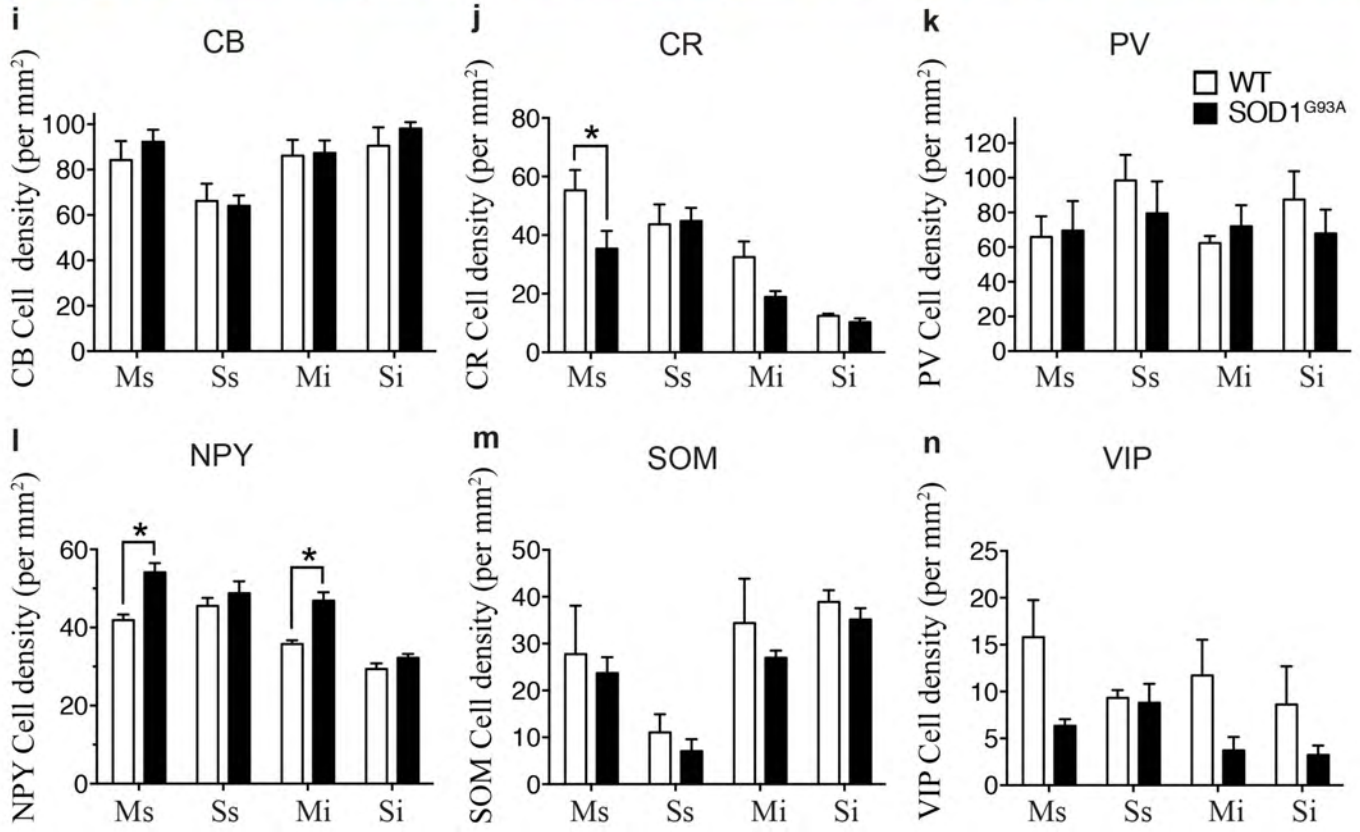
i
CB
CB Cell density (per mm2)
j
CR
CR Cell density (per mm2)
k
PV
PV Cell density (per mm2)
WT
SOD1G93A
l
NPY
NPY Cell density (per mm2)
m
SOM
SOM Cell density (per mm2)
n
VIP
VIP Cell density (per mm2)
Ms
Ss
Mi
Si
*

± 2 p/mm^2 SOD1^{G93A} Mi) ($P < 0.05$, two-way ANOVA, Bonferroni post-hoc) (**Figure 2.2 l**), an unexpected finding as interneurons in the cortex are generally not thought to undergo adult neurogenesis (Ernst & Frisen 2015). This suggests increased NPY density may more likely reflect increased expression of the NPY peptide on neurons. In the somatosensory cortex the density of NPY-neurons remained unchanged in both lamina (45 ± 2 p/mm^2 WT Ss, 48 ± 3 p/mm^2 SOD1^{G93A} Ss; 29 ± 1 p/mm^2 WT Si, 32 ± 1 p/mm^2 SOD1^{G93A} Si). Analysis of other neuropeptide expressing populations, SOM- and VIP-expressing neurons, identified no further differences in motor or somatosensory lamina compared to WT (**Figure 2.2 m, n**). These investigations demonstrate that at end-stage in the SOD1^{G93A} cortex, at a time of established cortical vulnerability in this ALS model (Jara et al 2012), distinct regions of the motor cortex undergo selective alteration involving the differential vulnerability of neurons expressing CR and NPY.

2.3.2 Contrasting and progressive alterations of NPY and CR populations throughout the SOD1^{G93A} time course

The early alteration of interneuron populations in the motor cortex could initiate a cascade of events resulting in an inability to maintain excitability in the cortex. In the TDP-43 model of ALS, SOM-expressing interneurons has been shown to initiate hyperexcitability in the motor cortex at an early disease stage (Zhang et al 2016). Therefore in this study the density of CR- and NPY-expressing populations was examined at earlier stages in the SOD1^{G93A} disease course: 8 weeks (from the earliest signs of symptoms in this model), 12 weeks and 16 weeks (Wooley et al 2005) (**Figure 2.3 a**). The mean density of CR-expressing neurons was decreased by 31% from (16 weeks) in the supragranular motor cortex of SOD1^{G93A} mice compared with WT (88 ± 13 p/mm^2 WT Ms, 60 ± 8 p/mm^2 SOD1^{G93A} Ms) ($P < 0.05$, two-way ANOVA, Bonferroni post-hoc) (**Figure 2.3 b**). This decrease was not significant in the infragranular lamina of the motor cortex (61 ± 8 p/mm^2 WT Ms, 46 ± 6 p/mm^2 SOD1^{G93A} Ms), and was not present in the somatosensory cortex (71 ± 12 p/mm^2 WT Ss, 48 ± 11 p/mm^2 SOD1^{G93A} Ss; 21 ± 9 p/mm^2 WT Si, 17 ± 2 p/mm^2 SOD1^{G93A} Si). The density of CR-expressing neurons remained unchanged relative to controls at earlier time points in the SOD1^{G93A} cortex at 8 and 12 weeks. This suggests either a loss of CR-expressing neurons, or a potential reduction in the expression levels of CR in this distinct interneuron population, occurs during the later symptomatic phase in this model and is restricted to the upper layers of the motor cortex.

Interestingly, in contrast to the end-stage increase in the density of NPY-expressing cells in the SOD1^{G93A} motor cortex (Fig. 2d), from symptom onset (8 weeks) the density of NPY-cells were

Figure 2.3. Calretinin-expressing interneurons are progressively lost during the symptomatic phase in the SOD1^{G93A} motor cortex.

a, CR-expressing interneurons were labelled throughout the SOD1^{G93A} disease course, showing neurons were present at comparable levels in SOD1^{G93A} and WT mice at 8 weeks (early symptom onset) and 12 weeks in motor (M) and somatosensory cortex (S). **b**, Analysis of 16 week symptomatic SOD1^{G93A} mice showed that CR-expressing interneurons were significantly decreased in the supragranular lamina of motor cortex (Ms, layers I-IV) compared to WT mice. CR-expressing interneurons were progressively reduced in the supragranular lamina of motor cortex (Ms, layers I-IV) in 20 week end-stage SOD1^{G93A} mice (arrow heads in **a**) (*$P < 0.05$, two-way ANOVA, Bonferonni's multiple-comparison test). Values in graphs represent means ± SEM, n = 6 mice per group. Scale bar in (**a**) 50μm.

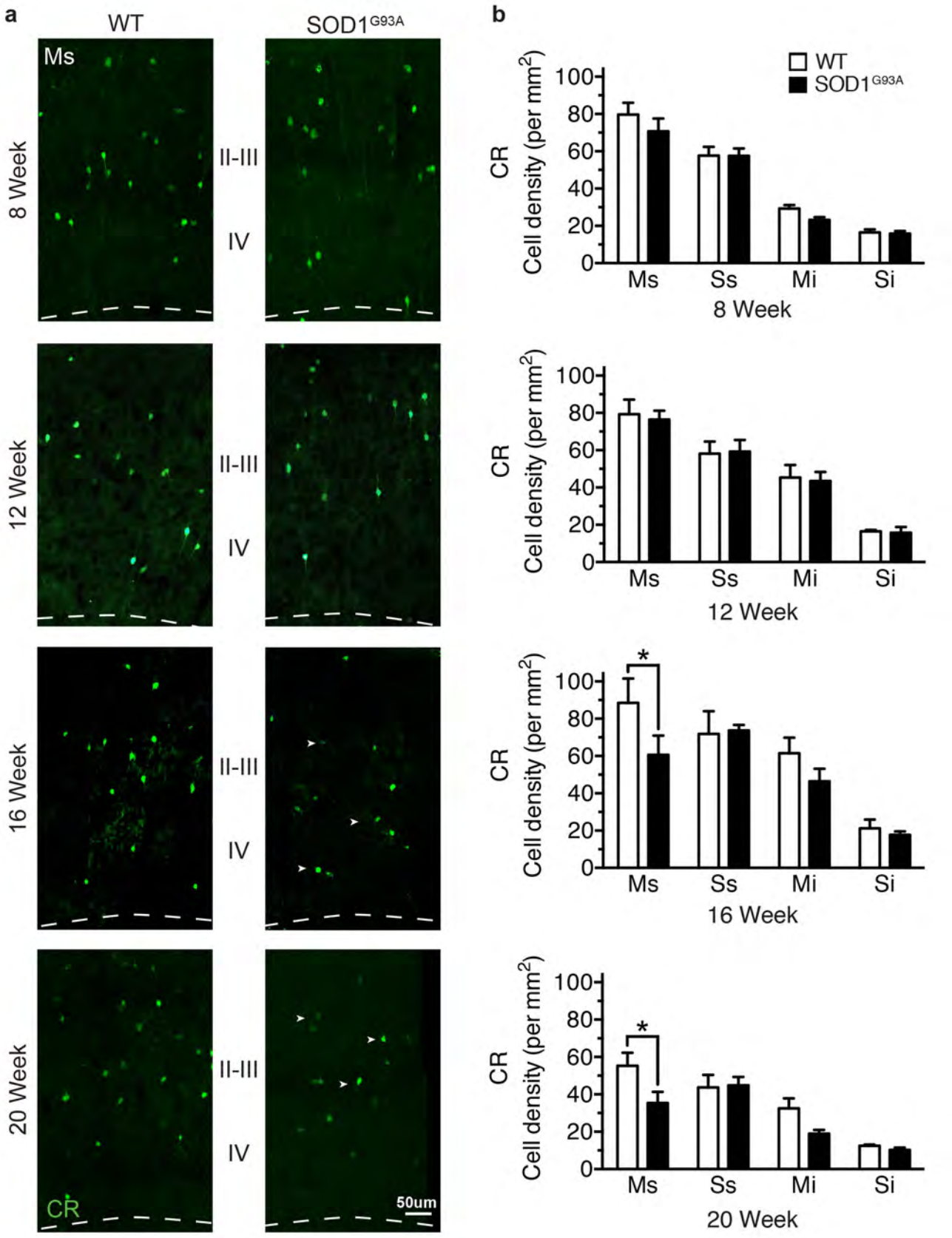
a
WT
SOD1G93A
Ms
8 Week
II-III
IV
12 Week
16 Week
20 Week
CR
50um
b
WT
SOD1G93A
CR
Cell density (per mm2)
100
80
60
40
20
0
Ms
Ss
Mi
Si
8 Week
12 Week
16 Week
20 Week
*

Figure 2.4. Neuropeptide Y populations are differentially altered from early symptom onset in the SOD1^{G93A} motor cortex.

a, NPY-expressing interneurons were labelled at different stages in the SOD1^{G93A} disease course: 8 weeks (early symptom onset), 12 weeks, 16 weeks and 20 weeks (end-stage). **b**, The mean density of NPY-expressing interneurons was significantly decreased in the supragranular lamina of the motor cortex (Ms, layers I-IV) in early symptomatic (8 week) SOD1^{G93A} mice compared to WT (arrow heads in **a**). NPY-expressing interneurons were present at comparable levels in SOD1^{G93A} and WT mice at 12 weeks and 16 weeks, with a late increase in cell density detected throughout the motor cortex at 20 weeks in end-stage SOD1^{G93A} mice (arrow heads in **a**). The somatosensory cortex showed no change in NPY-expressing interneurons at any stage of disease in supragranular (Ss, layers I-IV) or infragranular lamina (Si, layers V-VI) in SOD1^{G93A} and WT mice (*P < 0.05, two-way ANOVA, Bonferonni's multiple-comparison test). Values in graphs represent means ± SEM, n = 6 mice per group. Scale bar in (**a**) 100μm.

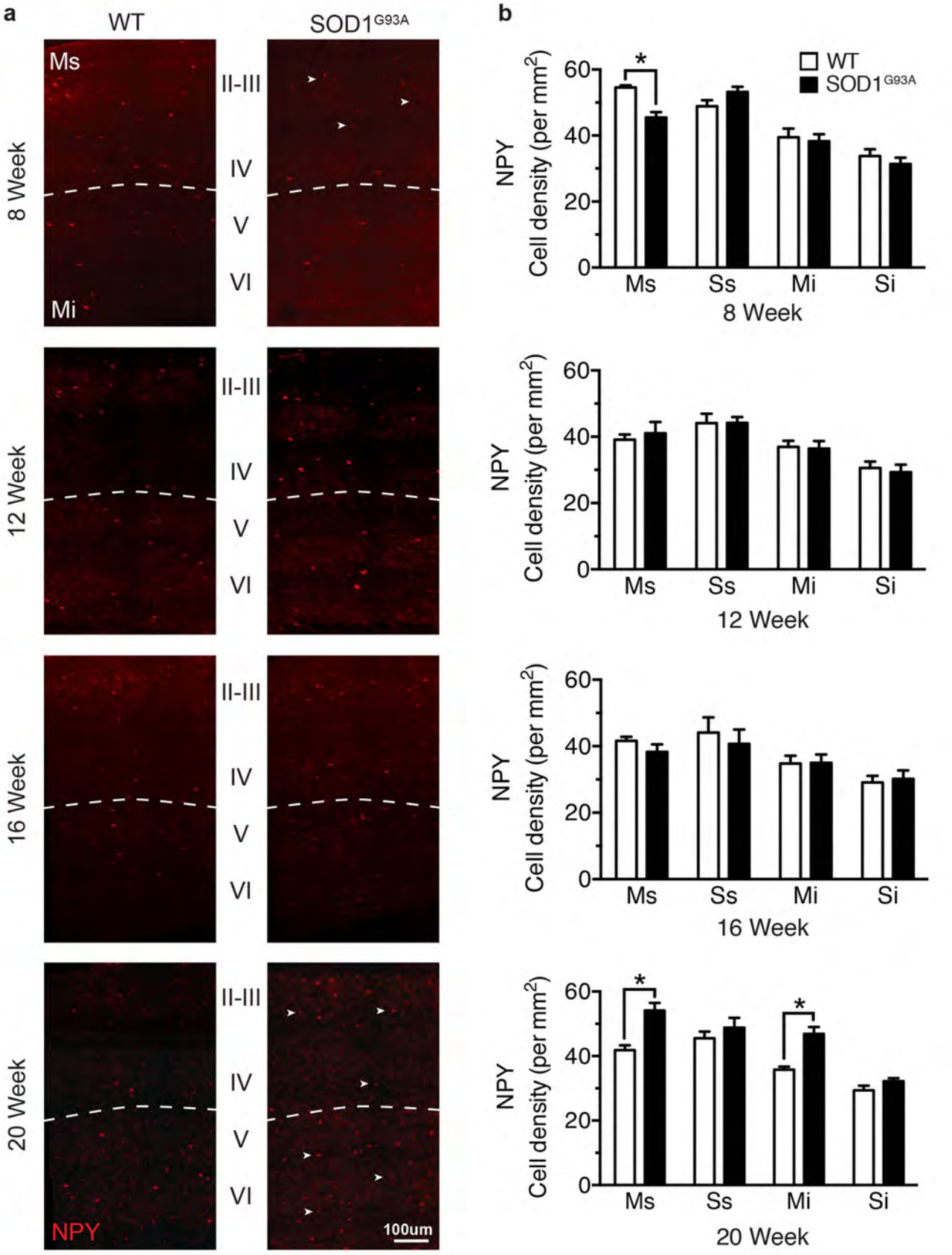
a
WT
SOD1G93A
Ms
Mi
8 Week
12 Week
16 Week
20 Week
II-III
IV
V
VI
NPY
100um
b
WT
SOD1G93A
NPY
Cell density (per mm2)
60
40
20
0
Ms
Ss
Mi
Si
8 Week
12 Week
16 Week
20 Week
*

significantly decreased by 17%, but only in the supragranular lamina of the SOD1^{G93A} motor cortex (55 ± 1 p/mm^2 WT Ms, 45 ± 2 p/mm^2 SOD1^{G93A} Ms) ($P < 0.05$, two-way ANOVA, Bonferroni post-hoc) (**Fig. 2.4 a-b**). The density of NPY-neurons remained unaltered in the infragranular lamina of the motor cortex (39.5 ± 3 p/mm^2 WT Ms, 38 ± 2 p/mm^2 SOD1^{G93A} Ms), and in other somatosensory regions relative to WT controls assessed at this 8 week time point (49 ± 2 p/mm^2 WT Ss, 53 ± 2 p/mm^2 SOD1^{G93A} Ss; 33 ± 2 p/mm^2 WT Si, 31 ± 2 p/mm^2 SOD1^{G93A} Si). Notably, the density of NPY-expressing neurons from SOD1^{G93A} mice were also unaltered in motor and somatosensory cortical regions investigated at 12 and 16 weeks relative to WT mice. These data suggest that changes to interneurons can occur early in the SOD1^{G93A} motor cortex, is progressive with CR-expressing neurons, and may alter over the disease course in relation to NPY-expressing neurons. This may indicate that the alteration of different classes of interneurons varies across the disease course and that interneuronal alterations are not a static phenomenon in the SOD1^{G93A} cortex. As an aside, it was also interesting to note that overall there were fewer cells counted in both the WT and SOD1^{G93A} mice with increasing age, most notable at the 20 week time point. However, this is consistent with developmentally programmed cell death of cortical interneurons that occurs with synaptic pruning in the neocortex of mice. By 18 weeks of age approximately 40% of neocortical interneurons undergo programmed cell death in the mouse neocortex (Southwell et al 2012), similar to the generalised decrease in density observed in the WT mice in this study.

2.3.3 Progressive CR-interneuron involvement in the supragranular SOD1^{G93A} motor cortex

A characteristic hallmark of neuronal degeneration is the alteration of neurite structure, which can precede overt changes in cell density, while augmenting connectivity patterns and the innervation field of neuronal populations (Kaas et al 1990, Darian-Smith & Gilbert 1994, Beirowski et al 2004, Lee et al 2008, Blizzard et al 2011). Due to the progressive nature of CR-neuronal alterations, CR-expressing interneurons were investigated to determine if they were abnormal in SOD1^{G93A} mice by examining branching patterns in 40µm coronal sections at two contrasting disease stages: an early symptomatic time point (8 weeks), prior to loss of CR-expressing neurons demonstrated at 16 weeks, and an end-stage time point, when CR-expressing interneuron loss had been established for a prolonged period in the SOD1^{G93A} disease course. Immunolabeling of the supragranular lamina of the motor cortex revealed extensive differences between CR-labelled neurites from end-stage (20 week) SOD1^{G93A} mice and WT controls. CR-neurons in WT tissue had well-developed and extensive neurite trees, whereas the same neurons in SOD1^{G93A} tissue exhibited a substantial reduction in neurite labelling (**Figure 2.5 b**). Quantification confirmed this

Figure 2.5. Calretinin-expressing neurites undergo progressive alterations in branching complexity from symptom onset in the supragranular SOD1^{G93A} motor cortex.

a-d, CR-labelled tissue sections were imaged and immunopositive neurons in the supragranular lamina assessed using cell tracing software to analyse neurite morphology (arrowheads, insets) at 8 weeks (**a**) and 20 weeks (**b**) in WT and *SOD1*^{G93A} tissue. The division of the neurite structure into primary, secondary, tertiary and quaternary order processes (as observed with CR-labelling) was used for all investigations. **c-d**, A proportional analysis was conducted to determine the extent of CR-labelled processes remaining on neurons in the supragranular motor cortex at both time points, showing a significant increase in neurons with no, or fewer, CR-labelled processes visible in early symptomatic (8 week) SOD1^{G93A} mice and in 20 week end-stage SOD1^{G93A} mice compared to WT. **e-h**, The mean branch length (**e-f**) and mean volume (**g-h**) of CR-labelled neurites were also assessed, demonstrating a pre-symptomatic increase in the length and volume of distal neurite processes in 8 week SOD1^{G93A} mice (**e**, **g**). Analysis of 20 week end-stage SOD1^{G93A} mice showed a significant reduction in the length and volume of CR-labelled processes compared to WT (**f**, **h**) (*$P < 0.05$, two-way ANOVA, Bonferonni's multiple-comparison test). Values in graphs represent means ± SEM, n = 6 mice per group. Scale bar in (**b**) 20μm.

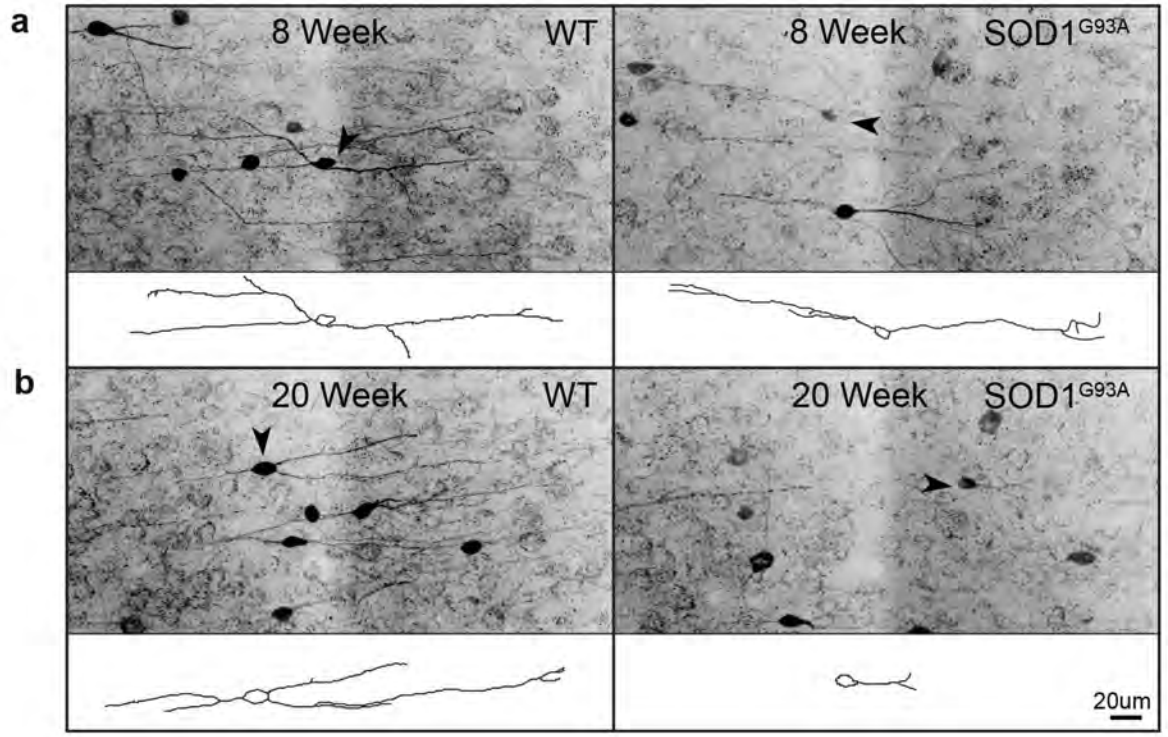
a
8 Week
WT
8 Week
SOD1G93A
b
20 Week
WT
20 Week
SOD1G93A
20um

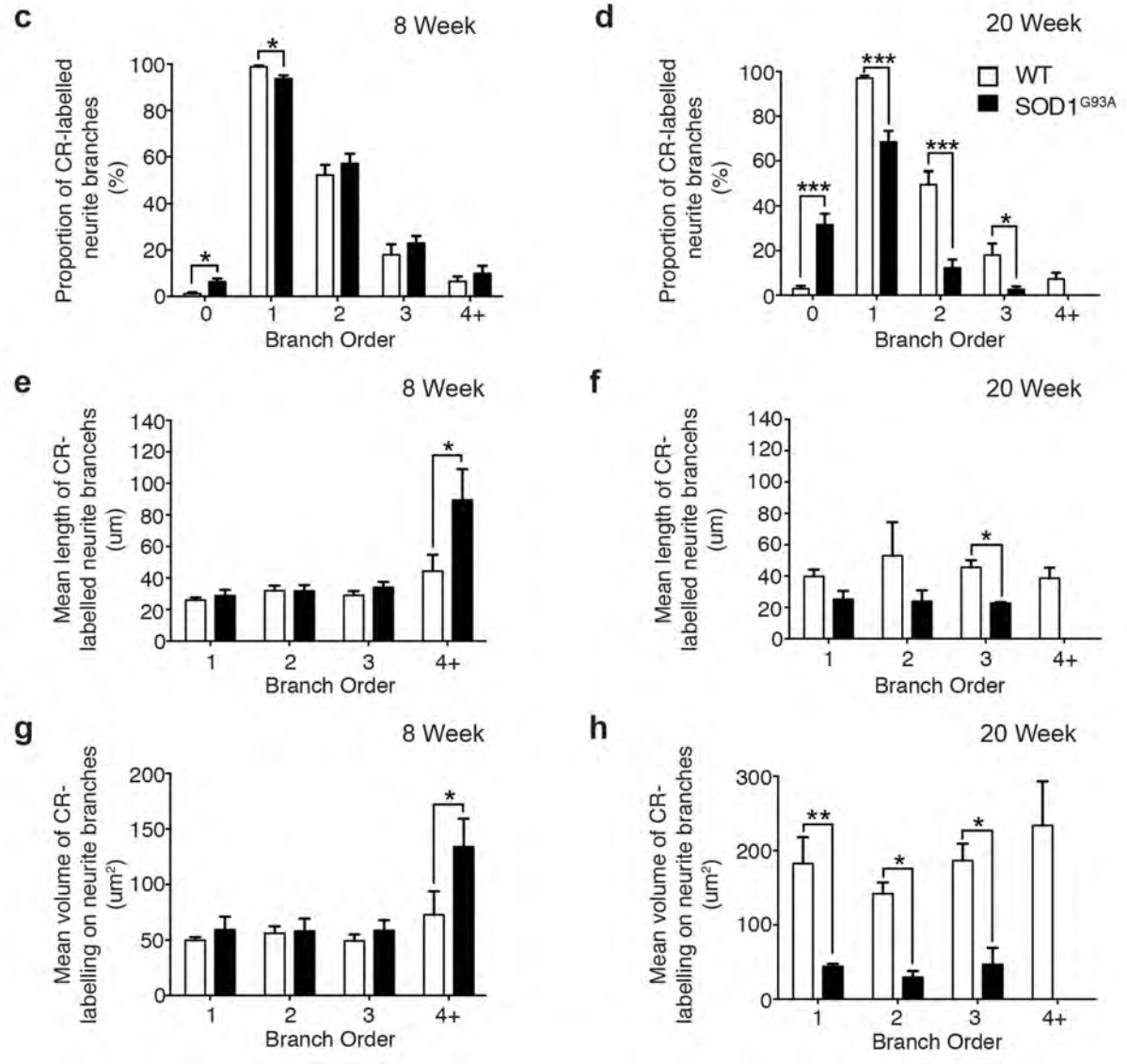
c
8 Week
Proportion of CR-labelled neurite branches (%)
Branch Order
d
20 Week
WT
SOD1G93A
Proportion of CR-labelled neurite branches (%)
Branch Order
e
8 Week
Mean length of CR-labelled neurite brancehs (um)
Branch Order
f
20 Week
Mean length of CR-labelled neurite brancehs (um)
Branch Order
g
8 Week
Mean volume of CR-labelling on neurite branches (um2)
Branch Order
h
20 Week
Mean volume of CR-labelling on neurite branches (um2)
Branch Order

observation, revealing a significant reduction in the proportion of CR-positive neurons with primary (~70%), secondary (~25%) and tertiary (~14%) order processes in the SOD1^{G93A} cortex compared with WT (Fig. 5d). This was accompanied by a nine-fold increase in the proportion of SOD1^{G93A} CR-neurons with no neurites visible (**Figure 2.5 d**). Likewise, the average length of tertiary order processes (~48%) (**Figure 2.5 f**) and the average area of primary (~75%), secondary (~79%) and tertiary (~75%) order processes (**Figure 2.5 h**) was significantly decreased in the SOD1^{G93A} motor cortex compared to WT. Overall group comparisons revealed that the SOD1^{G93A} genotype significantly reduced the average length (~38%) and volume (~78%) of all CR-labelled neurites, independent of branch order (**Figure 2.5 f, h**). These results demonstrate that at end-stage the remaining population of CR-expressing neurons have an irregular distribution of CR-immunoreactivity in their processes, which may translate into abnormal function in the motor cortex.

Next the CR-labelling patterns in early symptomatic tissue (at 8 weeks) were investigated to establish if alterations were present prior to loss of CR-expressing neurons. Cell tracing revealed a similar, although more subtle, pattern of alterations to SOD1^{G93A} CR-neurons at this time point (**Figure 2.5 a**). There was a significant reduction in the proportion of CR-expressing interneurons with primary neurites (~5%) and a small increase in cells with no processes visible (**Figure 2.5 c**). However, there was a trend towards a two-fold increase in the average length and area of neurites of CR-neurons in SOD1^{G93A} tissue, which was only significant in quaternary order processes (**Figure 2.5 e, g**). These results strongly suggest a potential involvement of CR-networks in relation to motor neuron circuitry defects previously observed in the motor cortex.

2.4 DISCUSSION

This current study sought to determine if there was cellular evidence indicating a loss of cortical inhibitory influence in the transgenic familial SOD1^{G93A} mouse model. It was hypothesised that specific interneuron populations would be altered in the motor cortex, with investigations performed to assess changes in cell density, distribution and morphology throughout cortical lamina at defined stages relative to disease progression. The interneuron pathology reported here strongly support a sequence of inhibitory alteration, which is restricted to the motor cortex, includes specific interneuron populations, and begins early in disease at a stage when, according to previous reports, corticospinal motor neurons are altered in the SOD1^{G93A} model (Jara et al 2012). Changes in CR- and NPY-expressing interneuron populations are evident from 8 weeks in the supragranular lamina of the motor cortex, progress to loss of CR-expressing neurons by 16 weeks, and include contrasting alterations of CR and NPY populations by end-stage disease at 20 weeks. The early involvement of both populations within the supragranular motor cortex indicates inhibitory cell deficits originate in the upper cortical layers (I-IV) of the motor cortex in the SOD1^{G93A} mouse model. A significant increase in the length of the most distal (terminal) CR-processes is also identified from 8 weeks, a number of weeks prior to their apparent loss at 16 weeks, and prior to a marked decrease in their process complexity by end-stage. While it remains unclear why interneurons are vulnerable to disease, it is likely that their involvement is related to motor-specific structural and functional alteration. The current discussion highlights the potential for CR and NPY interneuron populations to underlie dysfunction in the motor cortex, emphasising how contrasting changes may represent a convergence on excitability. The structural changes in the motor cortex are also discussed in relation to the current findings.

2.4.1 CR-interneurons and vulnerability to enhanced excitation

Cortical interneurons are essential for the regulation of normal excitability, but it is increasingly apparent that CR-interneurons in particular are susceptible to pathogenic changes in excitability. In this study CR-expressing interneurons had reduced density and showed morphological abnormalities in the SOD1^{G93A} mouse model. While it cannot be concluded if this represents loss of the protein or loss of the cell, there were changes consistent with altered network activity. In mouse models of epilepsy and in the epileptic human hippocampus increased excitability is accompanied by the loss of CR-containing interneurons and reorganisation of their neurites (Toth & Magloczky 2014). This is exemplified in the sclerotic hippocampus where the density of CR-immunopositive neurons is significantly decreased, while in non-sclerotic hippocampus CR-

interneurons are preserved (Toth et al 2010). When considered in the context of ALS, this may suggest a feedback mechanism whereby the loss of CR-interneurons translates to a loss of key excitatory neuronal populations, or vice verse. Additionally, it may suggest that reduced CR-populations are involved in a loss of circuitry control, resulting in the hyperexcitability observed in ALS, and epilepsy. As interneurons play such a critical role in the modulation of cortical circuitry (as discussed in section 1.2), a loss of interneuron populations can contribute to overstimulation of glutamate receptors via excessive release of glutamate, resulting in Ca^{2+} mediated neuronal injury and death (Zeman et al 1994). Hence, the finding of altered morphology as early as 8 weeks in this study raises the possibility that CR-interneurons may be involved in the initial alteration of the motor network. It remains to be determined if this is a developmental phenomenon or due to disease progression at this early symptomatic stage in the $SOD1^{G93A}$ mouse model.

2.4.2 The UMN circuit and CR-inhibitory networks in the $SOD1^{G93A}$ mouse

While the mechanism responsible for the observed interneuron deficits require further investigation, the timing of changes in the cortex correspond well with early changes in the corticospinal motor neurons in the $SOD1^{G93A}$ motor cortex. Results from this study indicate CR-interneuron networks are altered in the supragranular lamina of the motor cortex at 8 weeks. Within this region the majority of CR-interneurons reside within layer II/III, where they may directly synapse with apical processes from layer V corticospinal motor neurons and provide feedback or lateral inhibition (Cauli et al 2014). In $SOD1^{G93A}$ mice, it has been shown that at 8 weeks the apical dendrites of layer V motor neurons located within layer II/III are severely degenerated and have reduced spine density, while the basal motor neuron dendrites in layer V do not exhibit overt signs of degeneration (Jara et al 2012). This may suggest unique regional involvement of CR-neurons is initiated by, or responding to, alterations in spine density of the apical corticospinal motor neuron dendrites within layer II/III of the motor cortex. Therefore, the dendritic inhibition of pyramidal neurons may be less effective. In support of this, the apical dendritic spines of layer V projection neurons, typically receive excitatory inputs from thalamocortical neurons and from local layer II/III neurons (Brecht et al 2013), whereas basal spines preferentially receive inputs from distal sensory and motor nuclei (Hooks et al 2013). Recent works suggest corticospinal motor neuron spine loss can occur at 3 weeks in the $SOD1^{G93A}$ mouse model accompanied by increased functional excitatory synaptic activity onto layer V pyramidal neurons (Fogarty et al 2015). Hence mutant SOD1 may mediate increased excitability

through early changes to spine dynamics, leading to apical dendritic regression and inhibitory neuronal alteration; however, aberrant inhibition may also have the capacity to initiate pathology.

2.4.3 An initial vulnerability of CR-inhibitory networks in the SOD1^{G93A} mouse

It is increasingly recognised that the development of CR-interneurons is an activity dependent process and alterations in excitability can affect their morphology. In particular, the length of axonal arbours on both multipolar and bipolar populations is directly influenced by aberrant excitability during development (De Marco Garcia et al 2011). This raises the possibility that abnormal excitability may initiate abnormal maturation of the CR-interneuron innervation field. Furthermore, CR-interneurons are a unique inhibitory population in the cortical circuit, as they preferentially regulate the activity of other GABAergic inhibitory populations, and subsequently the actions of principal neurons via disinhibition (Gulyas et al 1996, Barinka & Druga 2010). In this manner, not only may CR-interneurons be more susceptible to early alterations in excitability, but they also have the ability to potentiate a wide reaching inhibitory and excitatory circuit dysfunction, due to their distinctive connectivity patterns and continual alteration throughout disease. The major excitatory input to corticospinal motor neurons is a pathway from layer II/III to layer V (Thomson & Lamy 2007); hence interneurons located within layer II/III may disproportionately influence corticospinal motor neuron activity via disynaptic feedforward inhibition (Cauli et al 2014). Indeed, the contrasting and somewhat unexpected involvement of NPY-interneurons may also support a continuum of pathogenic alterations triggered by altered excitability.

2.4.4 The contrasting alteration of NPY

As a loss of inhibitory influence is theorised in ALS, the finding of increased NPY-interneuron density at end-stage was an unexpected finding. A potential cause of this may be due to the effect of the SOD1^{G93A} mutation on cortical thickness, driving alterations at different rates across the time course. However, this is not expected to be the case as other interneuron populations are not similarly affected. Another more plausible scenario for this observation may include the role of NPY as an endogenous neuroprotective compound in the context of increased excitability. Neuropeptides are preferentially released during sustained neuronal stimulation (Drexel et al 2012), and are thought to protect neurons against increased pathogenic cortical activity (Tallent & Siggins 1999, Vezzani & Hoyer 1999, Tallent & Qiu 2008, Kovac & Walker 2013). Extensive literature from the epilepsy field supports a neuroprotective role for NPY as an endogenous anti-epileptic (Kovac & Walker 2013). Mice lacking NPY are more susceptible to spontaneous and

pharmacologically induced seizures, which can be reversed by intracerebral administration of NPY (Erickson et al 1996, Baraban et al 1997). As it is generally thought that interneurons in the adult cortex do not undergo neurogenesis (Ernst & Frisen 2015), this indicates that the increased NPY density observed in this study more likely reflects up-regulation and increased expression of the peptide on existing neurons in the cortex that may not typically express this peptide under normal physiological circumstances. Indeed, increased synthesis and release of NPY has been reported following seizure activity (Vezzani & Sperk 2004, Kharlamov et al 2007) and increased the density of interneurons expressing NPY are described following excitotoxin treatment (Bouilleret et al 2000). This indicates increased NPY expression by interneuron populations may be an advantageous intrinsic mechanism to counteract increased activity of cortical excitatory neurons, potentially up-regulating NPY expression on a greater proportion of neuron populations. Therefore, our finding of increased density of NPY-immunoreactive neurons at end-stage may be a direct consequence of increased activity in the motor cortex.

In line with this, it is quite interesting that the increased density of NPY populations was first restricted to the upper cortical layers of the motor cortex, where CR-populations are predominately altered, but by end-stage these NPY alterations were widespread throughout the entire motor cortex. This may suggest initial inhibitory deficits cause a localised change in excitability within the motor cortex, which spreads, resulting in increased NPY-immunoreactivity throughout the major excitatory pathways within the diseased motor cortex. In the context of our early results, this may suggest a late stage compensatory mechanism whereby NPY expression is upregulated to dampen the effects of altered excitability in motor circuitry. However, as this study demonstrates decreased density of NPY-interneurons at 8 weeks, excitability in the motor cortex may fluctuate throughout the disease course. In this respect, it is also interesting to note that both SOD1 and TDP-43 ALS models demonstrate the increasing involvement of neuropeptide systems, as somatostatin-interneuron density is reported to increase by late stages in TDP-43 mice (Zhang et al 2016). This is particularly important because it shows that not all interneuron populations may be involved in a similar manner in the disease, and the targeting of inhibitory populations for the restoration of normal excitability in the ALS cortex might best be considered in a subpopulation specific paradigm. It will be interesting and important to identify whether other genetic variants of the disease have a similarly distinct yet divergent interneuronal phenotype.

2.4.5 Conclusion

While the role of the cortex in motor neuron circuitry is only just beginning to be elucidated, it is apparent that in the $SOD1^{G93A}$ mouse specific inhibitory populations may have an underappreciated role in the disease. This study clearly demonstrates a novel timeline of interneuron involvement in the $SOD1^{G93A}$ motor cortex. This included the specific change of NPY- and CR-expressing interneuron populations. Changes originate in the upper cortical layers of the motor cortex from early symptom onset, and progress to involve the entire motor cortex by end-stage disease. It is important to note this study primarily uses immunohistochemistry to investigate interneuron populations; hence it remains to be determined how interneuron alterations functionally influence the disease, whether pathology is primary or secondary to excitability, due to a developmental phenomenon or disease progression and protective or pathogenic in the context of the disease. Nonetheless, these findings suggest that inhibitory involvement may not be a static phenomenon, but instead involves dynamic changes throughout disease.

Chapter 3

3 DIFFERENTIAL INTERNEURON PATHOLOGY IS A FEATURE OF THE HUMAN ALS MOTOR CORTEX

3.1 INTRODUCTION

It is important for pre-clinical insights gained from mouse models to be cross-validated in human disease, particularly as the major weakness of using animal models for ALS has been a failure to predict responses in humans and the subsequent failure to translate potential drug candidates into effective therapeutics (DiBernardo & Cudkowicz 2006, Ittner et al 2015, Justice & Dhillon 2016). Although fragmentary evidence of cortical interneuron involvement has been provided by previous human immunohistochemical studies (Ince et al 1993, Nihei et al 1993, Maekawa et al 2004), the current pilot study aimed to investigate interneurons in the ALS motor cortex to primarily establish the validity of findings from the $SOD1^{G93A}$ mouse model. It was hypothesised that specific interneuron populations affected in the $SOD1^{G93A}$ mouse would also be affected in ALS patients and associate with the extent of cortical pathology. This was reasoned as post-mortem neuropathology studies have shown reduced expression of $GABA_A$ receptor expression in the motor cortex of patients (Petri et al 2003) and both magnetic resonance spectroscopy imaging (MRSI) and positron emission tomography (PET) studies provide additional evidence for an early and diffuse loss of inhibitory cortical interneurons in the motor cortex. Moreover, the main inhibitory neurotransmitter, GABA, is reduced in the motor cortex of ALS patients (Foerster et al 2012) and PET scans reveal reduced binding of the GABA receptor ligand, flumazenil, in the motor cortex of sporadic ALS patients (Lloyd et al 2000), consistent with a loss of inhibitory interneurons. Longitudinal functional neuroimaging studies also suggest there is an initial phase of reduced intracortical inhibition, before loss of upper motor neurons (Mohammadi et al 2011), indicating inhibitory dysfunction may have an important role in motor neuron decline.

However, clinical and pathological heterogeneity may also be an important factor in the failure of drug studies to date and there is an emerging research priority to establish methods capable of stratifying patients clinically (Turner et al 2009, Marin et al 2016, Zach et al 2016). This is exemplified by recent attempts to map the onset and spread of disease pathology throughout different brain regions (Brettschneider et al 2013, Fatima et al 2015), and to differentiate ALS from FTD variants using neuropathological grading (Tan et al 2015), with both strategies based on the prevalence of TDP-43 pathology. Notably, the study by Bretteschneider and colleagues indicated that while pathology extends to prefrontal, temporal and hippocampal regions with disease progression, lesions may first develop in the motor cortex, brainstem motor nuclei and spinal cord α-motor

neurons. Hence, considerable efforts remain focused on determining the pathological basis of vulnerability in motor regions, particularly as elucidation of disease mechanisms that occur early in disease would be more beneficial for targeting therapeutics. Interestingly, clinical studies indicate that intracortical inhibitory involvement may act as an early determinant of disease progression in ALS cases (Menon et al 2014).

It is widely acknowledged that there is considerable clinical variation in the rate of disease progression in ALS, particularly as approximately 10% of all cases survive beyond 10 years of symptom onset (Chio et al 2011, Talbot 2014). Hence, it is notable that familial SOD1 mutation carriers with preserved intracortical inhibitory circuitry have a slower disease progression (Weber et al 2000), surviving an average of 13 years compared to three in sporadic patients (Andersen et al 1996, Turner et al 2005). Conversely, but complimentary, *in vivo* clinical imaging studies have shown that sporadic ALS patients with greater intracortical inhibitory dysfunction have a more rapid clinical decline and shorter disease duration (Shibuya et al 2016). These studies not only support a role for interneurons in pathogenesis, but also indicate that preservation of inhibitory circuit function may be a viable therapeutic option to slow the rate of disease progression in patients. Hence, there is a need to better understand the cellular basis of inhibitory involvement, as ultimately the group of cells affected may define the disease.

This study aimed to not only determine the validity of findings from the $SOD1^{G93A}$ model in Chapter 2, but also to extend upon our earlier work by determining the relationship of interneuron pathology with clinical profiles of patients and the pattern of interneuron involvement with pyramidal neuron loss, since this may be relevant to our understanding of the mechanisms of cell death. This pilot study was performed in a small case group with immunohistochemistry utilised in post-mortem ALS cases and control subjects to determine if end-stage pathology in the $SOD1^{G93A}$ motor cortex was also present in the ALS motor cortex, and consequently establish the validity of an underlying CR- and NPY-interneuronal phenotype in patients. To assess pyramidal pathology in ALS cases, labeling was performed against the non-phosphorylated epitope in neurofilament H using the antibody SMI32 as it preferentially binds to both pyramidal and motor neurons (Morrison et al 1987, Del Rio & DeFelipe 1994, Dzaja et al 2014).

3.2 METHODS

3.2.1 Human tissue

All cases were provided by the Victorian Brain Bank Network Australia. Informed consent for the collection of material was obtained prior to death and tissue use was approved by the University of Tasmania Human Ethics Committee and complies with the guidelines of the National Health and Medical Research Council (Permit #H0016154). All material had been previously de-identified. Blocks of primary motor cortex were provided as 10% formalin fixed blocks with post-mortem intervals ranging from 7-45 hours. Neuropathologist Professor Catriona McLean performed gross dissection. Human tissue was obtained from six patients with clinically defined ALS (age 68.81 ± 6.3 years, M = 4, F =2) and six age-matched controls without neurological symptoms (age 66.16 ± 8.5 years, M = 4, F = 2). See **Table 3.1** for case characteristics.

3.2.2 Histology and Immunoperoxidase labelling of postmortem human brain tissue

Forty micrometre thick cryostat sections were cut from frozen (-14^{o}C) optimal cutting compound-embedded blocks of postmortem human brain tissue (Leica CM 1850 cryostat), previously cryoprotected by sequential exposure to increasing concentrations of PBS/Sucrose (4%, 16%, 30%). Sections were stored at 4^{o}C in 0.01M PBS containing 0.1% w/v sodium azide (Sigma Aldrich, Australia) and prior to immunostaining were washed in 0.01M PBS (3 x 10 min). Human tissue was processed as free-floating sections using the immunoperoxidase method, with 3,3'-diaminobenzidine tetrahydrochloride (DAB) as the chromagen. Endogenous peroxidase activity was quenched with 0.3% hydrogen peroxide (H_2O_2) in methanol for 20 min to reduce background staining. Phosphate-buffered saline was used to all washes (3 x 10 min between each serum). Non-specific immunoglobulin (IgG) binding of the tissue was blocked by 3% normal horse serum in phosphate-buffered saline for 30 min. Primary antibodies were diluted in 0.6% Triton X-100 at room temperature with gentle agitation for 24 hrs (Calretinin, 1:500, Swant; Calbindin, 1:500, Millipore; Neuropeptide Y, 1:500, Abcam; SMI32, 1:500, Bioscience). For visualization of immunopositive elements, sections were incubated with either biotinylated secondary antibodies (goat anti-rabbit or anti-mouse IgG, Vector, 1:200) for 90 min, followed by avidin-biotinylated horseradish peroxidase complex (1:250, Vector, 45 min), or where appropriate, the peroxidase-polymer-based method with an HRP labelled polymer directly conjugated to the secondary antibody (goat anti-rabbit-IgG-HRP or anti-mouse-IgG-HRP, EnVision+ System, DAKO). The polymer-peroxidase system does not contain avidin or biotin, eliminating non-specific staining

Table 3.1. Human brain cases utilised for immunohistochemistry and analysis

Type	Age	Gender	Cortical Region	PMI	Site of onset	Duration	Family History
Control							
1	73.7	F	MC	26.5			
2	52.1	M	MC	33			
3	75.9	M	MC	50			
4	63.9	M	MC	68			
5	67.3	F	MC	24			
6	64.1	M	MC	24			
ALS							
7	74.4	F	MC	7	Left leg, arm & bulbar	~ 3.16	Unknown
8	62	M	MC	12.5	Right leg	~ 4.75	Unknown
9	78.1	M	MC	13.5	Bulbar (speech)	~ 3.5	Unknown
10	63.9	M	MC	14	Global (lumbar)	~ 2	Unknown
11	69.3	F	MC	45	Right leg	~ 3	Strong
12	65.2	M	MC	13.5	UMN involvement	~ 3	Unknown

Post mortem interval (hours), age of death and sex is noted for all cases. Where applicable MND disease duration (years), site of onset and family history is noted. MC, Motor cortex.

resulting from endogenous avidin-biotin. All sections were developed with DAB as the chromogen (Peroxidase substrate kit, Vector) until adequate staining had been achieved.

Sections were counterstained with haematoxylin (Peters 2010) to visualize cell nuclei, cell layers and the gray/white matter border within cortical regions. Briefly, sections were mounted on electrostatically charged slides (Flex, IHC microscope slides, Dako), stained with Mayer's haematoxylin (30 sec), washed in running tap water (5 min), blued in ammoniated water (30 sec) and washed in running water (5 min). Sections were then dehydrated through graded ethanol (75% EtOH, 95% EtOH, 1x2 min; 100% EtOH, 2x2 min) cleared in xylene (3x2 min) and mounted in DPX (Koch-light Lab Ltd, England). No primary and secondary antibody controls were processed in vehicle solutions to control for non-specific labelling and residual endogenous peroxidase activity.

3.2.3 Double immunolabelling for calretinin/SMI32

The protocol was similar to that described above for single immunostaining. After blocking the endogenous peroxidase activity with 0.3% H_2O_2 and the non-specific IgG binding with 3% normal horse serum, the sections were first incubated in primary antibody against calretinin (1:500, SWANT) for 24 hours at room temperature. Sections were incubated in EnVision-HRP secondary antibodies (goat anti-rabbit-IgG-HRP, EnVision, DAKO). In this case, calretinin was developed using DAB as a chromogen intensified with ammonium nickel-sulphate and cobalt chloride (0.1g in 10ml H_20) (DAB-Ni-$CoCl_2$, blue/black reaction product) (Hsu & Soban 1982). After the first immunostaining, the sections were washed extensively in phosphate-buffered saline and re-blocked for residual peroxidase activity and non-specific binding. The sections were then incubated in monoclonal mouse anti-SMI32 (1:500, Covance) for 24 hours at room temperature. After incubation in the HRP anti-mouse IgG secondary the second immunoperoxidase reaction was developed with DAB as the chromogen (brown reaction product). Sections were then dehydrated, cleared and mounted in DPX, as above. The immunopositive profiles at the light microscopic level were identified by their colour difference (i.e. calretinin-positive profiles were blue/black; the SMI32-positives were brown).

3.2.4 Imaging and Quantification

For quantitative purposes, all haematoxylin and immunostained DAB sections were analysed at the light microscopy level using an integrated stereology-brightfield system. Sampling was done using the Olympus BX-53 photomicroscope equipped with a Ludl X,Y motorized stage driven by

ProScan™III H31 controller (Prior Scientific, USA). The Visiopharm Integrator System 4.5.6.440 (Visiopharm, Hoersholm, Denmark) was used to quantify the density of DAB labelled cells in the primary motor cortex using the physical dissector technique (Foster et al 2014). Contours were drawn to delineate the gray matter (layers I-VI) from the white matter as visualized with haematoxylin staining. Counting was performed using a 20x objective (N.A. 0.75) and a counting frame 200 x 200 μm was systematically moved through all counting areas until the entire delineated area was sampled. Identical quantification parameters were used in all sampling. For each individual case and control, three representative sections were counted per cortical region and numbers used to generate an average value. Six ALS cases and controls were used for each analysis where possible. However, due to limited tissue availability, one ALS case was excluded from the Calbindin interneuron analysis. Data is reported as number of cells per mm^2. All cell counts were performed blinded to case status. Representative images were captured using a Zeiss LAB.A1 microscope with a 63x (N.A. 0.85), 40x (N.A. 0.65), 20x (N.A. 0.45) and 10x (N.A. 0.25) objective using Zen 2 software (Zeiss, Germany) and the digital AxioCam ICc 5 camera (Zeiss, Germany). Photomicrographs were processed using Adobe Photoshop CS6 (Version 13.0, USA).

3.2.5 Statistical analysis

Data was analysed using one-way ANOVA and using non-parametric two-tailed Students *t* tests. Statistical significance was set at $P < 0.05$. Average values were expressed as means ± standard error of mean. To examine individual-level relationships between the cell densities of neuronal populations assessed, a non-parametric Pearson's correlation r^2 was reported. Multiple regression analysis was used to determine if ALS case characteristics were predictors of neuronal densities (SPSS, Version 20). For comparisons of clustering between ALS cases and controls, cluster analysis (k-means) was performed (SPSS) with cluster number cross-validated with the Hierarchical Cluster Ward's method (Ward 1963, Kaufman & Rousseeuw 1990).

3.3 RESULTS

3.3.1 Optimisation of neuron labelling in post-mortem human tissue sections

Immunohistochemical labelling of human tissue was conducted using an immunoperoxidase-enzyme linked detection method. While immuno-fluorescence produced a high signal to noise ratio in mouse cortical sections, in human tissue labelling appeared indistinct and there was a high level of background. This was primarily due to autofluorescence caused by formalin fixation of human tissue and age-related pigment lipofuscin, which masks the primary signal (**Figure 3.1 a**). As a result, a light based immunoperoxidase detection method was used for all neuron labeling as it produces a coloured precipitate, that could be visualised by a light microscope, thus avoiding the non-specific signal that is otherwise detected using fluorescent microscopy (**Figure 3.1 b**). The optimal immunolabeling conditions were determined by trialing different primary antibody incubation times, different temperatures of incubations and by serial dilutions of primary antibody concentrations. After adequate labeling was established, the coloured chromagen precipitate was optimised to ensure a distinct and clear signal could be captured with the light microscope (**Figure 3.1 c**). A brown DAB precipitate was used for single labeling experiments and the chromagen developed to allow sufficient contrast with the blue haematoxylin nuclei staining (**Figure 3.1 d**). For double labeling experiments both DAB-Nickel (black) (**Figure 3.1 e**) and DAB-Nickel-Cobalt-Chloride (blue) were trialed against DAB. The blue DAB-Nickel-Cobalt-Chloride was chosen for double labelling as it produced a clear, distinct and less saturated signal that could be co-localised with DAB (**Figure 3.1 f**). To determine if endogenous immunoperoxidase activity was adequately quenched, and labeling observed was only due to binding of the secondary antibody, no primary and no secondary controls were performed (**Figure 3.1 g-h**).

3.3.2 Calretinin-immunoreactive neurons are reduced in the ALS patient motor cortex

To investigate whether, the interneuron phenotype we observed in the $SOD1^{G93A}$ mouse model of ALS reflects interneuron vulnerability relevant to human disease, we immunolabeled sections from the motor cortex of ALS patients and age-matched controls. In control tissue, CR-expressing neurons were small- and medium-sized aspiny bipolar cells with clear processes visible (**Figure 3.2 a, c**). In contrast, examination of the ALS motor cortex showed fewer CR-expressing cells in layers II-III and labelled processes appeared blebbed and beaded (**Figure 3.2 b, d**). Quantitation confirmed this observation, revealing a significant decrease in the density of CR-expressing interneurons in a subset of ALS cases in layer II-III of the motor cortex (**Figure 3.2 e**). Hierarchical cluster analysis demonstrated the presence of two distinct clusters of ALS cases when

Figure 3.1. Optimisation of human tissue labelling

a-c, Representative images of interneuron labelling in post-mortem cortical sections from human tissue. **a**, Immunohistochemical labelling of interneurons with fluorescent based labelling techniques shows a lack of specificity and clarity in human tissue, with high levels of autofluorescence and fluorescent lipofuscin granules visualised. **b**, An immunoperoxidase-enzyme linked method has an improved signal to noise ratio as auto fluorescence and fluorescent age-related lipofuscin granules are avoided. **c**, Immunoperoxidase labelling protocols produce a clear signal once optimised for antibody concentrations, non-specific binding and endogenous peroxidase activity. **d-f**, Images show optimisation of chromagen for neuron labelling. **d**, The brown chromogen DAB is chosen for single labelling protocols and for counterstaining with Haematoxylin. **e**, For double-labelling protocols the black chromogen DAB-Nickel (e) is too dark to assess co-localisation with DAB labelled neurons. **f**, The blue chromogen DAB-Nickel-Cobalt-Chloride (f) produces a lighter labelling more appropriate for co-localisation analysis with DAB labelled neurons. **g-h**, Representative images show no primary controls (**g**), and no secondary controls (**h**). Scale bar in (**a-h**) 25μm.

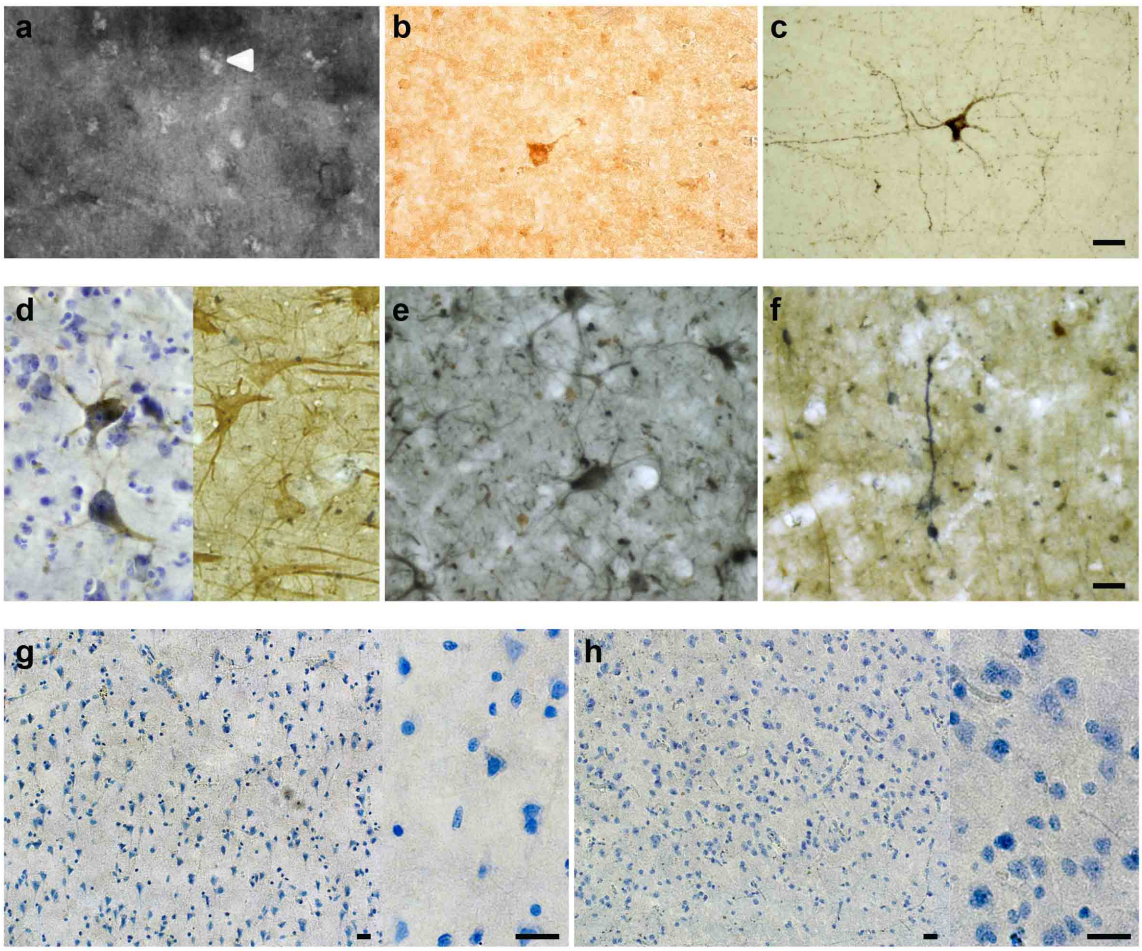
a
b
c
d
e
f
g
h

considering age, sex, disease duration and density of CR-expressing neurons. ALS Cluster 1 comprised three ALS cases that were unchanged from controls (ALS 1, 108 ± 3 cells per mm^2; Control, 99 ± 5 cells per mm^2), while ALS Cluster 2 comprised a further three cases that showed a significant decrease in CR-expressing neurons (~29%) compared to controls (ALS 2, 70 ± 3 cells per mm^2, $p < 0.006$). A multiple regression analysis was performed to discount the possibility that CR-pathology was a consequence of age, post-mortem interval, sex or disease duration (**Table 3.2**). However, independent variables did not account for the alteration in CR cell density identified in layer II-III of the motor cortex in the subset of ALS cases. Interestingly, a strong family history of ALS was present in one case from ALS Cluster 2, which may indicate a genetic component influences the extent of CR-density in cases. However, the full genetic history of cases was unavailable to investigate a genetic contribution to pathology. Nonetheless, these results suggest a differential involvement of CR-interneurons in ALS cases, with interneurons preserved in some cases and reduced in others.

3.3.3 NPY-immunoreactive neurons are increased in the ALS patient motor cortex

NPY-interneuron pathology was evaluated to determine cell type specific changes in the ALS motor cortex. In control tissue NPY-expressing interneurons were small aspiny bipolar and multipolar cells with fine processes (**Figure 3.2 a, c**). In contrast, NPY-expressing interneurons were densely labelled in ALS cases and there was a distinct increase in the extent of NPY immunoreactive fibers present in all layers of cases examined. Often, NPY intensely immunoreactive fibers were beaded and formed small clusters throughout the cortex that appeared unrelated to the distribution of NPY-expressing interneurons (**Figure 3.2 b, d**). Analysis revealed that the density of NPY-expressing interneurons was significantly increased (~200%) throughout the entire motor cortex compared to controls (ALS, 0.6 ± 0.1 cells per mm^2; Control, 0.3 ± 0.04 cells per mm^2) ($p < 0.05$, students *t* test) (**Figure 3.2 e**). There was no significant correlation between the density of NPY-interneurons and age, sex, post-mortem interval, or disease duration; however, it was interesting to note that the cases with the greatest increase in NPY-expressing interneurons compared to controls had the greatest preservation of CR-interneurons in ALS cases (ALS Cluster 1). Likewise, ALS cases with the least increase in NPY-expressing neurons had the greatest loss of CR-interneurons (ALS Cluster 2).

3.3.4 CB-expressing interneurons are unchanged in the ALS patient motor cortex

To determine if this pathology was generalised to calcium-binding proteins, or recapitulates the subtype-specific CR pathology identified in the $SOD1^{G93A}$ model, we assessed CB-expressing

Figure 3.2. Calretinin-expressing interneurons are reduced within the supragranular motor cortex of ALS cases.

Coronal sections of motor cortex from post-mortem control and ALS cases were labelled for CR-expressing interneurons. **a-b**, Representative images show CR-expressing interneurons in a control (**a**) and ALS case (**b**) labelled with DAB (brown) and nuclei stained with Haematoxylin (blue). **c-d,** High magnification images show normal bipolar and multipolar CR-expressing interneurons in control (**c**) motor cortex and abnormal CR-expressing interneurons with blebbed and beaded processes (highlighted with arrows) in ALS (**d**) motor cortex. **e**, CR-interneuron density was quantified within the supragranular lamina (layers II & III) of the motor cortex. Based on CR-interneuron density ALS cases clustered into two sub-groups as determined by Hierarchical Cluster Ward's method. ALS Cluster 2 had significantly reduced CR-interneuron density compared to controls (***$P < 0.0005$, unpaired Student's t test). Scale bar in (**a-d**) 25μm.

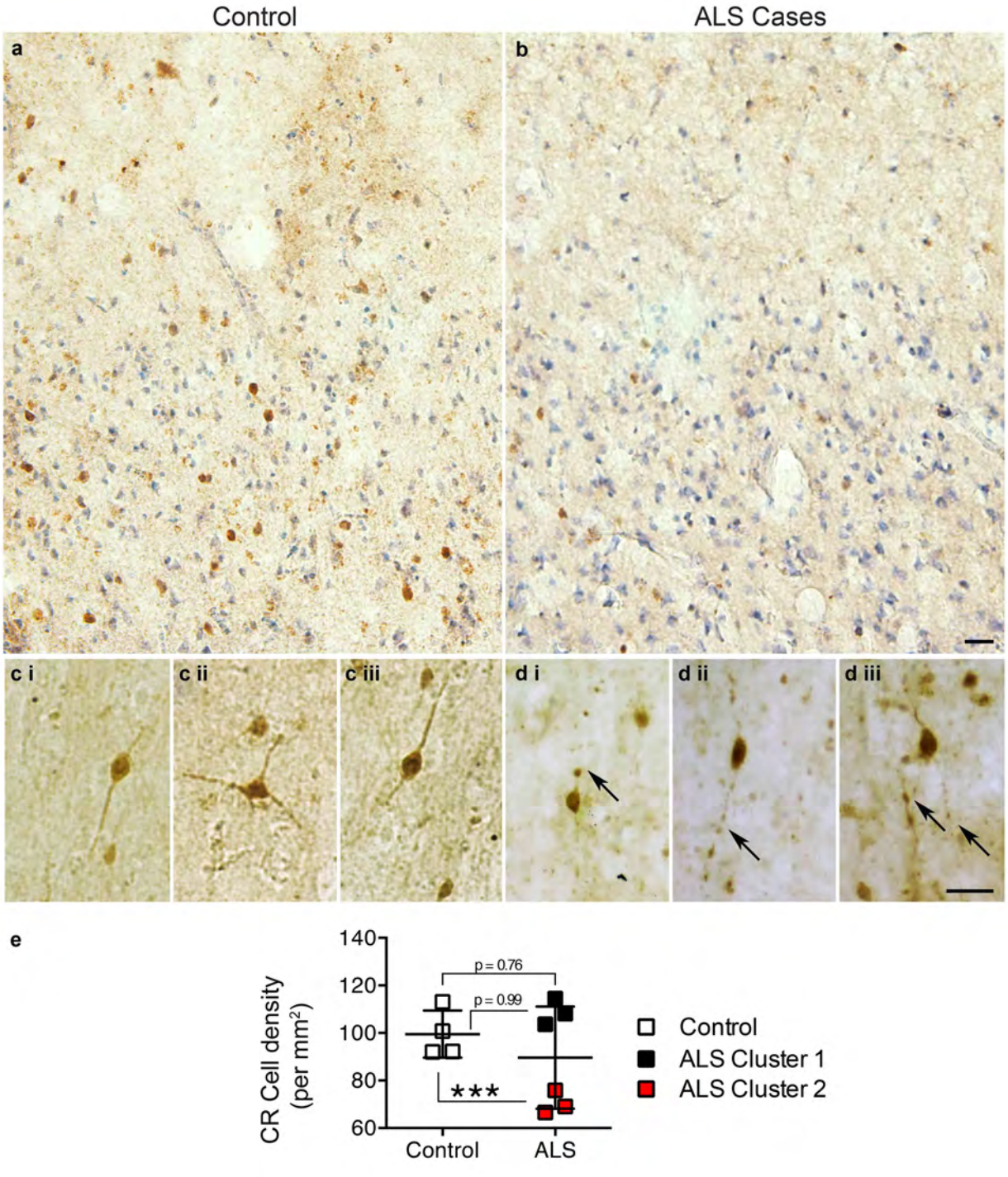
Control
ALS Cases
a
b
c i
c ii
c iii
d i
d ii
d iii
e
CR Cell density (per mm²)
140
120
100
80
60
p = 0.76
p = 0.99
***
Control
ALS
Control
ALS Cluster 1
ALS Cluster 2

Table 3.2. Multiple regression analysis of CR-density in human motor cortex

Dependent	Variable	Beta	t-value	P	VIF	Adj R2	F	p
CR-density	Age	0.334	0.2	0.875	1.246	0.016	1.020	0.622
	PMI	0.023	0.029	0.982	1.404			
	Sex	-32.16	-1.374	0.400	1.613			
	Duration	10.15	0.942	0.519	1.029			

Age, post-mortem interval (PMI), sex and duration of disease were not significant predictors of CR-density in the motor cortex of ALS cases and controls ($P > 0.05$). A model fit (adjR2) <0.1 suggests other independent variables may influence CR-density, as a variance inflation factor (VIF) of less than 2.5 is found for each independent variable.

Figure 3.3. Neuropeptide Y-expressing interneurons and fibres are increased within the motor cortex of ALS cases.

a-b, NPY-expressing neurons were labelled in the motor cortex of ALS cases and controls using immunoperoxidase DAB staining (brown). **a**, Layer II & III of the motor cortex of a normal control case shows intricate labelling of NPY-expressing neurons. **b**, In ALS cases immunoreactive fibre density is increased and neurons are irregular with prominent labelling as visualised in higher magnification images (arrows). **c-d**, Representative images show NPY-expressing neurons in control (**c**) and ALS cases (**d**) with neuronal nuclei counterstained with Haematoxylin (blue). High power view shows nuclei are visible in NPY-expressing neurons in controls (**cii, ciii**) while in ALS cases neurons have intense somatic NPY-labelling and beaded neurites (arrows) throughout tissue (**dii, diii**). **e**, The mean density of NPY-expressing neurons was significantly increased throughout the motor cortex (layers I-VI) in ALS cases compared to controls (*$P < 0.05$, unpaired Student's *t* test). Scale bar in low and high magnification images (**a-d**) 50μm.

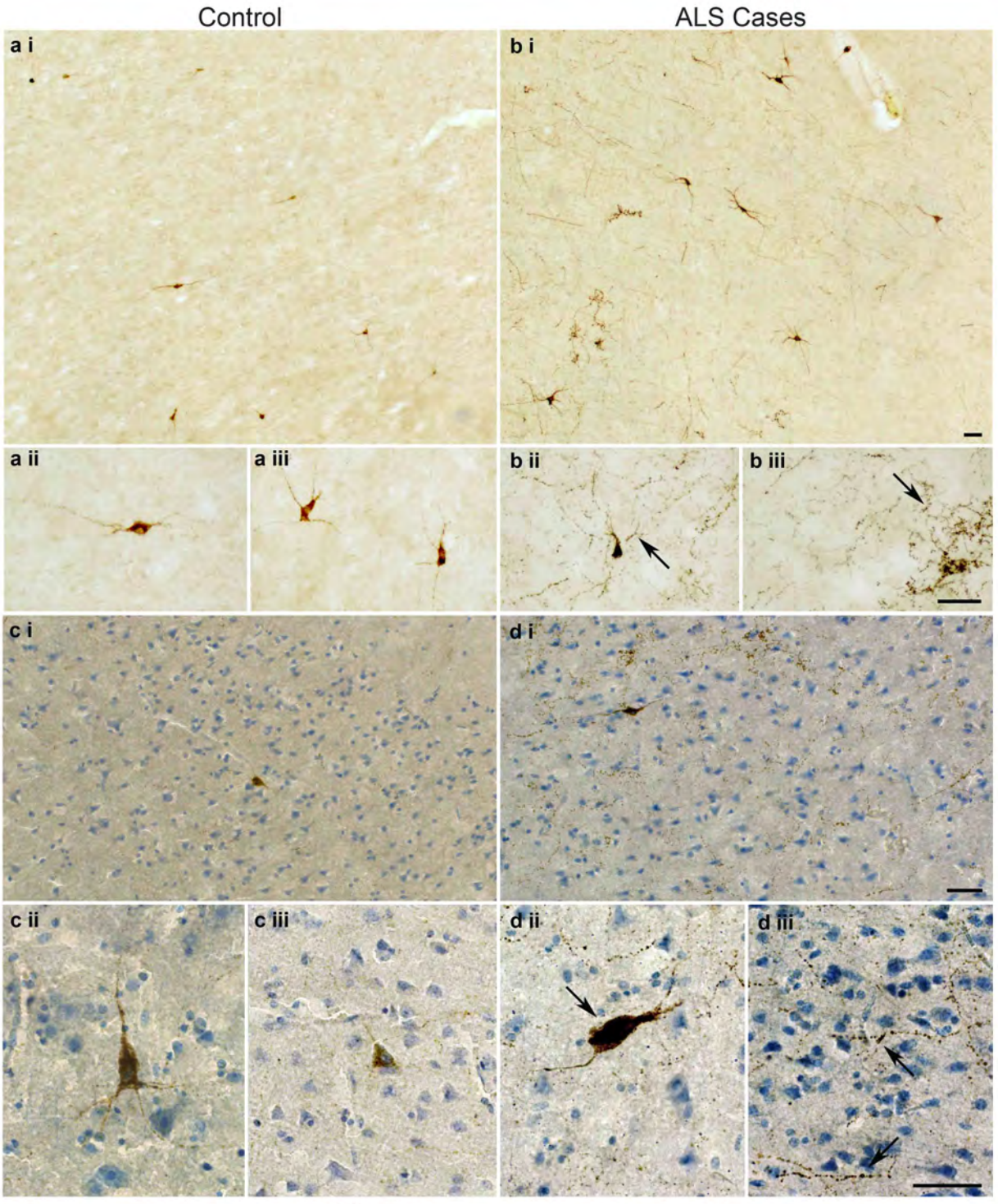
Control
ALS Cases
a i
b i
a ii
a iii
b ii
b iii
c i
d i
c ii
c iii
d ii
d iii

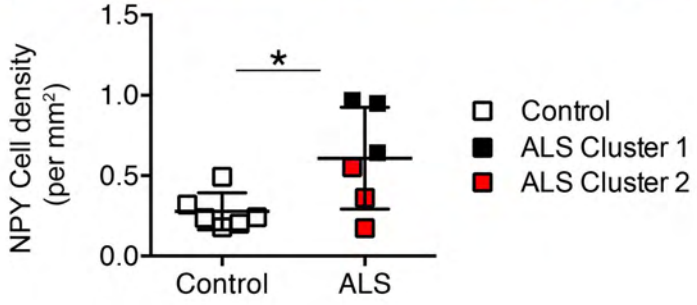
e
NPY Cell density (per mm²)
1.5
1.0
0.5
0.0
*
Control
ALS
Control
ALS Cluster 1
ALS Cluster 2

interneurons in layers II-III of the motor cortex. CB-expressing interneurons were predominantly medium sized bipolar and multipolar cells with complex dendritic trees visible (**Figure 3.4 a, c**). In ALS cases there was no overt differences in the appearance of CB-expressing interneurons (**Figure 3.4 b, d**). Analysis confirmed that the density of CB-expressing interneurons was unchanged compared to controls (ALS, 73 ± 7.6 cells per mm^2; Control, 71 ± 7.7 cells per mm^2) ($p < 0.05$, students *t* test) (**Figure 3.4 e**). There was no significant correlation of CB-interneurons with age, sex, post-mortem interval, or disease duration. These results indicate that CB-expressing interneurons are not affected in a similar manner to the CR-expressing interneurons in layers II-III of the ALS motor cortex.

3.3.5 Interneuron density in the ALS patient motor cortex is associated with SMI32 pyramidal cortical neuron pathology in ALS patients.

To determine if interneuron pathology was associated with cortical motor neuron pathology, SMI32-labeling was used to visualise the large pyramidal neurons in layer V (Campbell & Morrison 1989, Nihei et al 1993) in cases compared to controls. In control tissue large pyramidal populations were prominent in layers III and V (**Figure 3.5 a, c, e**), while in ALS cases the SMI32-expressing pyramidal neurons in layer V were atrophic and appeared to be decreased in density, particularly the medium and large SMI32-expressing neurons (**Figure 3.5 b, d**). Quantitation revealed that cases with the greatest reduction in SMI32-expressing pyramidal neurons in layer V had the greatest reduction in CR-expressing interneurons in the layer II-III of the motor cortex (ALS Cluster 2). Interestingly, the ALS cases that showed no alteration of CR-expressing interneurons (ALS Cluster 1) also showed minimal SMI32 pathology. Indeed, there was a strong and significant correlation between the density of SMI32-expressing pyramidal neurons from layers V and the density of CR-expressing interneurons from layers II-III within the ALS motor cortex (r^2 0.702, $P < 0.001$) (**Figure 3.5 g**). Similarly, there was also a positive correlation between the density of NPY-expressing interneurons and the density of SMI32-expressing pyramidal neurons in ALS cases (r^2 0.690, $P < 0.05$) (**Figure 3.5 h**). However, this correlation was not significant in controls, suggesting that this relationship is particular to the ALS cortex. Again, it was interesting to observe that the cases with the greatest increase in NPY-expressing interneurons compared to controls had the greatest preservation of CR-interneurons in the ALS cases, and also the least amount of SMI32-pyramidal neuron loss. Indeed, while there was no correlation between CB-expressing interneurons and SMI32-expressing pyramidal neurons (r^2 0.166, $P > 0.05$) (**Figure 3.5 i**), there was in fact a correlation between the extent of CR-expressing interneurons and the extent of NPY-expressing interneurons (r^2 0.672, $P < 0.05$)

Figure 3.4. Calbindin-expressing interneurons are unchanged within the motor cortex of ALS cases.

Cells expressing CB were labelled in the motor cortex of ALS cases and controls using immunoperoxidase DAB staining (brown) and counterstained with Haematoxylin (purple). **a-b**, Representative images show CB-expressing interneurons in layer II & III of the motor cortex of a control (**a**) and ALS case (**b**). **c-d**, High power images show clear labelling of CB-expressing interneurons and processes in controls (**c**) and comparable labelling in ALS cases (**d**). **e**, The mean density of CB-expressing interneurons was unchanged in layer II-III of the motor cortex in ALS cases compared with controls ($P > 0.05$, unpaired Student's t test). Scale bar in all low and high magnification images (**a-d**) 25μm.

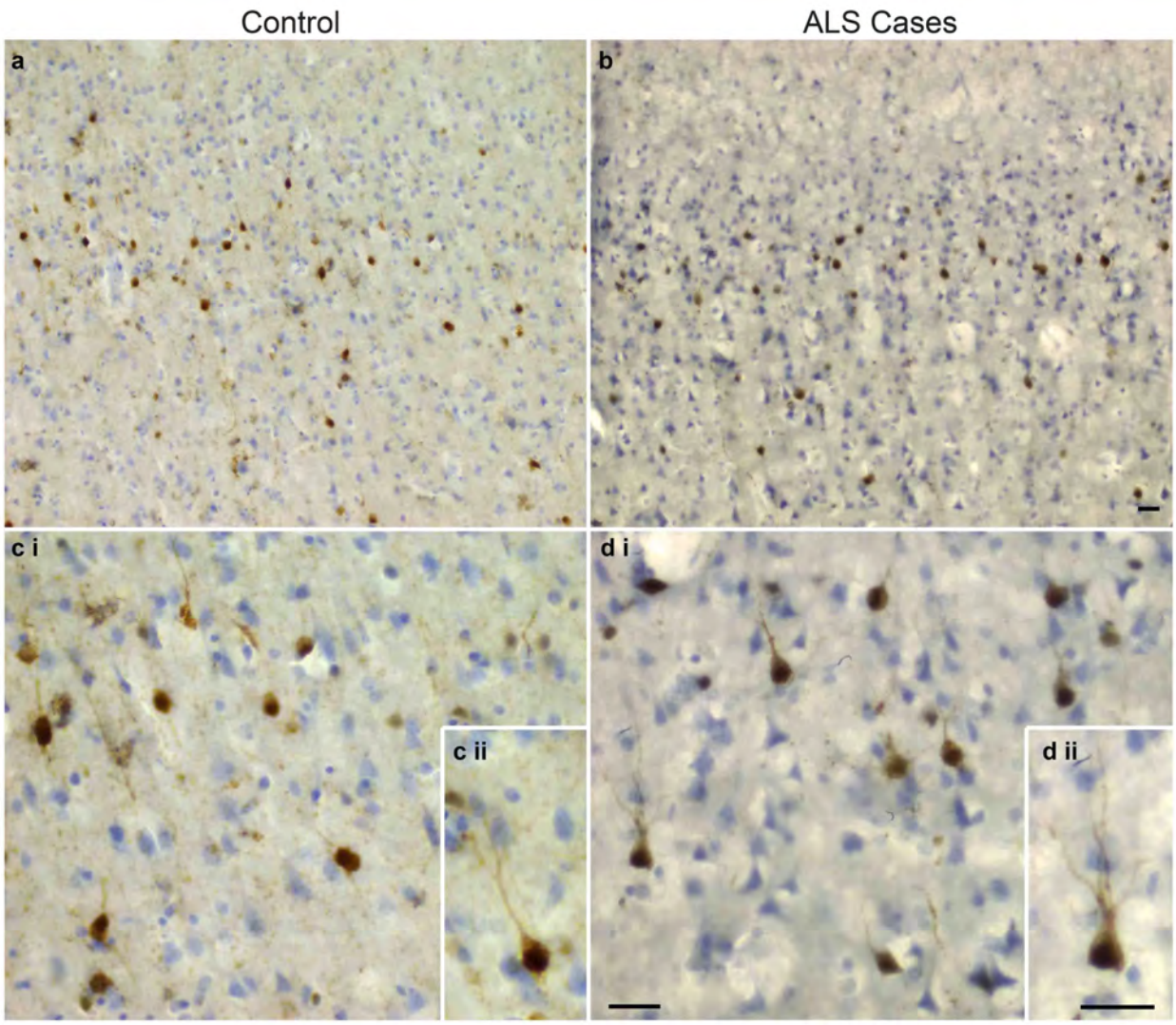
Control
ALS Cases
a
b
c i
c ii
d i
d ii

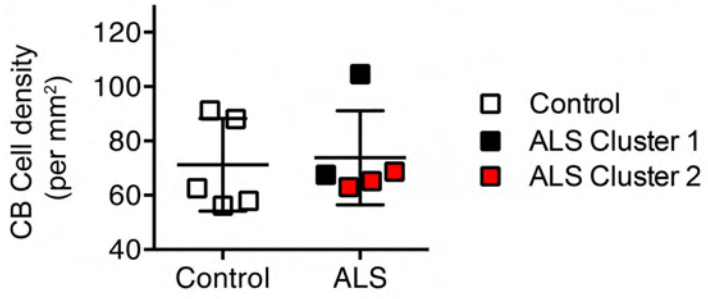
e
CB Cell density (per mm2)
120
100
80
60
40
Control
ALS
Control
ALS Cluster 1
ALS Cluster 2

(**Figure 3.5 j**). This may indicate that the vulnerability of the ALS motor cortex is associated with the extent of CR-, NPY- and SMI32-populations.

It is important to note that large spiny excitatory CR-neurons can be found in the mammalian cortex (Del Rio & DeFelipe 1997, Liu et al 2014), as well as the non-spiny smaller typically inhibitory populations. As such, SMI32/CR double labeling was performed to confirm that the change in CR-interneuron density in layer II-III is primarily associated with inhibitory aspiny interneurons, and the change in SMI32 density in layer V is not confounded by the excitatory spiny CR-population. In both cases and controls, less than 1% of cells labeled were found to be spiny excitatory cells (**Figure 3.5 f**), and none of these cells were located in layer II-III, nor did they differ in density between controls and ALS cases (**Figure 3.5 k**). The combined results of these experiments demonstrate that reduced interneuron cell density is present in a subset of ALS cases, is specific to aspiny CR interneurons, and correlates well with the extent of the change in NPY and SMI32 cell density.

Figure 3.5. SMI32-immunoreactive pyramidal neurons are reduced in the ALS motor cortex and correlate with interneuron density.

Neurons expressing SMI32 were labelled in the motor cortex of ALS cases and controls using immunoperoxidase DAB staining (brown). **a-b**, Representative images show SMI32-labelled pyramidal cells in the motor cortex in control (**a**) and ALS cases (**b**) with double labelling performed to visualise CR-expressing interneurons using DAB-Nickel-Cobalt Chloride (blue). **c-d**, In control motor cortex pyramidal neurons are normal (**c**), while in ALS tissue (**d**) cells appear atrophic and decreased in number with condensed nuclei visualised by Haematoxylin (purple). **e**, High magnification images show large Betz cells in control tissue with dendritic branches leaving from the entire circumference of the soma. **f**, A spiny double-labelled SMI32 and CR-expressing cell in layer V of the motor cortex (**i**) and a normal non-spiny CR-expressing interneuron (**ii**). **g-j**, Pearson's correlation analyses revealed positive correlations between the density of SMI32-expressing neurons, CR-expressing interneurons (**g**) and NPY-cells (**h**), but not between the density of SMI32-expressing neurons and CB-expressing interneurons (**i**), while CR-interneuron and NPY-cell density (**j**) is associated (*$P < 0.05$, Pearson's correlation r^2). **k**, Analyses shows a small proportion of large spiny CR-expressing cells are present in the cortex relative to non-spiny small CR-expressing interneurons, and are unchanged between controls and cases ($P < 0.05$, one-way ANOVA). Scale bar in (**a-f**) 50μm.

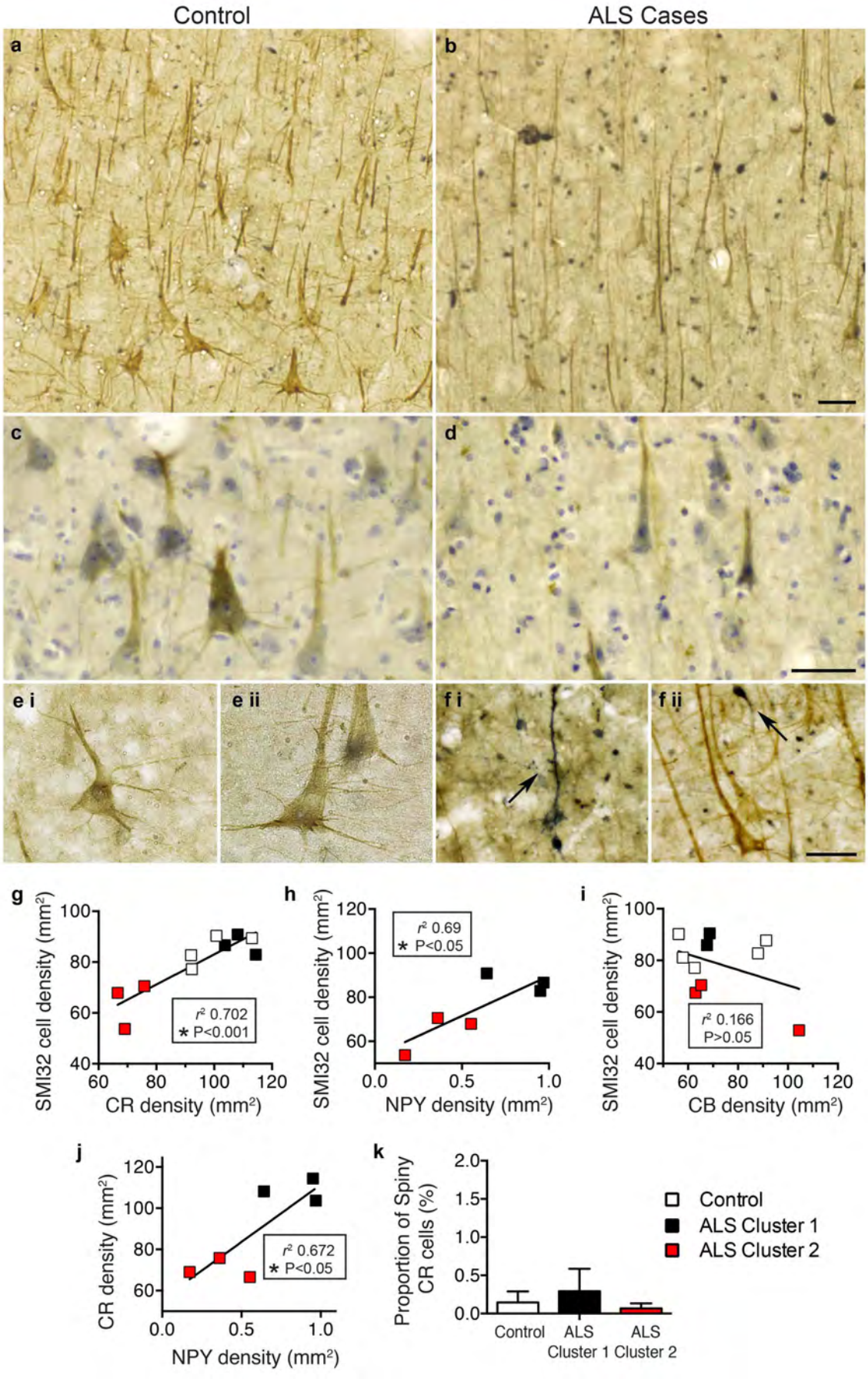
Control
ALS Cases
a
b
c
d
e i
e ii
f i
f ii
g
SMI32 cell density (mm²)
CR density (mm²)
r² 0.702
* P<0.001
h
SMI32 cell density (mm²)
NPY density (mm²)
r² 0.69
* P<0.05
i
SMI32 cell density (mm²)
CB density (mm²)
r² 0.166
P>0.05
j
CR density (mm²)
NPY density (mm²)
r² 0.672
* P<0.05
k
Proportion of Spiny CR cells (%)
Control
ALS Cluster 1
ALS Cluster 2
Control
ALS Cluster 1
ALS Cluster 2

3.4 DISCUSSION

In the ALS cortex, there is clinical evidence that the disease may be potentiated by dysfunction, degeneration or loss of inhibitory interneurons (Ziemann et al 1997, Martin & Chang 2012, Turner & Kiernan 2012). The previous findings from this thesis support the involvement of specific inhibitory populations, however, it was unknown if this was relevant to the human disease and how these populations may be implicated in the context of the ALS motor cortex. In this small pilot study investigations were performed to identify specific changes in subclasses of GABAergic interneurons that were previously identified in the $SOD1^{G93A}$ mouse. Additional analyses were performed to compare the relationship of interneuron pathology in the ALS motor cortex to the clinical profile of cases, and the pattern of interneuron involvement with pyramidal neuron loss. The current chapter advances our understanding of the selective vulnerability of interneurons in ALS and the potential cellular basis of functional imaging abnormalities reported in clinical studies.

3.4.1 The pattern of neuron loss in the ALS motor cortex

In ALS, traditional neuropathological techniques have been used to show that neuronal degeneration occurs frequently in the motor cortex. The most prominent changes reported are loss of the giant layer V pyramidal Betz cells and astrocytic gliosis (Brownell et al 1970, Udaka et al 1986, Nihei et al 1993, Nagy et al 1994). In this study, there is loss of the medium to large SMI32 cells. However, relatively less is known about the involvement of other neuronal populations in the motor cortex, particularly the inhibitory interneurons.

In the current investigation comparison of the brains of ALS patients and control subjects revealed changes in CR and NPY interneurons that largely recapitulated the interneuron pathology observed in the $SOD1^{G93A}$ mouse model. Similarly, CB-interneurons were found to be unaltered, which agrees with findings from the $SOD1^{G93A}$ study and a previous study in the ALS cortex (Ince et al 1993). However, there is a distinct difference in the extent of interneuron pathology in cases, exemplified by a significant loss of CR-expressing interneurons in 50% of ALS cases. While previous studies have reported a trend towards a decrease in the density of CR-interneurons in the ALS primary motor cortex, it was not clear if a similar clustering pattern was observed (Maekawa et al 2004).

More relevant to the current study, a recent investigation found a distinct divergence of interneuron pathology in the cortex of Huntington's disease patients (Kim et al 2014b). While heterogeneity was predominately centred on a differential loss of CB-interneurons, it was found that heterogeneity was associated with the symptom subtype exhibited by individual cases. Patients with dominant motor

symptoms had a loss of CB-interneurons, while no interneuron loss was observed in the primary motor cortex of cases with major mood disorder. This may indicate that the divergence in CR-pathology observed in this study may relate to the extent of motor and cognitive involvement in the cortex of ALS cases, particularly as the disease is now considered on a spectrum with frontotemporal dementia. However, due a lack of clinical information in this study we were unable to discern such an association and as such it cannot be ruled out as a cause of heterogeneous pathology. Moreover, while considerable evidence suggests that variable interneuron dysfunction may be linked to altered disease duration in the ALS motor cortex, in this study no associated with duration of disease, nor with age, gender or post-mortem interval is demonstrated in relation to interneuron involvement. However, due to a small sample size, such a correlation cannot be excluded and it will be important for future studies to explore such an association with an increased sample size. Nonetheless, the examination of cell morphology in this study showed major differences in the CR-interneuron populations, such as blebbing and beading of processes in ALS cases, which support their involvement in disease.

3.4.2 Relationship of heterogeneous interneuron pathology to pyramidal neuron loss

Interneurons are essential components of the cortical motor neuron network and may be central to network failure. Every segment of a pyramidal neuron, such as soma, dendritic branches and spines, and the initial axonal segment, receives dense GABAergic synaptic innervation [see reviews (Jones 1993, Buzsaki et al 2004)]. In ALS, clinical imaging studies suggest brain plasticity in motor networks is correlated with disease progression (Poujois et al 2013), and the extent of inhibitory alteration in the motor cortex is associated with increased excitability of the motor cortex (Menon et al 2014, Geevasinga et al 2015, Shibuya et al 2016). Hence, this study was interested in determining if such a correlation may be found in the interneuron and pyramidal pathology in the region.

The results of this study show a correlation between differential loss of CR-interneurons in the primary motor cortex and pyramidal neuron pathology. That is, in the primary motor cortex of ALS cases, the selective loss of CR-interneurons was associated with pyramidal neuron loss, measured by decreased density of layer V pyramidal neurons. Intriguingly, the converse was also shown with preservation of CR-interneurons associated with a lesser extent of pyramidal neuron pathology. This suggests that interneuron pathology and corticomotoneuronal pathology may be coupled in the ALS motor cortex. However, as CB-interneuron pathology is not associated with pyramidal neuron pathology, this indicates vulnerable networks may be associated with specific interneuron populations, such as the CR-interneurons.

From a functional view point, when looking at other diseases with demonstrated reductions in CR-interneurons, it is most interesting to find that in the epileptic human hippocampus the number of CR-cells lost also correlated with the severity of principal cell loss in the region (Toth et al 2010). This common neurological condition is by definition due to abnormal excessive or synchronous neuronal activity in the brain (Fisher et al 2005), which when comparing evidence for hyperexcitability in the motor cortex in ALS draws certain parallels. Thus, when considered in the context of ALS, this may suggest a pathogenic feedback mechanism whereby the loss of CR cells translates to a loss of principal cells, or vice verse. Additionally, it may also indicate that reduced CR populations are involved in a loss of circuitry control, contributing to the hyperexcitability observed in ALS, and epilepsy.

While it remains to be determined if CR-populations drive corticomotoneuronal degeneration, or respond to altered network feedback due to corticomotoneuronal degeneration, the differential nature of CR pathology in patients is not surprising. Previous literature has established that the extent of pyramidal neuron pathology in layer V of the motor cortex varies between patients (Nihei et al 1993, Maekawa et al 2004), as also observed in this study. Therefore, it was quite unexpected that there was an overall significant increase in NPY interneurons throughout the entire motor cortex of all ALS cases. However, in line with the clustering of ALS cases based on CR-interneuron pathology, it was an interesting observation to find that cases with the least amount of pyramidal and CR-pathology had the greatest increase in NPY cell density relative to controls. Indeed, this study shows a correlation of NPY-pathology with both pyramidal pathology and CR-pathology. This suggests that while CR-interneuron pathology may be detrimental in the motor cortex, increased NPY may be associated with a reduced extent of cortical damage. However, this correlation was only found in ALS cases, not controls, suggesting this may be a compensatory mechanism specifically related to an altered network in the ALS motor cortex. This may be supported by the apparent marked increase in NPY-immunoreactive fibres identified to varying degrees in all ALS motor cortices studied.

When considering the distinct morphological appearance of NPY-immunoreactive fibres in the ALS cortex, again similar parallels are observed with key-disease affected regions in the epileptic brain. Previous studies have shown an increase in the cell density and length of NPY immunoreactive fibres in hippocampal subfields with sclerosis in the epileptic human hippocampus (De Lanerolle et al 1989, Mathern et al 1995, Furtinger et al 2001), which mirror the NPY pathology detected in the present study. The striking similarity of this pathology is best demonstrated when directly comparing photomicrographs from works of Furtinger and colleagues (Furtinger et al 2001) with images from the present study (**Figure 3.6**).

Figure 3.6. NPY-immunoreactive fibres in the epileptic human hippocampus parallel NPY-pathology demonstrated in the ALS motor cortex.

a, Widespread NPY immunoreactivity is shown in a patient with hippocampal sclerosis as demonstrated by Furtinger and colleagues in 2001. **b**, Striking similarities are demonstrated in the NPY-immunoreactive fibres found in the ALS motor cortex in this study. High magnification images in both show the unusual pattern of NPY process labelling in both disease-associated regions. Scale bar in (**a-b**) 50μm.

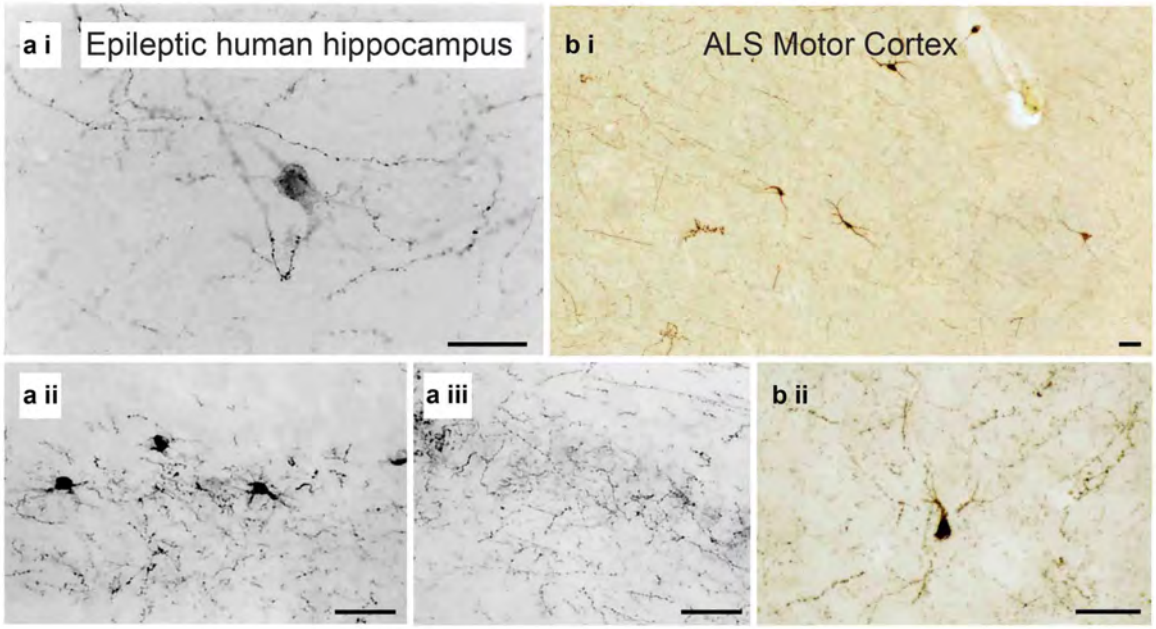
a i
Epileptic human hippocampus
b i
ALS Motor Cortex
a ii
a iii
b ii

While the mechanism responsible for NPY involvement in ALS is not yet known, it is tempting to speculate that this may again represent a mechanism related to increased excitability. Regarding modes of NPY expression, in normal neurological conditions NPY is contained and released by GABAergic interneurons, however in regions of pathogenically enhanced excitability it can be found upregulated in interneurons and aberrantly expression in non-neuronal populations (Marksteiner et al 1990, Rizzi et al 1993, Gruber et al 1994). This has been typically demonstrated in the hippocampus of mouse and rat strains that are susceptible to seizures, with NPY transiently upregulated in interneurons and granule cells/mossy fibres of the dentate gyrus from the pre-convulsive stage in animals (Schwarzer et al 1996, Vezzani et al 1996). Thus, it is possible that NPY-fibre immunoreactivity in this study may represent upregulation of the neuropeptide on either GABAergic or glutamatergic processes. While we confirm that CR-interneuron involvement is restricted to aspiny inhibitory SMI32 negative populations, future studies should also conduct co-localisation for equal assessment of NPY labelling. Hence while we cannot rule out the upregulation of NPY on pyramidal populations, it is important to note that irrespective of the mode of delivery, administration of NPY has been found to potently suppress epileptic activity in hippocampal slices from epilepsy patients (Patrylo et al 1999). Therefore, the demonstrated alteration of NPY reported here should remain of high interest in the context of cortical hyperexcitability demonstrated in the motor cortex of ALS patients.

3.4.3 Conclusion

Comparing the brains of ALS patients with control subjects revealed specific changes in CR and NPY interneurons that largely recapitulated the interneuron pathology observed in the $SOD1^{G93A}$ mouse model. However, a novel divergence of interneuron pathology across ALS patients identified heterogeneity in disease pathology, as demonstrated by the significant loss of CR-expressing interneurons in 50% of ALS cases. Nonetheless, the clear increase of NPY-expressing neurites in ALS cases and increased cell density supports a similar pathogenic process in the motor cortex of ALS patients and the $SOD1^{G93A}$ mouse model that warrants further investigation. Indeed, while future studies are required to fully elucidate the relationship of interneuron pathology with clinical characteristics of individual cases due to low case numbers, the results from this study suggest that both CR and NPY interneuron populations may have an important role to play in the ALS motor cortex. This study proposes that CR and NPY may be critical determinants of altered excitability in the ALS cortex, due to profound similarities with the epileptic human cortex. The divergence of pathology between cases may indicate innate differences/vulnerabilities in the cortex that may be associated with the extent of cortical dysfunction. Whether this relates to variable disease

progression rates in patients remains to be determined, however, due to the correlation with pyramidal pathology this may be of interest for future studies. Moreover, the differences in cases may highlight the potential for therapeutic intervention aimed at modulating these populations to restore or maintain network functions.

Chapter 4

4 THE SOD1^{G93A} MUTATION ALTERS CORTICAL INTERNEURON DEVELOPMENT AND INTRINSIC ELECTRICAL PROPERTIES *IN VITRO* IN MOUSE MODEL OF ALS

4.1 INTRODUCTION

It is increasingly apparent that a long pre-clinical and pre-symptomatic period may exist in ALS patients, in which underlying pathogenic processes initiated much earlier in life, may remain innocuous until protective and compensatory mechanisms that mask primary pathogenic events become overwhelmed or saturated, culminating in the ALS phenotype [see review (Eisen et al 2014)]. Evidence for this relates to the identification of pathological changes in animal models shortly after birth, predating the first clinical abnormalities by 2-3 months (Bendotti et al 2001, Ozdinler et al 2011, Jara et al 2012, Vinsant et al 2013), and more recently, the detection of cortical hyperexcitability in sporadic and familial ALS patients months prior to measurable lower motor signs or symptoms (Menon et al 2014). In familial ALS, these early pathogenic processes may be initiated by the expression of mutant proteins during early embryonic life. Indeed, investigation of one of the most well documented familial mutations, the SOD1^{G93A} mutation, has demonstrated increased motor neuron excitability during early postnatal development *in vitro* (Pieri et al 2003, Kuo et al 2004) and prior to symptom onset *in vivo* (Fogarty et al 2015). This indicates that there is likely underlying bio-molecular dysfunction occurring in ALS patients throughout life, but also that compensatory mechanisms may mask these early alterations for months in ALS mouse models, and potentially for decades in humans.

In the context of previous findings from this thesis, this raises the question of whether changes in interneurons are casual and/or adaptive in nature. When considering this first possibility it is important to note that while mutant SOD1^{G93A} has been shown to cause intrinsic damage to motor neurons, expression in motor neurons alone is reportedly insufficient to cause disease (Clement et al 2003), supporting the view that the disease pathogenesis is critically dependent on dysfunction of other cell types (Boillee et al 2006a, Ilieva et al 2009). Indeed, SOD1 is ubiquitously expressed in all cells of the CNS throughout life (Gurney et al 1994), including interneurons, and while the intrinsic vulnerability of cortical interneurons has yet to be investigated in ALS, the intrinsic electrophysiological properties of cortical neuronal populations have been found to be altered in response to expression of the SOD1^{G93A} mutation *in vitro* (Pieri et al 2009). However, as interneurons are primarily considered an adaptive cell type (Jones 1993, Mendez & Bacci 2011, Lehmann et al 2012) the alternate scenario may include the alteration of cortical interneurons secondary to changes in network excitability. Indeed, it is increasingly recognised that interneuron

development is an activity-dependent process (Cancedda et al 2007, De Marco Garcia et al 2011, Kepecs & Fishell 2014), and it is demonstrated that motor neuron hyperexcitability is present at both embryonic and presymptomatic stages in ALS models (Kuo et al 2004, van Zundert et al 2008, Martin et al 2013) and also in patient-derived motor neurons (Wainger et al 2014, Devlin et al 2015). Therefore, there is potential for interneuron dysfunction to initiate, or be responding to, changes in excitability during development.

In order to investigate these possibilities, the current study aimed to determine if cortical interneuron development was impaired in the presence of the $SOD1^{G93A}$ mutation *in vitro*. For these analyses, complementary culturing, immunohistochemical and electrophysiological techniques were used to investigate the intrinsic electrical properties of cortical interneurons, as well as their structural maturation and normal development *in vitro*. To aid in the identification of cortical interneurons, WT and $SOD1^{G93A}$ transgenic mice were crossed with the Gad67-GFP mouse, which expresses a fluorescent green protein under the interneuron-specific glutamate decarboxylase 67 (GAD67) promoter (Tamamaki et al 2003). Primary cortical cultures were derived from E15.5 Gad67-GFP::$SOD1^{G93A}$ and Gad67-GFP::C57Bl6 (WT) transgenic mice, as this represents an embryonic stage when cortical interneurons generated from both the caudal/lateral ganglionic eminence (Miyoshi et al 2010) and medial ganglionic eminence should be present in the cortex (Miyoshi et al 2007).

4.2 METHODS

4.2.1 Animals

All procedures were approved by the Animal Ethics Committee of the University of Tasmania and conducted in accordance with the Australian Code of Practice for the care and Use of Animals for Scientific Purposes, 2013. Gad67-GFP knock-in transgenic mice were developed by Prof. Nobuaki Tamamaki (Kyoto University) (Tamamaki et al 2003) and were a kind donation form Prof. John Bekkers (ANU). These mice express green fluorescent protein (GFP) in GABAergic neurons arising from the ganglionic eminence under the control of the mouse Gad67 promoter, one of the two genes encoding isoforms of the GABA synthesizing enzyme, glutamic acid decarboxylase (Suzuki & Bekkers 2010a). These mice were intercrossed with the $SOD1^{G93A}$ mouse line (previously described in Chapter 2.2.1) purchased from the Jackson Laboratory (CA, USA), both maintained on a C57BL/6 background, to generate double transgenic Gad67-GFP::$SOD1^{G93A}$ mice. Animals were bred at the University of Tasmania. Animals were housed in individually ventilated cages at 20^{o}C, on a 12 hour light-dark cycle, with access to food and water *ad libitum*. Gad67-GFP transgenic littermates were used as controls.

4.2.2 Primary neuronal cortical culture

Primary mouse cortical neuron cultures were derived from individual mouse embryos, as previously described (Brizuela et al 2015). Briefly, Gad67-GFP and $SOD1^{G93A}$ transgenic mice were time mated, the pregnant females killed by CO_2 exposure at 15.5 days of gestation, and the embryos removed. Genotyping of embryos for Gad67-GFP was performed by fluorescence imaging using 470nm light on a Carestream Image Station 4000MM pro (Carestream Molecular Imagin, USA).

Neocortical hemispheres were dissected from individual embryos, meninges removed and placed into 5ml Hanks Buffered Salt Solution (HBSS; Thermo-Fisher Scientific, USA). Cortical tissue was dissociated by enzymatic digestion with 0.025% w/v Trypsin at 37^{o}C for 5min. The digestion was halted with the addition of 1ml of pre-warmed medium (Neurobasal^{TM} supplemented with 2% v/v B-27, 10% v/v fetal calf serum, 0.5mM L-glutamine, 25μM glutamate and 1% streptomycin penicillin; Thermo-fisher Scientific, USA). Tissue pieces were allowed to settle and after removal of the medium, dissociation was completed by resuspension of cells in 500μl of pre-warmed medium and gently triturated. Cell viability and concentration was assessed using trypan blue vital dye exclusion (Sigma-Aldrich, USA). Cortical neurons dissociated from individual embryos were then plated at a

density of 3.5 x 10^4 cells/mm^2 on 19mm diameter glass coverslips, pre-coated with 0.001% poly-L-lysine (Sigma-Aldrich, USA) in 0.01M PBS (pH 7.0).

Twenty-four hours after plating, initial plating media was removed and replaced with serum-free growth medium (Neurobasal^{TM} media, supplemented with 2% v/v B-27, 0.5mM L-glutamine and 1% streptomycin penicillin; Thermo-fisher Scientific, USA). This promoted the selective growth of neuronal populations (Brewer 1995). Half of the media was replaced every three to four days with fresh media. Cultures were maintained in a humidified incubator at 37^oC in 5% CO_2 for up to 15 days in vitro (DIV). Cultures were either fixed at 3, 7, 10 or 14 DIV for synaptic analysis, or 10 DIV for interneuronal, electrophysiological and morphological assessments.

4.2.3 Genotyping

After single Gad67-GFP-positive embryos had been cultured, they were subsequently genotyped for the SOD1^{G93A} transgene using a multiplexed quantitative polymerase chain reaction protocol (real-time qPCR). DNA was extracted from either cortical tissue obtained at embryonic dissection, or from the mature genetically isolated cultures at 10-14 DIV, using an Extract-N-Amp Tissue PCR tissue kit (Sigma-Aldrich) according to the manufacturer's instructions. The presence of the SOD1^{G93A} transgene was assessed as previously described in Chapter 2.2.2, and copy number analysed in order to monitor genetic drift according to standard protocols (Leitner et al 2009).

4.2.4 Electrophysiology

Cortical neurons cultured on glass coverslips (10 DIV) were superfused at 24 ± 1^oC with bicarbonate-buffered solution [155mM NaCl, 3.5mM KCl, 2mM $CaCl_2$, 1.5mM $MgCl_2$, 10mM glucose; osmolarity adjusted to 305-310mOsm/kg by the addition of D-sorbitol (all Sigma)]. For recordings, patch electrodes were prepared from borosilicate glass capillaries (1.5mm O.D. x 0.86mm I.D.) (Harvard Apparatus, UK) and had a resistance of 7-9Ω when filled with a internal solution containing 130mM K-gluconate, 4mM NaCl, 10mM HEPES, 0.5mM $CaCl_2$, 10mM BAPTA, 4mM MgATP, 0.5mM Na_2GTP, set to a pH of 7.4 (KOH), and an osmolarity of 290 ± 5 mOsm/kg with D-sorbitol. Whole-cell patch clamp recordings of GABAergic cortical interneurons, selected based on GFP expression, were collected using an Axopatch 200B amplifier (Molecular Devices, USA), with a holding potential of -70mV. Recordings were made using a gap free protocol for 3 minutes and 10 seconds, sampled at 10Hz and filtered at 5Hz using PClamp9.2 software (Molecular Devices). Access resistance was recorded before and after each recording. Data was not included if the cells access resistance was ≥ 15 MΩ, or if the access resistance changed by ≥ 10%

during the course of the recording. Access resistance did not significantly differ between groups. Voltage-gated sodium and potassium currents were evoked with a series of voltage steps (-70 to 50mV, 10mV increments), and were analysed using the programs Igor (WaveMetrics) and Axograph scientific. The peak net inward current (reflecting the difference between the inward I_{Na} and the other voltage-dependent outward currents) was quantified after subtracting the capacitive current, and assumed ohmic leak current was scaled from the response to hyperpolarizing pulses (Clarke et al 2012). Voltage responses to current injection were recorded from the cell's resting potential (applying 25 pA steps for 200 ms from – 100 to 500pA). Post-recording, the patch electrode was removed from the neuron, which was later identified by the detection of neurobiotin.

4.2.5 Immunocytochemistry of cortical cultures

Neuronal cultures were fixed with 4% PFA for 30min at room temperature and washed in 0.01M PBS three times for ten minutes. Fixed cultures were then blocked for non-specific binding (0.3% Triton X-100 in 0.01M PBS with 10% normal bovine serum) for 1hr at room temperature and incubated in primary antibody combinations in diluent (0.01M PBS with 5% normal bovine serum) at 4^{o}C overnight. Specimens were then washed a further three times for ten minutes and incubated in appropriate secondary antibodies (Alexa Fluor anti-rat 488, anti-rabbit 647, anti-mouse 647) diluted in PBS (1:1000, Molecular Probes) for 90 minutes at room temperature. DAPI (1:10000 dilution, 5mg/ml stock) was added for the final ten minutes to visualise nuclei. Specimens were then thoroughly washed with PBS and mounted with Permafleur media (DAKO) onto slides.

Cultures were probed for Gad67-GFP expression (enhanced by rat anti-GFP, 1:3000, Nacalai tesque) along with interneuronal markers (rabbit anti-CB, 1:2000, Millipore; rabbit anti-CR, 1:2000, Swant; mouse anti-PV, 1:2000, Swant; rabbit anti-NPY, 1:2000, Abcam; rabbit anti-SOM, 1:1500, Immunostar; rabbit anti-VIP, 1:2000, Immunostar), synaptic markers (rabbit anti-synaptophysin, 1:1000, Millipore; mouse PSD-95, 1:500, Abcam) and vesicular transporters (rabbit anti-VGAT, 1:500, Synaptic Systems; mouse anti-VGLUT-1, 1:500, Synaptic Systems).

Visualization of neurobiotin-filled patched cells was achieved by incubation of specimens with fluorescently conjugated Alexa Fluor® streptavidin-546 (Molecular Probes^{TM}; 0.1% Triton X-100), prior to incubation with primary antibodies. This approach was used to identify patched neurons for post-hoc morphological analyses.

4.2.6 Confocal microscopy of cortical cultures

Neurons were visualized using a spinning disk laser confocal (UltraView®VOX, Perkin Elmer) on an inverted microscope (Nikon TiE, Nikon) equipped with a 20x (Plan-Apo 0.75), 40x (Plan-Apo 0.95) and 60x (Plan-Apo 1.2) objective lenses. Images were acquired using an Orca R2 camera (C106000, Orca, Hamamatsu) and analysed using imaging capture software (Velocity v6 3.0, 2013, Perkin Elmer). Z-stack images of interneuronal populations were captured with a 20x objective (10μm, 1μm intervals), neurobiotin-filled interneurons on a 40x objective (5μm, 0.5μm intervals) and synaptic markers with a 60x objective (5μm, 0.5μm intervals).

4.2.7 Image analysis and cell tracing

Interneuron subtype proportions represented by Gad67-GFP interneurons were determined in Image J (NIH) by quantifying the relative expression of interneuron marker fluorescence co-localised with Gad67-GFP expression, and presenting data relative to total GFP expression [arbitrary units (AU)]. For morphological analyses, reconstruction of the streptavidin-positive processes of patch clamped interneurons was completed with tracing of cells through Z-stack series using the cell tracing software Neurolucida^{TM} (MBF Bioscience, USA). Each interneuron, that met the inclusion criteria for electrophysiological assessment (access resistance < 15 MΩ), was evaluated with Neurolucida^{TM} Explorer II to determine the total branch orders, numbers and length (MBF Bioscience, USA). The complexity of the neurite arbors was also assessed by performing a Sholl analysis with concentric circles placed at 10μm intervals radiating outward from the cell body.

4.2.8 Statistical analysis

To determine the effect of SOD1^{G93A} mutation on cortical interneuron maturation, developmental and functional data was statistically analysed using GraphPad Prism (Version 5.0, La Jolla, CA). For all electrophysiological assessments, data from Gad67-GFP cortical interneuron populations was pooled based on morphological features and two interneuron groups considered: bipolar interneurons with two-neurobiotin filled processes on opposite poles of the cell soma, and multipolar interneurons with at least three processes originating from the cell soma (Cauli et al 2014). For all electrophysiological statistical comparisons unpaired Student's *t* tests were performed, with the exception of frequency and amplitude assessments, which was evaluated with paired Student's *t* tests. Unpaired Student's *t* tests were also used to determine differences between the compositions of interneuron cultures and to evaluate the morphology of whole-cell patch clamped interneurons, with the exception of cumulative frequency distribution plots, which were assessed with the Kolmogorov-Smirnov test to compare cumulative distributions. To examine relationships between neuronal

morphology and electrophysiological parameters, a non-parametric Pearson's r^2 was reported. $P < 0.05$ was considered statistically significant. Data is expressed as means ± standard error of mean. Unless otherwise stated, a minimum of three separate cultures was used for each experiment, with 3 technical replicates per culture (n = 3).

4.3 RESULTS

4.3.1 Characterisation of Gad67-GFP interneurons *in vitro*

To determine the effect of the $SOD1^{G93A}$ mutation on cortical interneurons, cortical cultures derived from E15.5 Gad67-GFP::$SOD1^{G93A}$ and Gad67-GFP::C57Bl6 (WT) transgenic mice were initially characterised for key interneuronal and synaptic markers. Utilising immunocytochemistry, the current investigation identified that growing and developing interneurons with the SOD1 mutation showed no significant changes in expression and localization of synaptic proteins compared to WT interneurons (**Figure 4.1**). Cortical interneurons followed a distinct pattern of development, with the pre-synaptic protein synaptophysin and post-synaptic density 95 (PSD-95) transitioning from a diffuse pattern of expression at 3-7 DIV to become punctate and extended along elaborate neurite processes at 10-14 DIV (**Figure 4.1 a-d**). The maturation of interneuron populations was also examined by expression of the vesicular glutamate transporter (VGLUT-1) and the vesicular GABA transporter (VGAT) with Gad67-GFP soma and processes across the 3-14 DIV time course (**Figure 4.1 e-h**), there was no overt differences observed between the co-localisation and expression of these vascular proteins in $SOD1^{G93A}$ and WT populations. At 3-7 DIV, Gad67-GFP-positive interneuron soma and processes had distinct and robust co-localised VGLUT-1 expression (appearing white in images) that was markedly reduced by 10-14 DIV. In comparison, co-localisation of VGAT with GFP (yellow in images) at 3-7 DIV was diffuse and non-specific, but by 10-14 DIV had become distinctly punctate along GFP-positive cell soma and processes. This suggests that $SOD1^{G93A}$ Gad67-GFP cortical interneurons undergo a similar pattern of maturation to WT populations.

To examine if the migration of interneurons was affected by the $SOD1^{G93A}$ mutation, the composition of WT and $SOD1^{G93A}$ cortical cultures was characterised to determine if the proportion of different inhibitory types represented by Gad67-GFP cortical interneurons was altered in $SOD1^{G93A}$ cortical cultures, and by association, the migration of interneurons to the cortex from the ganglionic eminence. Immunocytochemistry revealed a diverse range of interneuron populations present in both the Gad67-GFP::$SOD1^{G93A}$ and Gad67-GFP::C57Bl6 (WT) cultures at 10 DIV (**Figure 4.2**). Labelling of the calcium-binding proteins CB, CR and PV showed clear and distinct cortical interneurons co-localised with GFP expression (**Figure 4.2 a-c**). Similarly, labelling of the neuropeptides, NPY, SOM and VIP identified heterogeneous interneuron populations co-localised with GFP that had a range of different morphologies (**Figure 4.2 d-f**). Assessing the extent of co-localised interneuronal and GFP fluorescence, relative to total GFP express (AU), showed no significant change in the proportion of populations represented by Gad67-GFP expression in WT and

Figure 4.1. Development of Gad67-GFP interneurons *in vitro*.

To examine neuronal maturity, dissociated Gad67-GFP interneurons were grown as a monolayer on a poly-L-lysine substrate and synaptic labelling performed at 3 DIV, 7 DIV, 10 DIV and 14 DIV. **a-b**, At 3-7 DIV triple labelling for GFP (green), the pre-synaptic maker synaptophysin (Syn, red) and post-synaptic density protein 95 (PSD-95, cyan) was diffuse in WT (**a i, b i**) and $SOD1^{G93A}$ (**a ii, b ii**) interneurons. **c-d**, At 10-14 DIV immunoreactivity for synaptophysin and PSD-95 was punctate and co-localised with GFP-positive processes and cell soma in WT (**c i, d i**) and $SOD1^{G93A}$ (**c ii, d ii**) interneurons. **e-h**, Labelling of the vesicular transporters for GABA (VGAT, red) and glutamate (VGLUT-1, cyan). **e-f**, At 3-7 DIV VGAT labelling was diffuse and VGLUT-1 was co-localised with GFP at illustrated by arrows (white in images). **g-h**, At 10-14 DIV VGAT labelling is punctate and co-localised with GFP processes as illustrated by arrows (yellow in images), while VGLUT-1 is not co-localised with GFP processes. Scale bar in (**a-h**) 20μm.

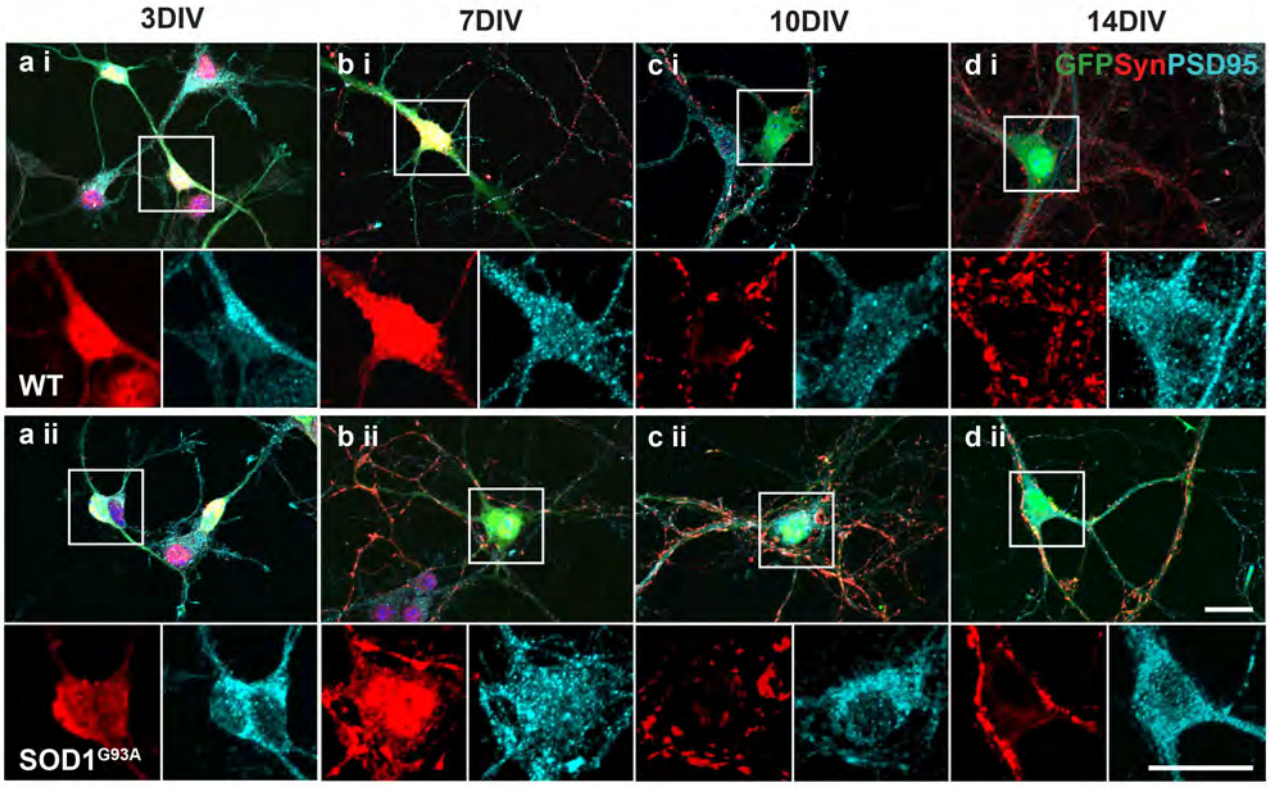
3DIV
7DIV
10DIV
14DIV
a i
b i
c i
d i
GFPSynPSD95
WT
a ii
b ii
c ii
d ii
SOD1G93A

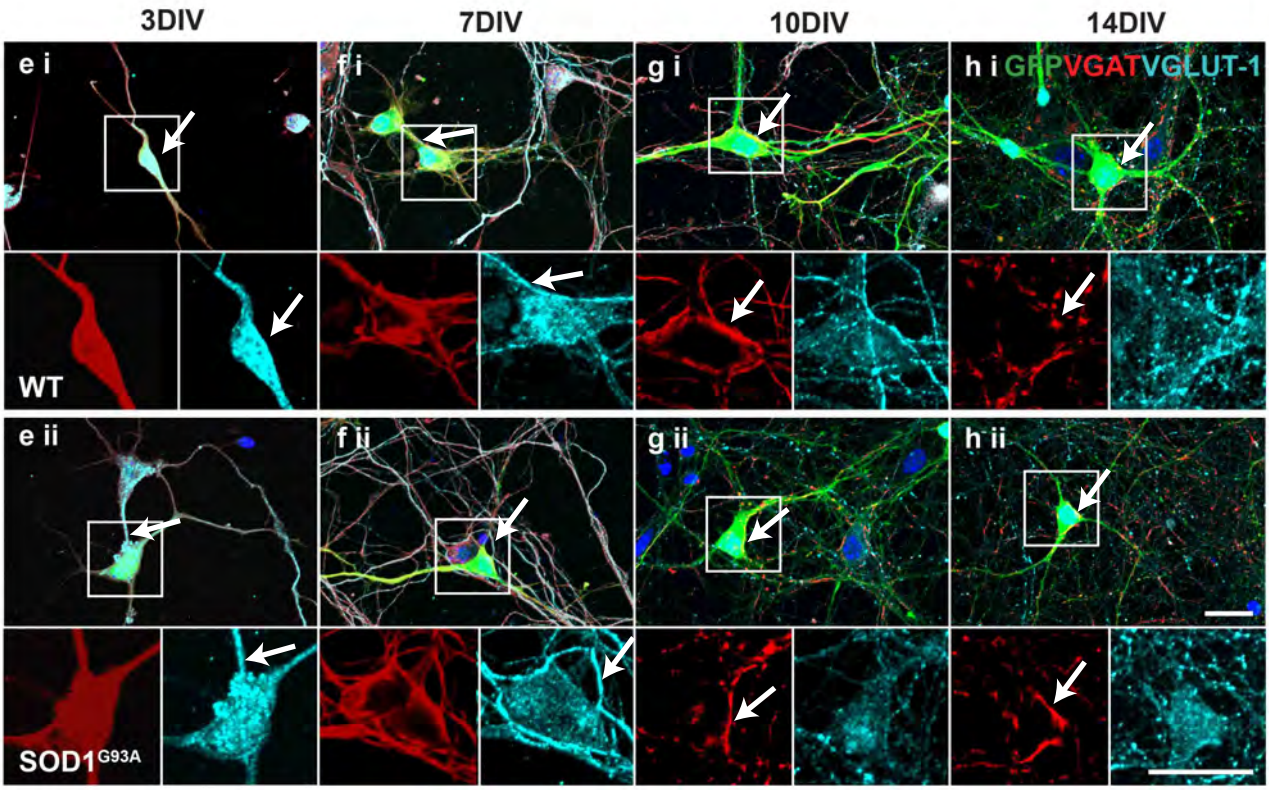
3DIV
7DIV
10DIV
14DIV
e i
f i
g i
h i GFPVGATVGLUT-1
WT
e ii
f ii
g ii
h ii
SOD1G93A

Figure 4.2. Characterisation of Gad67-GFP interneurons *in vitro*.

To determine the characteristics of Gad67-GFP^{+} interneurons *in vitro*, primary cortical cultures were derived from E15.5 embryos and grown as a monolayer on a poly-L-lysine substrate in order to label interneuron populations at 10 DIV. **a-c**, Cells were labelled for the calcium-binding proteins, calbindin (CB, **a**), calretinin (CR, **b**) and parvalbumin (PV, **c**), and the neuropeptides, neuropeptide Y (NPY, **d**), somatostatin (SOM, **e**) and vasoactive intestinal peptide (VIP, **f**) in Gad67::WT (**i**) and Gad67::SOD1^{G93A} (**ii**) cortical cultures. Double labelling of interneuronal markers with Gad67-GFP identified key inhibitory cortical interneuron populations co-localised with GFP, as shown in inserts. **g**, Analysis of the relative expression of interneuron marker fluorescence co-localised with Gad67-GFP expression, relative to total GFP expression, revealed no significant difference in the proportion of interneuron subtypes represented by Gad67-GFP interneurons in WT and SOD1^{G93A} cultures ($P < 0.05$, unpaired Student's *t* test). Scale bar in (**a-f**) 20μm.

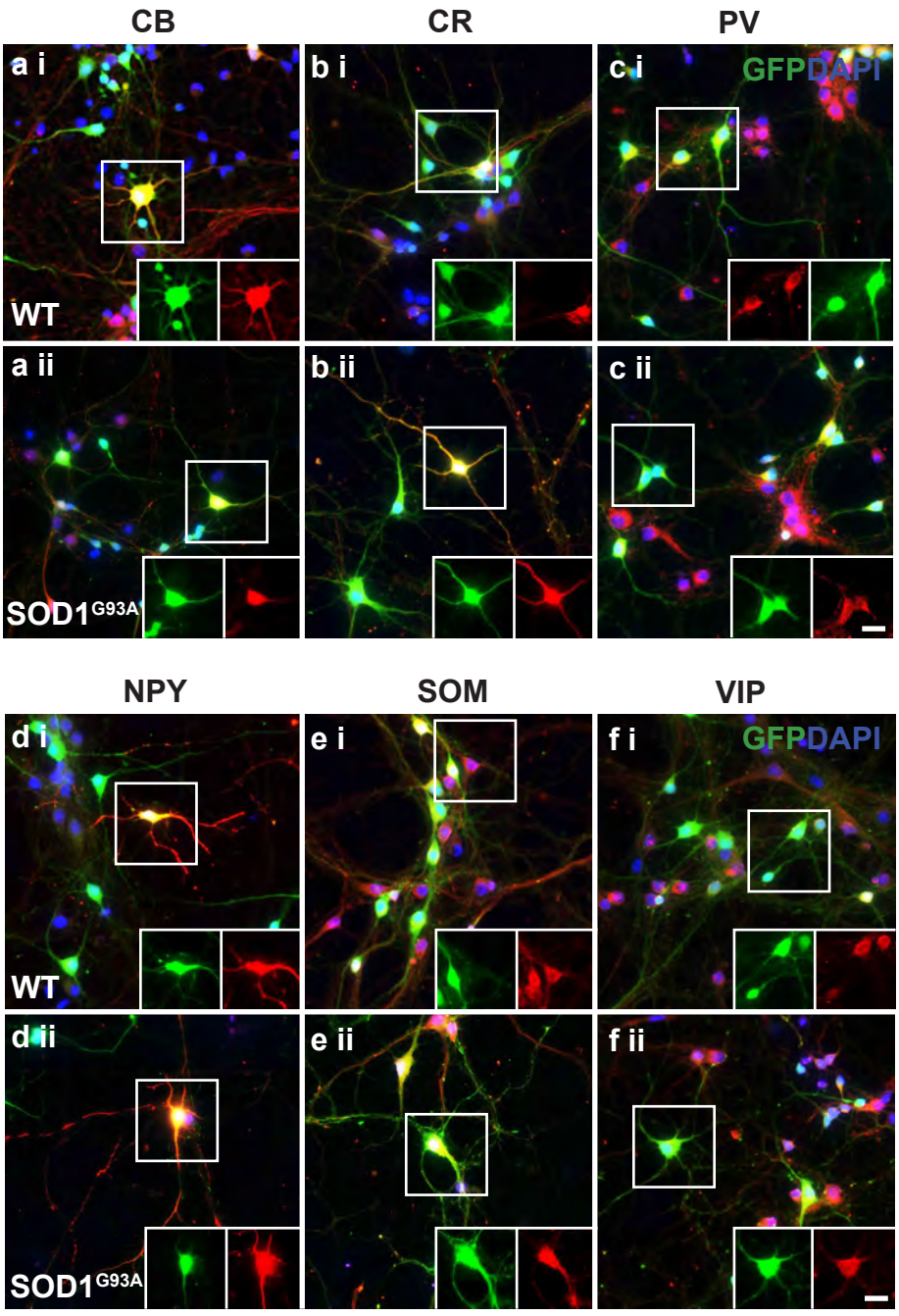
CB
CR
PV
a i
b i
c i
GFPDAPI
WT
a ii
b ii
c ii
SOD1G93A
NPY
SOM
VIP
d i
e i
f i
GFPDAPI
WT
d ii
e ii
f ii
SOD1G93A

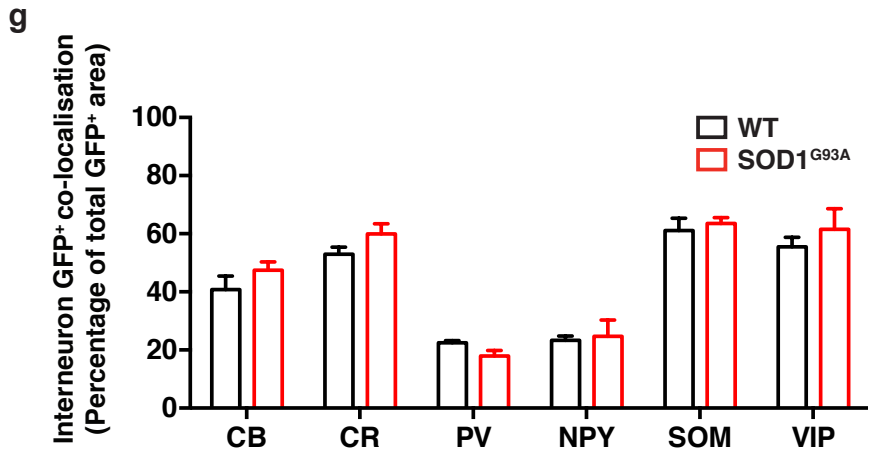
g
Interneuron GFP+ co-localisation
(Percentage of total GFP+ area)
100
80
60
40
20
0
WT
SOD1G93A
CB
CR
PV
NPY
SOM
VIP

SOD1^{G93A} cultures (P > 0.05, unpaired Student's *t* test) (**Figure 4.2 g**). These data indicate that the SOD1^{G93A} mutation might not initially affect the proportion of Gad67-GFP cortical interneurons *in vitro*.

4.3.2 The SOD1 mutation affects the electrophysiological profile of Gad67-GFP interneurons

Having established that a similar proportion of interneuron subtypes was represented by Gad67-GFP interneuron populations in SOD1^{G93A} and WT cultures, the next aim was to determine whether Gad67-GFP interneurons had altered intrinsic electrophysiological properties at this early stage of development, as has been demonstrated in motor neurons that express the SOD1^{G93A} mutation (Pieri et al 2003). Whole-cell patch clamp recordings were made from GFP-positive interneurons that were 10 DIV, which were concurrently filled with neurobiotin for post-hoc identification with streptavidin-546 labelling. As interneurons have incredibly varied electrophysiological properties (Markram et al 2004), for these analyses cortical interneurons were separated into two subclasses based on their neurite morphology (Cauli et al 2014): bipolar interneurons were considered GFP-positive interneurons with two neurobiotin filled processes originating from opposite sides of the cell soma (**Figure 4.3 a-d**) and multipolar interneurons, Gad67-GFP-positive cells with at least three neurobiotin filled processes originating from the cell body (**Figure 4.4 a-d**).

The electrophysiological profile of bipolar interneurons was first investigated and it was determined that WT populations at 10 DIV had a mean resting membrane potential (RMP) of ~ -60 mV (**Figure 4.3 e**), a capacitance of ~24 pF (**Figure 4.3 f**), an input resistance of ~610 MΩ (**Figure 4.3 g**), and a peak inward current at 0 mV of ~ -1.6 nA (**Figure 4.3 h**). Passive membrane properties are consistent with in vivo parameters of P8 E15.5-born CGE-derived cortical interneurons, although the capacitance appears lower (Karayannis et al 2012). The average threshold to excite WT bipolar interneurons was found to be ~ -42 mV (**Figure 4.3 j**), the average frequency of action potentials ~8 Hz (**Figure 4.3 k**) and the minimal strength of stimulus that can excite the cells (rheobase) ~210 pA (**Figure 4.3 l**). In the SOD1^{G93A} Gad67-GFP bipolar interneurons the previously mentioned parameters were unchanged compared to controls, including: RMP, capacitance, input resistance, peak inward current, threshold, frequency and rheobase (P > 0.05, unpaired Student's *t* test). However the peak outward current was significantly increased in SOD1^{G93A} interneurons (~1.4 ± 0.13 nA) compared to WT populations (~0.8 ± 0.07 nA, P < 0.05, unpaired Student's *t* test) (**Figure 4.3 i**). Additionally, the action potential waveform duration was significantly increased in SOD1^{G93A} interneurons (~10.48 ± 0.69 ms) compared with WT bipolar interneurons (~4.72 ± 0.99 ms, P < 0.05, unpaired Student's *t* test) (**Figure 4.3 m**). To analyse intrinsic excitability, frequency-current (*f-I*)

Figure 4.3. The SOD1^{G93A} mutation affects the peak outward current and intrinsic excitability of bipolar Gad67-GFP interneurons at 10 DIV.

To investigate the innate electrophysiological properties of bipolar interneurons, data of whole-cell patched clamped interneurons with two neurobiotin-positive processes visible was pooled. **a**, Phase image of whole-cell patch clamped bipolar interneurons (**a**) from Gad67::WT (**a i**) and Gad67::SOD1^{G93A} (**a ii**) primary cultures. **b-d**, Patched interneurons were GFP-positive (**b**), with neurobiotin-filled interneurons labelled by streptavidin-546 (**c**) used to post-hoc identify bipolar morphology based on co-localised labelling with GFP (**d**). Graphs show the average electrophysiological data for WT and SOD1^{G93A} cultures at 10 DIV, with individually patched interneurons represented as data points. **e-m**, Intrinsic parameters of bipolar SOD1^{G93A} interneurons showed no change relative to controls in resting membrane potential (RMP, **e**) capacitance (**f**), input resistance (**g**), peak inward current (**h**), threshold (**j**), frequency (**k**) or rheobase (**l**), while peak outward current was significantly increased in SOD1^{G93A} interneurons (**i**), as was the duration of action potential waveform (**m**) (*$P < 0.05$, unpaired Student's *t* test) **n**, The average frequency of action potentials plotted against injected current show that the intrinsic excitability of bipolar SOD1^{G93A} interneurons is significantly decreased compared with WT populations (*$P < 0.05$, paired Student's *t* test). Scale bar in (**a-d**) 20μm.

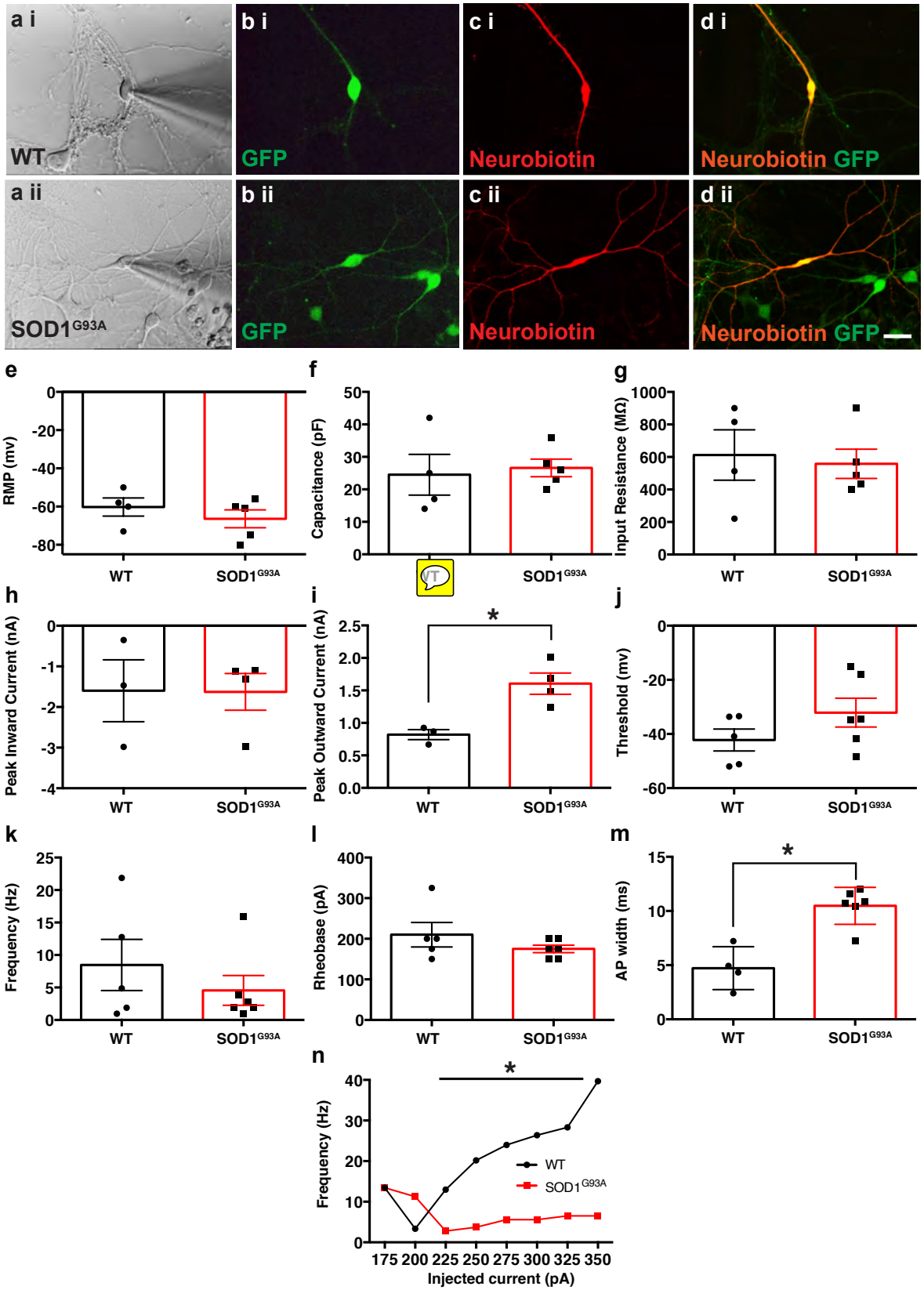
a i
b i
c i
d i
WT
GFP
Neurobiotin
Neurobiotin GFP
a ii
b ii
c ii
d ii
SOD1G93A
GFP
Neurobiotin
Neurobiotin GFP
e
RMP (mv)
0
-20
-40
-60
-80
WT
SOD1G93A
f
Capacitance (pF)
50
40
30
20
10
0
WT
SOD1G93A
g
Input Resistance (MΩ)
1000
800
600
400
200
0
WT
SOD1G93A
h
Peak Inward Current (nA)
0
-1
-2
-3
-4
WT
SOD1G93A
i
Peak Outward Current (nA)
2.5
2.0
1.5
1.0
0.5
0.0
*
WT
SOD1G93A
j
Threshold (mv)
0
-20
-40
-60
WT
SOD1G93A
k
Frequency (Hz)
25
20
15
10
5
0
WT
SOD1G93A
l
Rheobase (pA)
400
300
200
100
0
WT
SOD1G93A
m
AP width (ms)
15
10
5
0
*
WT
SOD1G93A
n
Frequency (Hz)
40
30
20
10
0
*
WT
SOD1G93A
175 200 225 250 275 300 325 350
Injected current (pA)

relationships were generated from responses to a series of depolarising current steps (100 to 500pA, in 25 pA increments, 200 ms duration). Comparisons were performed on data pooled from recordings of bipolar cells and it was found that SOD1^{G93A} interneurons fired at significantly lower rates than WT interneurons ($P < 0.05$, paired Student's *t* test) (**Figure 4.3 m**). This suggests that at this early developmental stage the SOD1^{G93A} mutation may alter the intrinsic excitability and intrinsic properties of bipolar interneurons.

To assess whether this altered electrophysiological profile was unique to bipolar interneurons, multipolar interneurons were next examined. Similar to bipolar interneurons, the RMP, capacitance, input resistance, peak inward current, threshold, frequency and rheobase were unaltered in Gad67-GFP-positive SOD1^{G93A} multipolar interneurons compared to Gad67-GFP-positive WT multipolar interneurons ($P > 0.05$, unpaired Student's *t* test) (**Figure 4.4**). At 10 DIV the WT multipolar interneurons had a RMP of ~ -68 mV (**Figure 4.4 e**), a capacitance of ~32 pF (**Figure 4.4 f**), an input resistance of ~520 MΩ (**Figure 4.4 g**), and a peak inward current at 0 mV of ~ -1.9 nA (**Figure 4.4 h**). The average threshold to excite WT bipolar interneurons was found to be ~ -36 mV (**Figure 4.4 j**), the average frequency of action potentials ~6 Hz (**Figure 4.3 k**), rheobase ~171 pA (**Figure 4.3 l**) and action potential duration ~6 ms (**Figure 4.3 m**). However, SOD1^{G93A} derived multipolar interneurons had contrasting alterations in peak outward current and action potential waveform compared to bipolar populations. While the action potential waveform duration was unaltered compared to WT multipolar populations, the peak outward current in SOD1^{G93A} multipolar interneurons was decreased (SOD1^{G93A}, ~1.1 ± 0.2 nA; WT, ~2.0 ± 0.2 nA, $P < 0.05$), in direct contrast to the magnitude of response observed in SOD1^{G93A} bipolar interneurons (**Figure 4.4 i**). Assessment of intrinsic excitability showed that SOD1^{G93A} multipolar interneurons also fired at significantly lower rates compared with WT populations ($P < 0.05$, paired Student's *t* test) (**Figure 4.4 n**). This indicates that there are differential responses of bipolar and multipolar interneurons to the expression of the SOD1^{G93A} mutation, however the intrinsic excitability of these populations appears to be similarly affected.

4.3.3 The SOD1 mutation affects the morphological development of Gad67-GFP interneurons

During development the maturation of cortical interneuron processes has been shown to be an activity-dependent process, with perturbed excitability shown to differentially influence the neurite path length of discrete interneuron populations (De Marco Garcia et al 2011, Le Magueresse & Monyer 2013). As the intrinsic excitability of interneurons was altered, and the peak outward current was differentially altered, the next aim of this study was to determine whether the presence of the

Figure 4.4. The SOD1^{G93A} mutation affects the peak outward current and intrinsic excitability of multipolar Gad67-GFP interneurons at 10 DIV.

To investigate the innate electrophysiological properties of multipolar interneurons, data of whole-cell patched clamped interneurons with more than two neurobiotin-positive processes visible was pooled. **a**, Phase image of whole-cell patch clamped multipolar interneurons (**a**) from Gad67::WT (**a i**) and Gad67::SOD1^{G93A} (**a ii**) primary cultures. **b-d**, Patched interneurons were GFP-positive (**b**), with neurobiotin-filled interneurons labelled by streptavidin-546 (**c**) used to post-hoc identify multipolar morphology based on co-localised labelling with GFP (**d**). Graphs show the average electrophysiological data for WT and SOD1^{G93A} cultures at 10 DIV, with individually patched interneurons represented as data points. **e-m**, Intrinsic parameters of multipolar SOD1^{G93A} interneurons showed no change relative to controls in resting membrane potential (RMP, **e**) capacitance (**f**), input resistance (**g**), peak inward current (**h**), threshold (**j**), frequency (**k**) rheobase (**l**), or action potential waveform duration, (**m**) while peak outward current was significantly decreased in SOD1^{G93A} interneurons (**i**) (*$P < 0.05$, unpaired Student's *t* test). **n**, The frequency of action potentials evoked for a range of current injections show that the intrinsic excitability of multipolar SOD1^{G93A} interneurons is significantly decreased compared with WT populations (*$P < 0.05$, paired Student's *t* test). Scale bar in (**a-d**) 20μm.

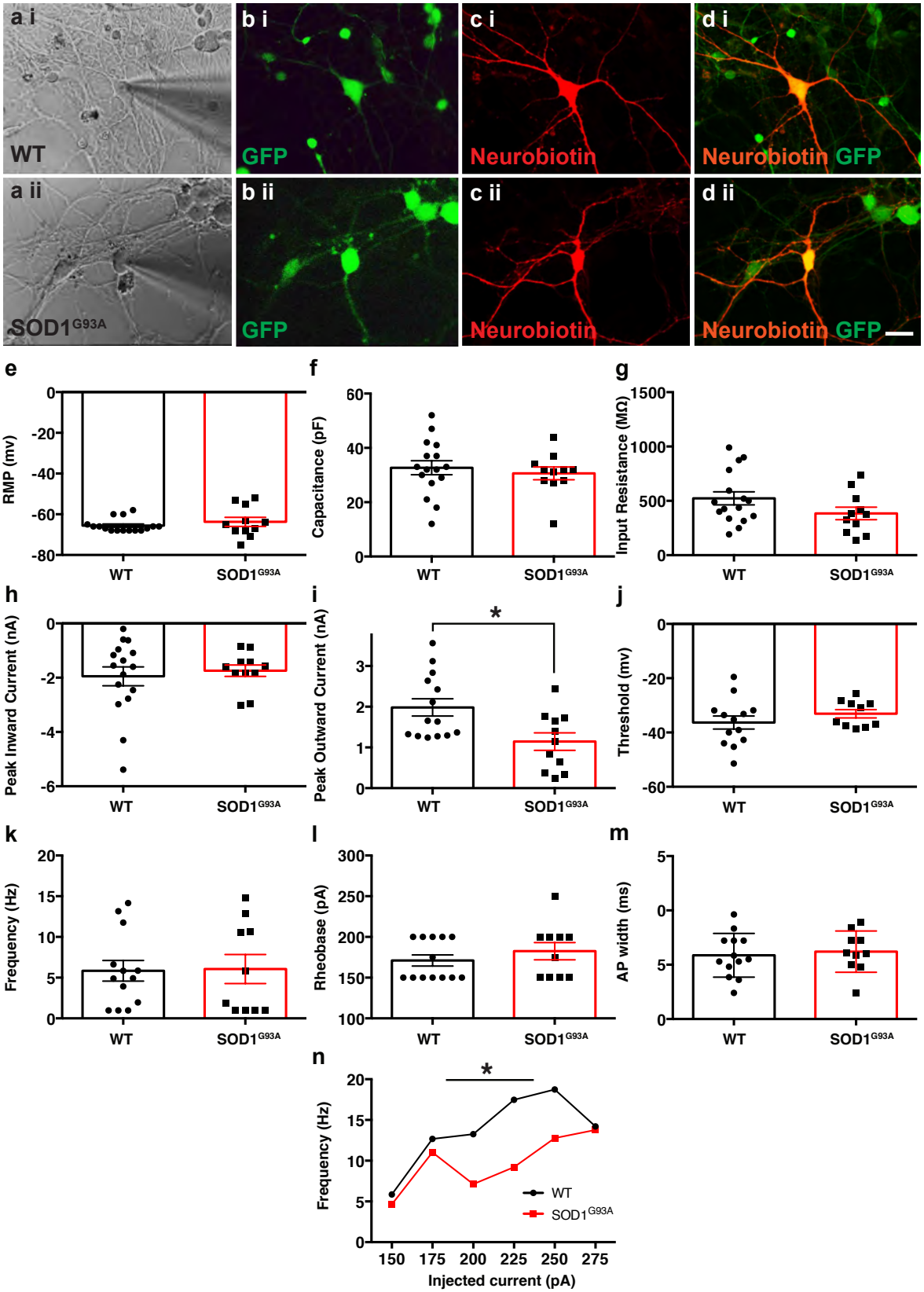
a i
WT
b i
GFP
c i
Neurobiotin
d i
Neurobiotin GFP
a ii
SOD1G93A
b ii
GFP
c ii
Neurobiotin
d ii
Neurobiotin GFP
e
RMP (mv)
0
-20
-40
-60
-80
WT
SOD1G93A
f
Capacitance (pF)
60
40
20
0
WT
SOD1G93A
g
Input Resistance (MΩ)
1500
1000
500
0
WT
SOD1G93A
h
Peak Inward Current (nA)
0
-2
-4
-6
WT
SOD1G93A
i
Peak Outward Current (nA)
*
3
2
1
0
WT
SOD1G93A
j
Threshold (mv)
0
-20
-40
-60
WT
SOD1G93A
k
Frequency (Hz)
20
15
10
5
0
WT
SOD1G93A
l
Rheobase (pA)
300
250
200
150
100
WT
SOD1G93A
m
AP width (ms)
5
0
5
0
WT
SOD1G93A
n
*
Frequency (Hz)
20
15
10
5
0
WT
SOD1G93A
150
175
200
225
250
275
Injected current (pA)

SOD1 mutation altered the development of interneuron morphology *in vitro*. To examine interneuron morphology, neurobiotin filled whole-cell patch clamped Gad67-GFP interneurons were post-hoc labelled with streptavidin-546 and reconstructed to assess neurite complexity. Morphological assessment was divided into bipolar and multipolar interneuron populations. The initial examination of bipolar interneurons identified cells with well-developed neurite trees (**Figure 4.5 a**), which morphologically resembled previous descriptions of cortical bipolar interneurons (Freund & Buzsaki 1996) and appeared similar to $SOD1^{G93A}$ populations (**Figure 4.5 b**). This was confirmed by the assessment of neurite complexity by Sholl analysis ($P > 0.05$, unpaired Student's *t* test) (**Figure 4.5 c**), and the additional examination of branch order, total neurite tree path length and total branch numbers ($P > 0.05$, unpaired Student's *t* test) (**Figure 4.5 d-f**), which were also unaltered in cumulative frequency distribution plots of $SOD1^{G93A}$ bipolar interneurons compared with WT populations ($P > 0.05$, Kolmogorov-Smirnov test, n = 16 interneurons analysed across n = 5 cultures per genotype) (**Figure 4.5 g-i**).

In contrast, assessment of the multipolar $SOD1^{G93A}$ interneurons revealed a larger and more complex neurite tree (**Figure 4.6 a**) compared with multipolar WT interneurons (**Figure 4.6 b**). By performing a sholl analysis it was determined that $SOD1^{G93A}$ most significantly affected branching in the intermediate zone of the multipolar interneuron neurite arbor, ~100-250μm from cell soma ($P < 0.05$, unpaired Student's *t* test) (**Figure 4.6 c**). By examining branch orders on neurite trees it was confirmed that multipolar $SOD1^{G93A}$ interneurons had increased complexity compared with WT multipolar interneurons ($SOD1^{G93A}$, 15 ± 1.6; WT, 11 ± 0.7, $P < 0.05$) (**Figure 4.6 d**). This was emphasised by a significant increase in total neurite tree path length ($SOD1^{G93A}$, 2467 ± 264μm; WT, 3801 ± 506μm, $P < 0.05$) (**Figure 4.6 e**) and total branch number of multipolar interneurons ($SOD1^{G93A}$, 135 ± 13; WT, 98 ± 10, $P < 0.05$) (unpaired Student's *t* test) (**Figure 4.6 f**). The right-shifted cumulative frequency plots, showing that $SOD1^{G93A}$ multipolar interneurons have more neurite branches, a longer neurite path length and total branch numbers relative to WT multipolar interneurons, further highlighting this phenotype ($P < 0.05$, Kolmogorov-Smirnov test, n = 31 interneurons analysed across n = 6 cultures per genotype) (**Figures 4.6 g-i**). These date indicate that although the intrinsic electrophysiological profiles of both bipolar and multipolar interneurons are altered, multipolar interneuron populations may be more susceptible during morphological development. Of note, a correlation analysis found that multipolar interneuron morphology was not correlated with firing frequency of these cells relative to total branch number ($SOD1^{G93A}$, R^2 0.01, $P > 0.72$) and length ($SOD1^{G93A}$, R^2 0.05, $P > 0.51$), nor was branch number ($SOD1^{G93A}$, R^2 0.02, $P > 0.66$) and length ($SOD1^{G93A}$, R^2 0.06, $P > 0.43$) correlated to their peak outward current.

Figure 4.5. The SOD1^{G93A} mutation does not affect the morphological development of Gad67-GFP bipolar interneurons at 10 DIV.

In order to assess the morphology of bipolar interneurons *in vitro*, patch-clamped Gad67-GFP interneurons were post-hoc labelled for neurobiotin to visualise processes. **a-b,** Bipolar interneurons (with only two processes extending from the cell soma) positive for GAD67-GFP and neurobiotin were identified and reconstructed from Gad67::WT (**a**) and Gad67::SOD1^{G93A} (**b**) primary cultures. Each concentric circle represents 10μm, and each dashed line represents 50μm, from the cell soma. (**c-f**), Traced interneurons show that neurite complexity by Sholl analysis (**c**), magnitude of branching order (**d**), total neurite tree path length (**e**), and total branch number (**f**) were unaltered in bipolar SOD1^{G93A} interneurons compared with WT interneurons ($P > 0.05$, unpaired Student's *t* test). **g-i**, The similarity of SOD1^{G93A} bipolar interneurons with WT populations is emphasised by overlap of measures in cumulative frequency distribution plots ($P > 0.05$, Kolmogorov-Smirnov test to compare cumulative distributions).

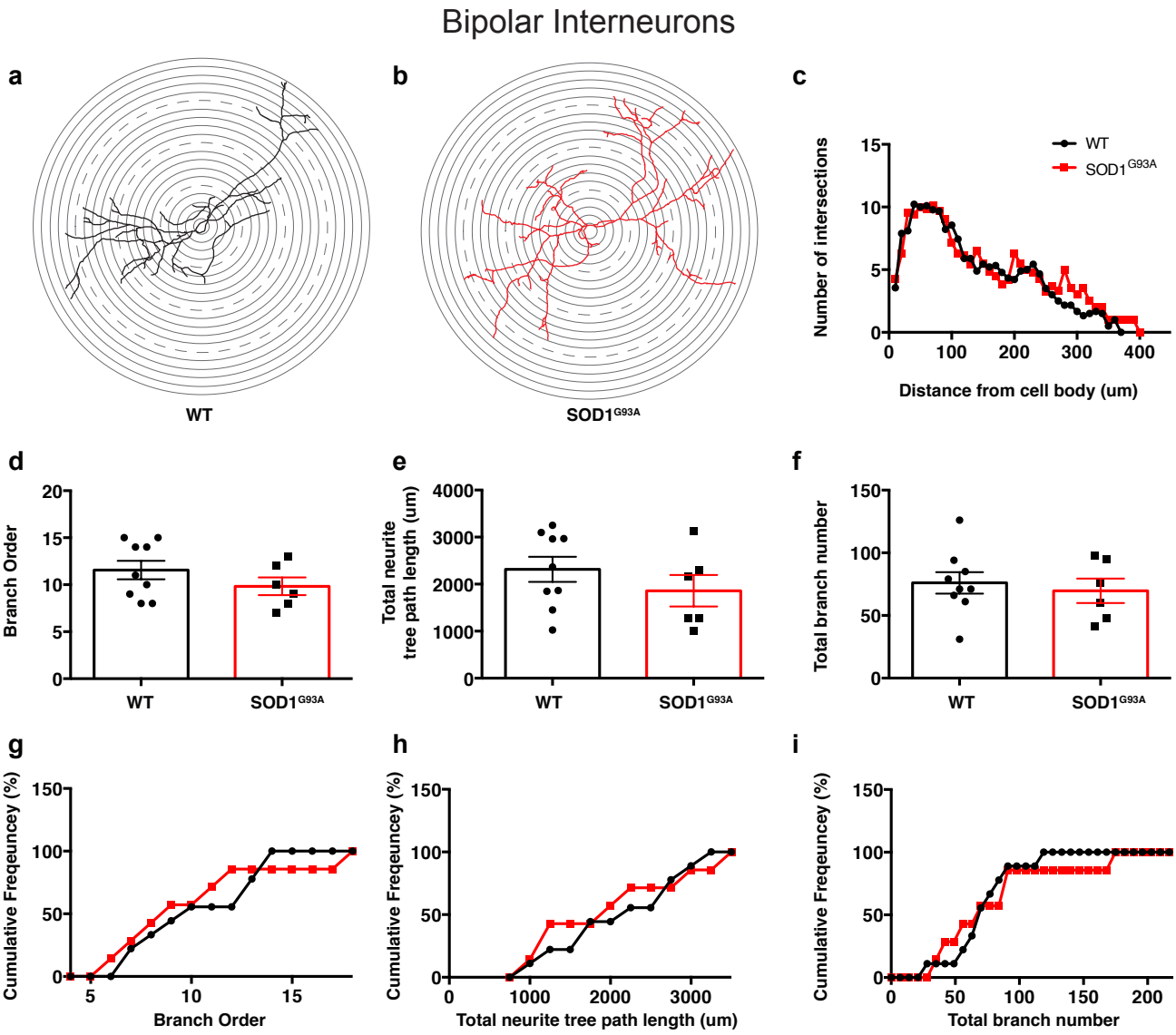
Bipolar Interneurons
a
b
c
WT
SOD1G93A
Number of intersections
Distance from cell body (um)
WT
SOD1G93A
d
e
f
Branch Order
Total neurite tree path length (um)
Total branch number
g
h
i
Cumulative Freqeuncey (%)
Branch Order
Total neurite tree path length (um)
Total branch number

Figure 4.6. The SOD1^{G93A} mutation affects the morphological development of Gad67-GFP multipolar interneurons at 10 DIV.

a-b, To assess the morphology of multipolar interneurons *in vitro*, patch-clamped Gad67-GFP interneurons (with more than two processes extending from the cell soma) positive for neurobiotin were identified and reconstructed from Gad67::WT (**a**) and Gad67::SOD1^{G93A} (**b**) primary cultures. Each concentric circle represents 10μm, and each dashed line represents 50μm, from the cell soma. **a-c**, In traced neurons (**a-b**) the bolded dashed lines represent the 100-250μm zone from the cell soma in which SOD1^{G93A} multipolar interneurons have significantly increased neurite complexity compared to WT populations (**c**) as demonstrated by Sholl analysis (*P < 0.05, unpaired Student's t test). **d-f**, Graphs show the magnitude of branching order (**d**), total neurite tree path length (**e**), and total branch number (**f**) was significantly increased in multipolar SOD1^{G93A} interneurons compared with WT populations (*P < 0.05, unpaired Student's t test). **g-i**, A greater percentage of multipolar SOD1^{G93A} interneurons had higher order processes (**g**), a longer total neurite path length (**h**), and an increased total branch number (**i**) as emphasised by the right shift in the cumulative frequency distribution plots compared to WT distributions (*P < 0.05, Kolmogorov-Smirnov test to compare cumulative distributions).

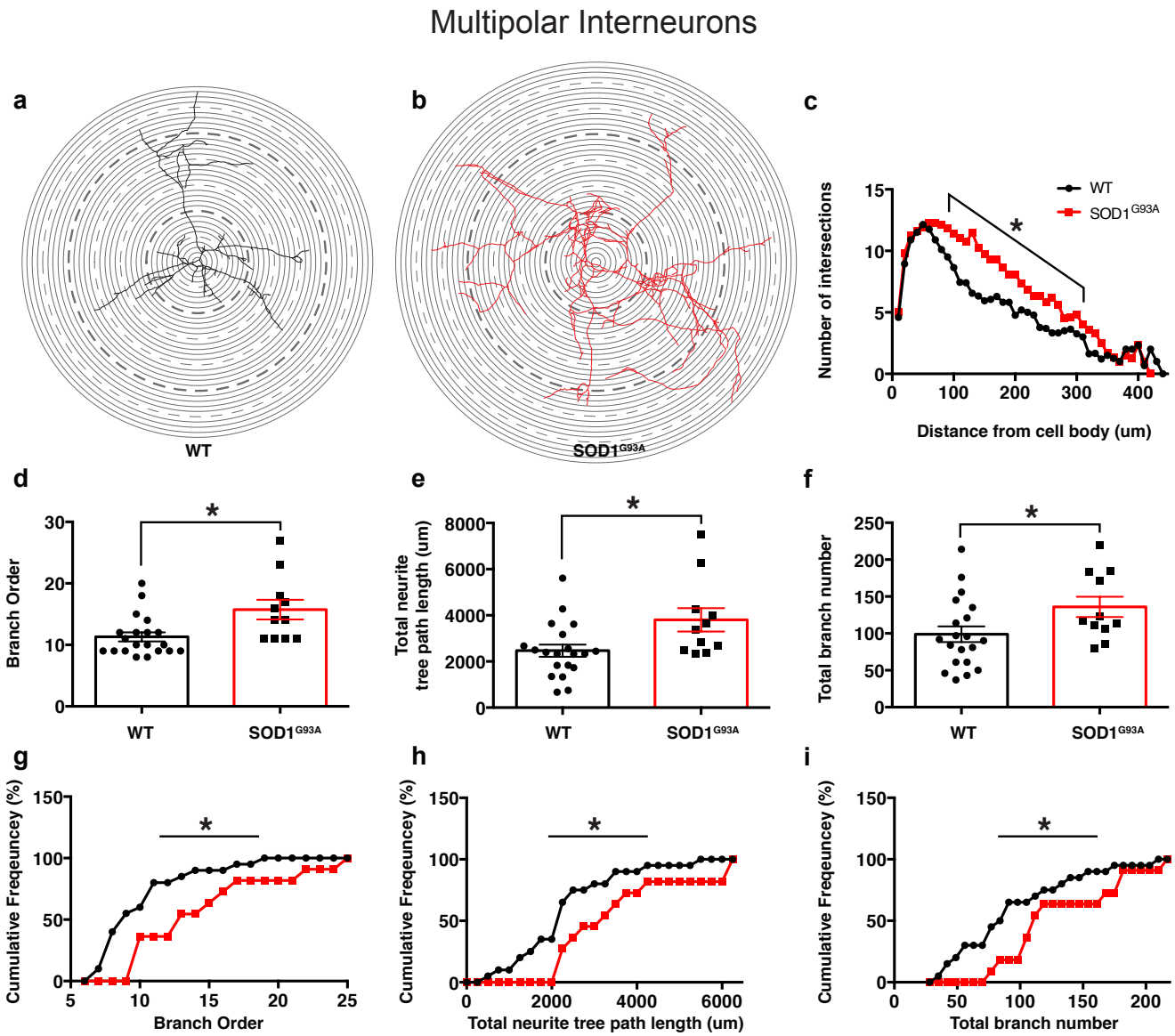
Multipolar Interneurons
a
b
c
WT
SOD1G93A
Number of intersections
Distance from cell body (um)
WT
SOD1G93A
d
e
f
Branch Order
Total neurite tree path length (um)
Total branch number
g
h
i
Cumulative Freqeuncey (%)
Branch Order
Total neurite tree path length (um)
Total branch number

4.4 DISCUSSION

ALS is a non-cell autonomous neurodegenerative disease in which pathogenic processes initiated during early post-natal development may insidiously prime networks to fail later in life. The previous findings form this thesis support the early and continual involvement of specific interneuron populations throughout the disease course of the $SOD1^{G93A}$ mouse. In addition, the recapitulation of findings in the ALS motor cortex has suggested that cortical interneuronal involvement may be related to pathology and potentially to pathophysiology in this key disease-affected region. However, several aspects of the role of cortical interneurons in disease remain unclear, including whether they are inherently vulnerable in the ALS network, potentially due to alterations in network excitability, or whether they may be innately susceptible to the expression of ALS mutations, such as the $SOD1^{G93A}$ mutation, at the cellular level. The current chapter investigated the effect of the $SOD1^{G93A}$ mutation on cortical interneuron maturation, morphological development and intrinsic function *in vitro*, in order to firstly ascertain if cortical interneurons are altered during development and secondly, to determine the validity of intrinsic or activity-driven alterations.

4.4.1 Cortical interneurons are susceptible to $SOD1^{G93A}$ during development

In this chapter, electrophysiological and morphological data provide considerable evidence for abnormal cortical interneuron development, which includes the alteration of neurite morphology and intrinsic firing properties; parameters that are also altered in motor neurons with the $SOD1^{G93A}$ mutation. It is demonstrated that cortical interneurons develop appropriate passive membrane properties in both control and $SOD1^{G93A}$ cortical interneurons, including membrane capacitance, input resistance and resting membrane potential. However, it is revealed that reduced spontaneous intrinsic activity and altered peak outward current occur in $SOD1^{G93A}$ derived cortical interneurons. Additionally, there appears to be a differential involvement of the peak outward current and action potential waveform in bipolar and multipolar populations. The action potential waveform was slower in $SOD1^{G93A}$ bipolar interneurons compared with WT equivalents, while it was unaltered in $SOD1^{G93A}$ multipolar interneurons. The peak outward current was decreased in $SOD1^{G93A}$ multipolar interneurons and increased in $SOD1^{G93A}$ bipolar interneurons, while in both cell populations an intrinsic reduction in excitability appears to be a consistent feature. This novel data indicates that early interneuron dysfunction may arise from altered biophysical properties that differentially influence the peak outward current and the action potential waveform in bipolar and multipolar cortical interneurons, which may contribute to the initiation of downstream degenerative pathways that predate their role in cortical circuits later in life.

4.4.2 A role for potassium channels?

Previous studies in animal models and in FALS patients have focused on persistent sodium currents as a mechanism of motor neuron hyperexcitability (Kuo et al 2005, Pieri et al 2009, Vucic & Kiernan 2010), however, more recently studies in patient-derived motor neurons have suggested the additional importance of voltage-activated potassium channels (Wainger et al 2014, Devlin et al 2015). Devlin and colleagues used modelling to predict that the mode of alteration of motor neurons derived from patients with TARDBP and C9orf72 mutations was likely reflected by perturbation of sodium and potassium currents (Devlin et al 2015). While they speculate that a general switch from hyperexcitability to hypoexcitability may result from a loss of ion channels in these cells, Wainger and colleagues demonstrate that patient-derived motor neurons with a SOD1 mutation have no difference in sodium current peak amplitudes, but instead a reduction in delayed-rectifier current magnitude attributed to decreased function of voltage-activated potassium channels (Wainger et al 2014). Administration of the Kv7 channel activator retigabine was found to reverse hyperexcitability observed in this model. In line with a more generalised mechanism of potassium channels involvement in the disease, hyper-methylation and down-regulation of potassium channel genes has also been observed in epigenetic studies of sporadic ALS (Figueroa-Romero et al 2012). While the pathways connecting disease-causing mutations with altered ion channels remain to be elucidated, the epigenetic suppression of potassium channels may indicate a convergent susceptibility in the disease, which may be instigated by accumulation of environmental stressors throughout a person's life, or at birth, through inherited mutation.

Of relevance to this study, a previous publication has described a subtype-specific response of interneurons to the expression of the Kir2.1 inward-rectifier potassium ion channel (Karayannis et al 2012). In this study, Kir2.1 expression in interneurons derived from the caudal ganglionic eminence induced intrinsic hypoexcitability, leading to a marked developmental change in intrinsic electrophysiological properties, specifically, a slower duration of the action potential waveform. In addition, there was a distinct lack of intrinsic or activity-dependent compensation for these alterations. This may be relevant to the findings of this study, as the majority of interneurons derived from the caudal ganglionic eminence are bipolar interneurons (Fogarty et al 2007), and the predominant response of these cells to $SOD1^{G93A}$ expression in this study was through altered intrinsic electrophysiological properties, namely altered peak outward current, intrinsic hypoexcitability and the bipolar-specific slowing of the action potential waveform. Therefore, as there is a precedent for perturbation of potassium channels in both sporadic and familial ALS (Wainger et al 2014), it may be likely that the alteration of bipolar cortical interneurons is also

initiated by aberrant function of potassium channels. However, such a model does not explain the alterations observed in the multipolar populations.

In multipolar interneurons hypoexcitability was identified similar to bipolar interneurons, but the action potential waveform was unaltered and an inverse response to the peak outward current was demonstrated in addition to the presence of a more elaborate neurite tree. A number of factors may contribute to the different responses observed in bipolar and multipolar interneurons, including the distinctly different embryonic origins of bipolar and multipolar interneuron subtypes. As bipolar interneurons arise from the caudal ganglionic eminence and multipolar interneurons are predominately generated within the medial ganglionic eminence (Fogarty et al 2007, Miyoshi et al 2007, Colasante & Sessa 2010), by a developmental classification system they are considered distinctly different interneuron classes. Moreover, interneurons generated within these areas are conferred distinct ion channel properties, morphology and immunohistochemical profiles that delineate further distinct classification of interneuron subtypes (Wonders & Anderson 2006). Therefore, distinct ion channels present on bipolar and multipolar interneuron subtypes could determine their response, and innate vulnerability to the $SOD1^{G93A}$ mutation, particularly if the $SOD1^{G93A}$ mutation interacts with specific subsets of ion channels, as has been indicated by previous research (Kuo et al 2005, van Zundert et al 2008).

A SOD1-dependent pathogenic mechanism targeting specific ion channels on interneurons could explain the different responses in peak outward current and action potential waveform, as these measures of neuronal activity are both highly influenced by ion channel composition and kinetics (McBain & Fisahn 2001). Therefore, it would be interesting to employ pharmacological approaches to further explore specific ion channels involved in the peak outward current and action waveform duration. This may provide further insight into SOD1-dependent mechanisms, and allow for better comparison of ALS literature about early modification of circuitry in the developing ALS cortex.

4.4.3 The morphology of select cortical interneuron populations is affected during development in the presence of the $SOD1^{G93A}$ mutation

While this study suggests an importance of the intrinsic biophysical properties of cortical interneurons in relation to development of normal function, altered morphological development may also be an important feature of the innate interneuron response to the presence of the $SOD1^{G93A}$ mutation. Post-hoc labelling of whole-cell patch clamped interneurons demonstrated a distinct difference between the presence and absence of a morphological phenotype in multipolar and bipolar interneuron subtypes, respectively. While there is limited understanding of the key factors required

for normal maturation of interneuron morphology throughout development (Le Magueresse & Monyer 2013), it is increasingly recognised that the maturation of GABAergic neurotransmission is a protracted process that takes place in discrete steps and results from a dynamic interaction between developmentally directed gene expression and brain activity (Ben-Ari 2002). The differentiation of interneuronal subtypes is primarily attributed to this first process, and is largely defined prior to migration out of the ganglionic eminence (Wonders & Anderson 2006, Le Magueresse & Monyer 2013). However, a study by De Marco Garcia and colleagues has demonstrated that the migration and development of particularly neurite arbor length may be an activity-dependent process that differentially affects discrete interneuron populations (De Marco Garcia et al 2011). Therefore, in the context of the increased neurite arbor demonstrated in multipolar $SOD1^{G93A}$ derived interneurons, this may reflect a change in the innervation field of these cells secondary to altered excitability in the cortical culture.

It remains to be determined what may initially drive any altered excitability in the presence of the $SOD1^{G93A}$ mutation, whether this is caused by interneurons directly, or quite possibly by an initial alteration of excitatory pyramidal neurons in the culture. However, it appears that the alteration in morphology of multipolar $SOD1^{G93A}$ interneurons is not directly correlated with the altered firing frequency or peak outward current of these cells. It is widely documented that hyperexcitability does exist in the $SOD1^{G93A}$ model at developmental stages (Kuo et al 2004, Pieri et al 2009). If excitatory neurons do initiate alterations in excitability it could be possible that they may contribute to the development of altered intrinsic excitability of interneurons (Pieri et al 2009). However, as it is poorly understood to what extent the intrinsic firing properties of interneurons are determined by activity during development, or are pre-determined by a genetic trajectory (Le Magueresse & Monyer 2013), further investigations will be required to establish if interneuron deficits develop independent of pyramidal neurons with the $SOD1^{G93A}$ mutation. Nonetheless, this data indicates that bipolar and multipolar interneurons have innately different responses to the presence of the $SOD1^{G93A}$ mutation. Whether this is mediated by altered network activity through excitatory neurons or by distinct ion channel compositions in a cell autonomous manner remains to be determined.

4.4.4 The maturation and composition of cortical cultures interneurons was similar in WT and $SOD1^{G93A}$ derived cultures.

Another possibility that requires further investigation is the notion that differences in the morphology of cortical interneuron populations might be caused by developmental acceleration of populations from distinct sub-regions of the ganglionic eminence. *In vitro* studies have suggested that alterations

in motor neuron populations may be due to an accelerated pace of maturation (van Zundert et al 2008, Quinlan et al 2011), however this was indicated by a decreased capacitance of motor neurons relative to controls, which was not observed in this study. Moreover, the synaptic and vesicular development of populations appeared unaltered in cultures, as evidenced by a similar pattern of somatic and neurotic labelling over the time course. The pattern of synaptophysin and PSD-95 labeling is consistent with normal developmental maturation of cultures (Thiel 1993, Nikonenko et al 2008) and the pattern of punctate VGAT labeling is consistent with inhibitory cell maturation (Chaudhry et al 1998). Therefore, the rate of *in vitro* development is observed to be seemingly normal, although as this later observation is not quantitative, cell sorting and quantitative expression studies may improve the strength of these interpretations.

Nonetheless, as previously mentioned, the development of interneuron networks can also be modified by altered migration in response to perturbed excitability at critical stages of development (De Marco Garcia et al 2011). Several genetic fate-mapping studies have shown that the pre-cursors of distinct cortical interneuron subtypes are generated within different regions of the ganglionic eminence [see review (Wonders & Anderson 2006)]. Pre-cursors of cortical interneurons expressing CB, PV, SOM, as well as multipolar CR interneurons, are generated exclusively from the medial ganglionic eminence, while precursors of all bipolar CR-expressing interneurons, and most NPY-expressing interneurons are generated in lateral/caudal ganglionic eminences (Fogarty et al 2007, Miyoshi et al 2010, Miyoshi & Fishell 2011). Therefore, if the mutation affected either the development or migration of interneuron subtypes from distinct regions of the ganglionic eminence, then it may bias the subtypes present in the cortex and those assessed in the E15.5 embryonic cortical cultures. As an index of potential migratory deficits, the proportion of subtypes represented by Gad67-GFP interneurons was assessed in cortical cultures, and it was found that there was no overt difference in the proportion of Gad67-GFP interneuron subtypes. Although, this result may be treated with some caution, as a better measure of interneuron migratory deficits is the use of genetic fete mapping studies. An additional consideration is that, although some Gad67-GFP interneurons are present in the neocortex by E15.5, when cortical tissue was dissociated for culture, not all have migrated from the ganglionic eminence at E15.5, nor are all interneurons in the culture labelled by GFP (Tamamaki et al 2003). As such, conclusions are limited to the proportion of Gad67-GFP interneurons that are present in the Gad67-GFP neocortex at E15.5, which are cultured, and to those that are labelled by GFP. In this respect, it is important to note that the Gad67-GFP population typically increases in number between 4 and 9 DIV, due to cell proliferation, and this population

reach a maximum size by 9-11 DIV (Southwell et al 2012). Therefore, a good representative population of Gad67-GFP interneurons is present *in vitro* at 10 DIV.

Irrespective of the need to further define the exact developmental stage when interneuron development may first become altered and the need to explore potential cortical migration deficits, it appears that there is considerable evidence for altered cortical interneuron development in the presence of the $SOD1^{G93A}$ mutation. Why this remains subclinical for such a long period, remains to be determined, however, possible explanations include the incredible capacity for inhibitory circuitry to compensate for alterations in networks through homeostatic regulatory mechanisms (Karayannis et al 2012). In the context of these current findings, it may be posited that divergent responses of bipolar and multipolar interneurons, represent a priming bipolar population, and a compensatory multipolar population that masks the effects of network dysfunction until it becomes critically saturated later in life. It will be of interest for future studies to examine how these populations functionally integrate in the ALS cortical network, particularly as there is potential for perturbation of these populations through sporadic epigenetic, and familial inherited, disease pathways.

4.4.5 Conclusion

In summary, these results indicate for the first time that distinct intrinsic biophysical properties and intrinsic firing properties of cortical interneuron populations may be innately susceptible to ALS mutations. In comparison, a distinction is made between a morphological phenotype in bipolar and multipolar cortical interneuron populations, which may highlight the unique vulnerability or contribution of these populations in the excitable ALS network. Additionally, this study demonstrates the sensitive nature of electrophysiological studies of interneuron populations, and highlights the potential importance of subtype-specific interneuronal studies to delineate the true complexity and contribution of these populations in the disease setting. Furthermore, in the context of the previous findings in this thesis, demonstrated immunohistochemical alteration of distinct populations in Chapter 2, it is suggested that further studies should be conducted to resolve the contribution of these fundamental cell types to disease circuitry in a subtype-specific manner. Collectively, this study supports an excitatory/inhibitory phenotype in the ALS condition, which may contribute to pathogenesis through the early initiation of aberrant network development, particularly as interneurons shape the functional maturation of the cortex.

Chapter 5

5 GENERAL DISCUSSION

While once considered a pure motor neuron disorder with limited cortical involvement, the view of ALS has evolved substantially in the last decade, and it is now considered a more genetically complex, multi-systemic disease with important pathogenic involvement of neuronal and non-neuronal cells. Indeed, while the classical neuropathological description of ALS focuses on degeneration of both upper and lower motor neurons, and undoubtedly the relationship between the two is fundamental to the understanding of ALS pathogenesis, it is now recognised that up to 50% of ALS patients have cognitive impairment. Frontotemporal dementia, the most common form of dementia after Alzheimer's disease, is considered part of the ALS disease spectrum, as evidenced by a combination of clinical neuroimaging, neuropathological and detailed genetic studies.

In keeping with the increased role of the cortex in the disease, TMS studies have suggested for a number of years that cortical hyperexcitability may have a central role in the disease, however, it was unclear what that role may be and the underlying basis for such a phenomenon. It was theorised that it may be caused by inhibitory deficits, but there was little evidence for this, and the non-cell autonomous view of the disease was not yet fully appreciated. Therefore, the potential role of interneurons to underlie this phenomenon was unknown, and the view of the disease in the context of an inhibitory vulnerability was largely overlooked until advancement in clinical imaging and TMS studies was able to further scrutinize the inhibitory system.

Now there is increasing evidence, including from the studies presented in this thesis, to support a role for interneurons in the disease (**Figure 5.1**).

5.1 CHARACTERISATION OF CORTICAL INTERNEURON INVOLVEMENT IN THE SOD1^{G93A} MOUSE

Chapter 2 of this thesis sought to determine if there was a cellular basis for interneuron dysfunction in the SOD1^{G93A} mouse model of ALS, in particular if cortical interneurons were affected in key disease-associated regions, and how this may manifest relative to disease progression. It was hypothesised that specific interneuron populations would be altered in the motor cortex, due to evidence of inhibitory deficits in the ALS cortex (Vucic & Kiernan 2006b, Menon et al 2014, Shibuya et al 2016) and increased excitability described in both transgenic SOD1^{G93A} models and SOD1^{G93A} patients (Vucic et al 2008, Pieri et al 2009). Data revealed a subtype-specific involvement of CR- and NPY-expressing interneurons in the motor cortex, which was apparent from symptom-onset, and supports an inhibitory phase of disease that coincides with the onset of motor neuron degeneration in this model (Ozdinler et al 2011, Jara et al 2012, Vinsant et al 2013). Changes in both

Figure 5.1. Timeline of changes in motor neuron pathology, motor neuron excitability relative to interneuron alterations in the SOD1^{G93A} mouse.

The most important and earliest abnormalities reported for the excitatory/inhibitory imbalance in the transgenic SOD1^{G93A} mouse model are shown. Weeks before motor neurons are lost and overt clinical symptoms appear (P60), widespread pathological abnormalities and changes in upper motor neuron excitability (blue) are detected in this ALS model. Inhibitory alterations (red) occur throughout the disease time course (black), but may constitute an early step in the initiation of the disease. At an early developmental stage when motor neurons are reported to be hyperexcitable, cortical interneurons are hypoexcitable and have altered morphology. Prior to symptom-onset, layer V upper motor neurons begin to degenerate and spines are reduced on their layer II/III apical dendrites at a similar time as CR neurites are altered and NPY-interneurons are decreased throughout the motor cortex. Hypoglossal motor neurons are also reported to be hyperexcitable from P70. By P90 when both upper and lower motor neurons have begun to be lost, CR-interneurons begin to be lost from the motor cortex. Weeks later (P120) NPY-interneuron cell density is increased in the motor cortex prior to end-stage in this mouse model.

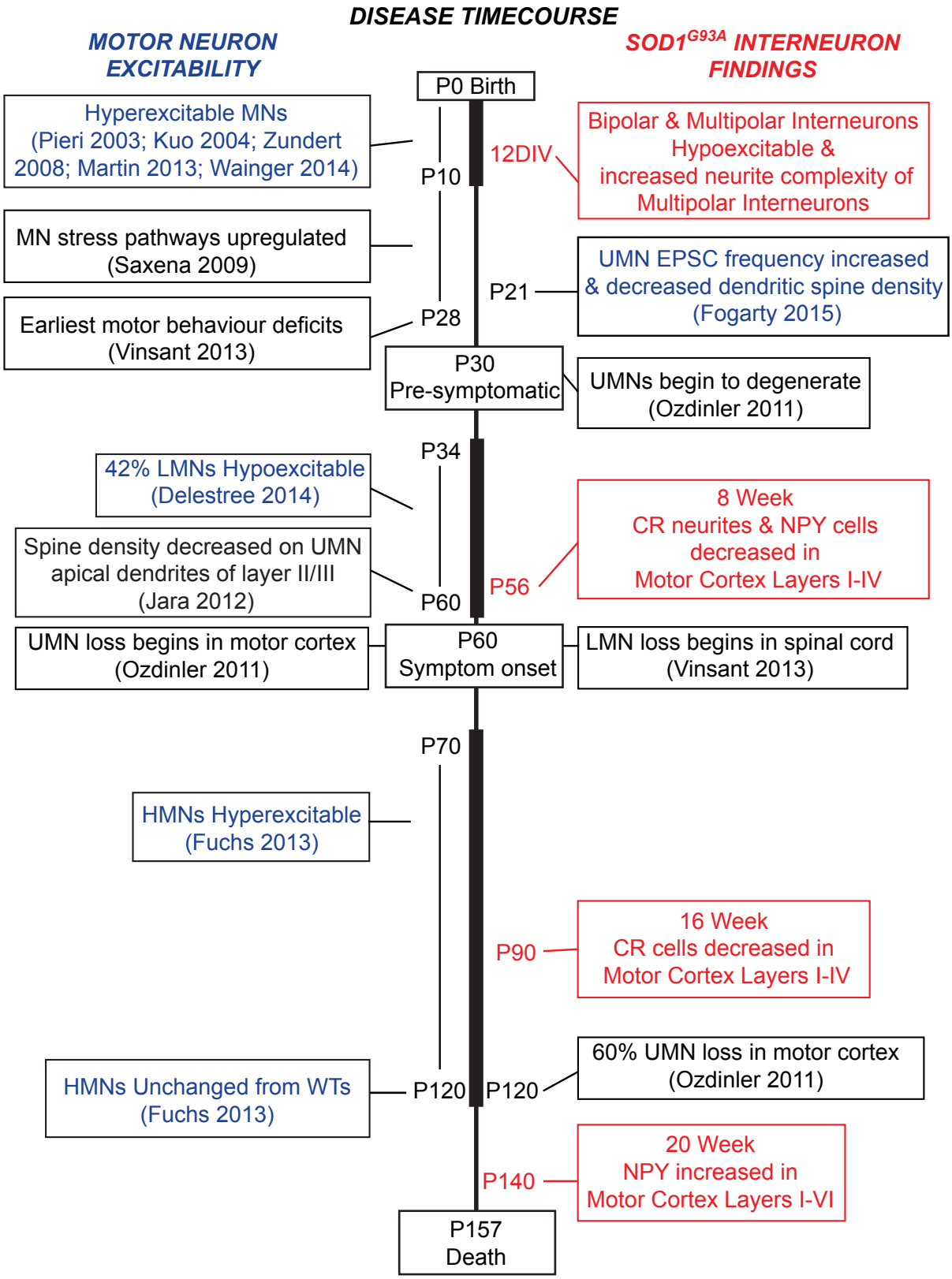
DISEASE TIMECOURSE
MOTOR NEURON EXCITABILITY
SOD1G93A INTERNEURON FINDINGS
P0 Birth
Hyperexcitable MNs (Pieri 2003; Kuo 2004; Zundert 2008; Martin 2013; Wainger 2014)
12DIV
Bipolar & Multipolar Interneurons Hypoexcitable & increased neurite complexity of Multipolar Interneurons
P10
MN stress pathways upregulated (Saxena 2009)
P21
UMN EPSC frequency increased & decreased dendritic spine density (Fogarty 2015)
Earliest motor behaviour deficits (Vinsant 2013)
P28
P30 Pre-symptomatic
UMNs begin to degenerate (Ozdinler 2011)
P34
42% LMNs Hypoexcitable (Delestree 2014)
8 Week CR neurites & NPY cells decreased in Motor Cortex Layers I-IV
Spine density decreased on UMN apical dendrites of layer II/III (Jara 2012)
P56
P60
UMN loss begins in motor cortex (Ozdinler 2011)
P60 Symptom onset
LMN loss begins in spinal cord (Vinsant 2013)
P70
HMNs Hyperexcitable (Fuchs 2013)
P90
16 Week CR cells decreased in Motor Cortex Layers I-IV
HMNs Unchanged from WTs (Fuchs 2013)
P120
P120
60% UMN loss in motor cortex (Ozdinler 2011)
P140
20 Week NPY increased in Motor Cortex Layers I-VI
P157 Death

interneuron populations were initially localised to the upper cortical layers of the motor cortex, where it was suggested that they either initiate or respond to degeneration of layer V motor neuron apical dendrites (Jara et al 2012). CR-interneurons showed a progressive alteration throughout the disease, with increased process length initially detected upon symptom onset, and a progressive decline in numbers demonstrated later in the disease, providing support for a loss of inhibitory function in the disease.

However, an interesting and unexpected finding of these studies was the contrasting nature of NPY-interneuron involvement. While initially decreased in the supragranular lamina of the motor cortex, it was increased by end-stage throughout the entire motor cortex. It was theorised that the observed late-stage increase in NPY may represent attempted compensatory mechanisms aimed at counteracting increased excitation, which may be an interesting avenue to explore in future studies for assessment of therapeutic potential (Vezzani & Sperk 2004, Kharlamov et al 2007). Indeed, extensive literature from the field of epilepsy has suggested that an increase in NPY and decrease of CR are both hallmarks of an excitable neuronal network (Kovac & Walker 2013, Toth & Magloczky 2014). While it remains to be determined if this represents a loss of these inhibitory cell populations, or a loss of the proteins that are typically used to characterise to them, it is important to note that both the proteins these cells express have important roles in modulating network excitability. More specifically, calretinin deficient cells have altered intrinsic neuronal excitability (Gall et al 2003) and CR knockout mice have a motor phenotype that worsens dramatically with increasing age, attributed to a failure of normal motor adaptation (Schwaller et al 2002). Indeed, in epilepsy studies loss of CR-expressing populations is also linked to a decline in network function (Toth & Magloczky 2014). In comparison, the release of NPY is closely associated with an anti-epileptic neuroprotective role in neuronal networks, as increased synthesis of the peptide is described after increased excitability in epilepsy models (Vezzani & Sperk 2004, Kharlamov et al 2007). Collectively, these results suggest that interneurons have an important role in disease pathophysiology within the motor cortex, and that they may have an underappreciated role in the disease, particular related to the onset of motor deficits.

5.2 IDENTIFYING INTERNEURON PATHOLOGY IN THE MOTOR CORTEX OF ALS CASES

The previous findings from Chapter 2 support the involvement of specific inhibitory populations in the $SOD1^{G93A}$ motor cortex; however, it was unknown if this was relevant to the human disease and how these populations may be implicated in the context of the ALS motor cortex. As such, Chapter 3 used a targeted approach to determine if the inhibitory phenotype detected in Chapter 2 translated to

the human cortex, and hence validate and build on the insights gained from the SOD1^{G93A} model. It was hypothesised that specific interneuron populations affected in the SOD1^{G93A} mouse would also be affected in ALS patients and associate with the extent of cortical pathology. For these analyses, the CR-, NPY- and CB-interneuron populations were selectively investigated, as they had distinctly different patterns of involvement in the SOD1^{G93A} mouse. Although only a small pilot study with a limited case numbers, the histopathological analysis provided by Chapter 3 successfully highlights a similar pattern of interneuron involvement in the ALS motor cortex to that previously reported in the SOD1^{G93A} mouse model (Chapter 2). The findings of this chapter may also highlight a novel relationship between interneuron pathology and pyramidal cell loss in the ALS motor cortex that has not been previously described.

While an interesting finding was the divergence of CR-interneuron pathology demonstrated in 50% of ALS cases, a perhaps more thought-provoking finding was the positive correlation of CR-cell loss with the extent of layer V pyramidal cell loss within the motor cortex. While direct causation of this relationship remains to be determined, it may be interesting to further investigate, as a greater extent of intracortical inhibitory dysfunction has been linked to more rapid clinical decline and shorter disease duration in sporadic ALS patients (Shibuya et al 2016). Conversely, familial SOD1 mutation carriers with preserved intracortical inhibitory circuitry have a slower disease progression (Weber et al 2000). In the context of the cortical hyperexcitability demonstrated in patients, this may suggest that the capacity of cortical interneurons to maintain their inhibitory functions is an important homeostatic mechanism to preserve motor neuron function and health in the ALS motor cortex. The differential involvement of CR-interneurons may also suggest innate differences in the vulnerability of specific interneurons in patients, which may influence the clinical phenotype. While such a link was not demonstrated in this study, it cannot be ruled out due to the nature of the small number of cases in this pilot study, particularly in the context of the genetic and clinical heterogeneity demonstrated in ALS.

Again we saw an increase in NPY-interneurons in ALS cases, as previously seen at end-stage in the SOD1^{G93A} motor cortex in Chapter 2. However, adding to these previous findings a correlation of NPY-interneurons was demonstrated between pyramidal neurons and CR-interneurons. In support of the neuroprotective role inferred from epilepsy literature discussed in Chapter 2, ALS cases with the greatest increase in NPY-populations relative to controls, had the greatest preservation of CR-interneuron and pyramidal cell density, whereas those cases with NPY-interneuron density most similar to controls had the most CR-interneuron and pyramidal cell loss. Again a comparison could be drawn between NPY involvement in ALS and that of epilepsy, as the apparent increase of NPY-

immunoreactive fibers was similar to that previously identified by other studies in the epileptic brain (Furtinger et al 2001).

Collectively, this study supported the findings and interpretations of Chapter 2, advancing our understanding of the selective vulnerability of cortical interneurons in the ALS motor cortex and the potential cellular basis of functional imaging abnormalities reported in clinical studies. Furthermore, given the surmised central role of cortical hyperexcitability in the disease, and the neuroprotective role of NPY as endogenous anti-epileptic, it again highlights the need for further investigation of these dynamic inhibitory interneuron populations, in regards to their potential to modify or compensate pathogenic excitability in the cortical motor network.

5.3 TESTING THE THEORY OF INTRINSIC INTERNEURON VULNERABILTY IN THE SOD1^{G93A} MOUSE

While the results of Chapter 2 and 3 provide support to the overarching hypothesis that ALS pathogenesis involves cortical interneuron dysfunction, they cannot differentiate if cortical interneuron involvement is instigated primary, or secondary to, increased excitability in the disease. As described previously inhibitory cell types are highly adaptive such that they may both respond to, or initiate, alterations in network excitability in the disease setting. Although increasingly recognised as a non-cell autonomous disorder (Boillee et al 2006a, Ilieva et al 2009), which is theorised to require multiple hits in order for disease symptoms to manifest (Al-Chalabi et al 2014), there is relatively limited knowledge of the innate vulnerability of interneurons in ALS. Key questions that may be central to understanding the role of these populations in disease, include determining if the motor-specific involvement of populations described in Chapters 2 and 3 are caused by their placement in a vulnerable network, secondary to altered states of excitability, or whether there is an innate susceptibility of these cells that may insidiously prime networks to fail later in life. Therefore, Chapter 4 of this thesis aimed to determine the effect of the SOD1^{G93A} mutation on interneuron development, with the hypothesis that the SOD1 mutation would affect the intrinsic function of interneurons and their normal development *in vitro*, adding to the timeline of findings from this thesis (**Figure 5.1**). This was theorised, as there is considerable evidence of increased hyperexcitability during early neonatal and embryonic stages in ALS models (Pieri et al 2003, Kuo et al 2004), and intrinsic alteration of motor neuron and excitatory cortical neuron populations is demonstrated (Pieri et al 2009, Quinlan et al 2011), while it is also appreciated that aspects of interneuron development are an activity-dependent process (Cancedda et al 2007, De Marco Garcia et al 2011, Kepecs & Fishell 2014).

Data from Chapter 4 suggests for the first time that cortical interneuron populations are innately susceptible to the presence of an ALS mutation, with intrinsic firing parameters and intrinsic excitability altered in both multipolar and bipolar cortical interneurons. While the contrasting alteration of key firing parameters suggests differential responses to the disease, potentially due to innate differences of cells and embryonic origins, these findings critically indicate that distinct interneurons may have a role in instigating an excitatory/inhibitory balance from early stages of development. The hypoexcitable nature of these interneurons could contribute to reduced network inhibition and increased network hyperexcitability. Therefore, inferring a potential primary role of cortical interneuron dysfunction in the disease, which must remain compensated for throughout the majority of disease until compensatory mechanisms fail, inhibitory function is lost, potentially through loss of CR-interneurons, and the disease manifests as cortical hyperexcitability. It is then proposed that this later phase of network hyperexcitability, underscored by inhibitory decline, transitions to hypoexcitability as cells undergo excitotoxic glutamatergic overload, and are lost from the functional network, resulting in the phenotypic motor neuron decline (**Figure 5.2**).

Importantly, potential compensation exerted by interneuron in the disease may have merit as differences in the ability of interneuron subtypes to respond through activity-dependent processes is demonstrated through the differential morphological response of bipolar interneurons compared with multipolar interneurons. Interestingly, the demonstration of increased neurite path length in multipolar interneurons in this chapter was comparable to the increased length of processes reported at symptom onset in CR-interneurons in Chapter 2. The alteration of neurite path length is thought to be an activity-dependent mechanism (De Marco Garcia et al 2011), which may suggest that altered morphology reflects an adaptive response to increased excitability in the cortex and cortical cultures with the $SOD1^{G93A}$ mutation. However, this morphological response of interneurons was not universally demonstrated, with bipolar interneurons largely unchanged compared to controls in this respect. This may indicate that while select inhibitory populations do have an ability to compensate for the pathogenic environment initiated in the disease, others do not.

5.4 FUTURE DIRECTIONS AND LIMITATIONS

This thesis focused on characterising the extent and timing of cortical interneurons in the motor cortex of the most widely used model of ALS the $SOD1^{G93A}$ mouse, the validity of interneuron involvement in the ALS motor cortex and the potential for cortical interneurons to be intrinsically susceptible to a known ALS mutation during development. The characterisation of cortical interneurons in Chapter 2 and 3 primarily utilised immunohistochemical assessment to investigate

Figure 5.2. Potential mechanisms of inhibitory system contribution to motor neuron failure in amyotrophic lateral sclerosis.

Based on the developmental occurrence of inhibitory and excitatory motor neuron deficits, and the subsequent timeline of structural alterations, a model is proposed in which this early inhibitory/excitatory imbalance may initiate a diverse cascade of secondary compensatory mechanisms, including CR-interneuron alterations, which will influence the development and functioning of neuronal circuits and prime motor networks to fail later in life. **a**, In normal physiological conditions, heterogeneous populations of interneurons innervate different domains of upper motor neurons, and provide regulatory inhibition of excitability. **b-g**, In a pathogenic disease setting, interneurons may be involved in multiple facets of excitability misregulation. **b-c**, Primary interneuronal dysfunction originating during early development (**b**) may result in upper motor neurons becoming hyperexcitable through loss of inhibition (**c**). **d-e**, Secondary interneuronal dysfunction may occur when upper motor neurons are initially hyperexcitable (**d**), leading to inappropriate interneuron development and function (**e**). Therefore, the failure of either interneurons or motor neurons to regulate excitability can lead to the motor system being primed to fail. **f**, The inhibitory system has an innate capacity for plasticity. Therefore, a degree of compensation and restoration of normal excitation by the inhibitory system may exist in the preclinical phase of disease. **g**, Onset of disease may become apparent when compensatory mechanisms become saturated or fail, due to accumulation of age-related pathogenic mechanisms, including inhibitory failure, leading to the failure of excitability regulation in the motor circuit and motor neuron degeneration.

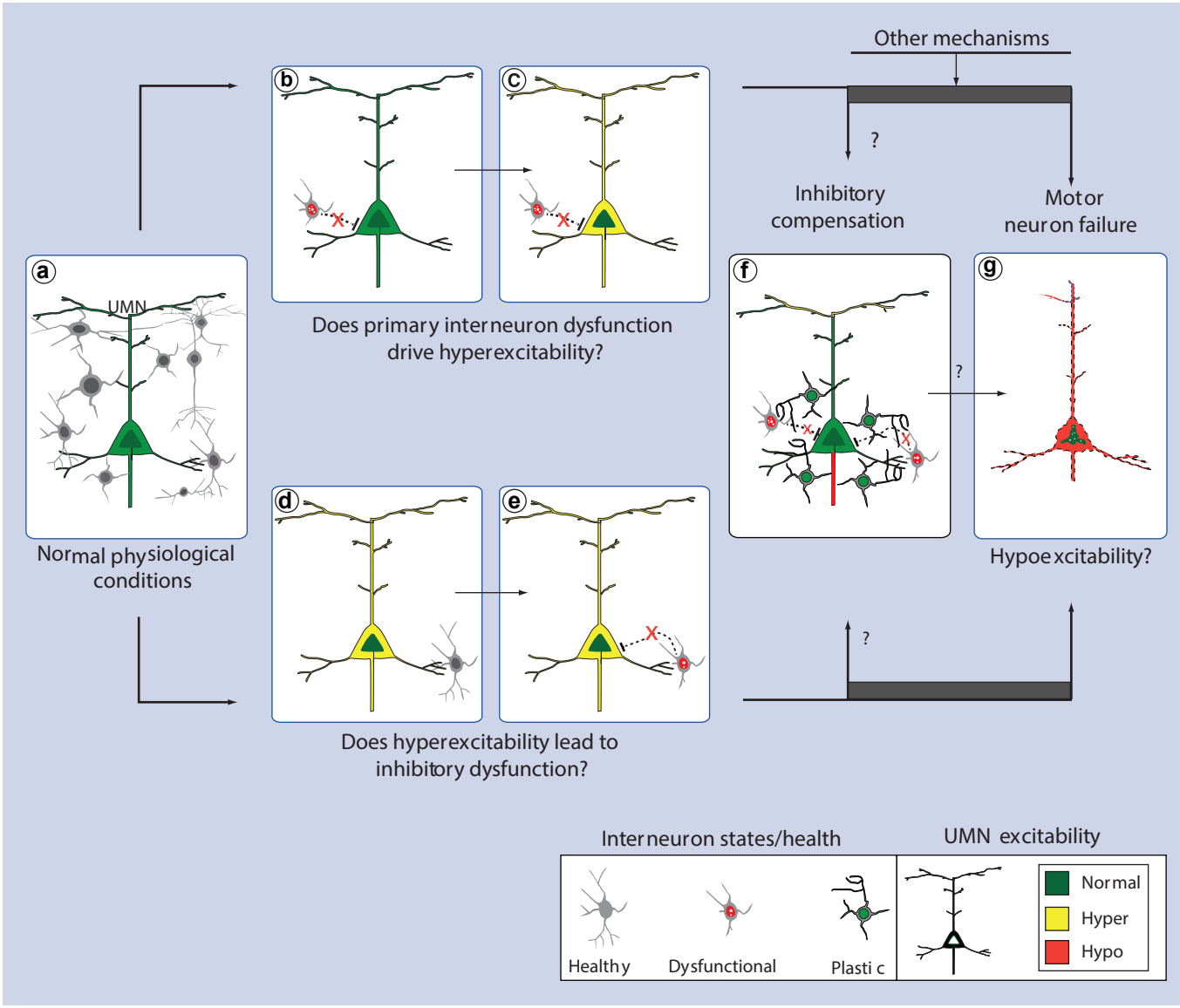

"Inhibitory dysfunction in amyotrophic lateral sclerosis: future therapeutic opportunities, Clark et. al., 2015"

potential involvement in the disease. While, the immunohistochemical assessment of human post-mortem tissue is traditionally utilised to great affect in many neuropathological case studies (Nihei et al 1993, Neumann et al 2006, Brettschneider et al 2013, Kim et al 2014a, Fatima et al 2015), alternative assessment strategies might include the quantification of mRNA abundance via in situ hybridization protocols to support changes in protein levels detected by immunohistochemistry (Liu et al 2010). Another method that can surpass such limitations is the use of transgenic mice that have Cre driver lines specific for distinct interneuron subtypes in the cortex (Taniguchi et al 2011). This may prove a more specific approach for investigating both CR- and NPY-interneuron populations, for example by crossing the B6(Cg)-Calb2$^{tm1(cre)Zjh}$/J CR-transgenic mouse with the SOD1^{G93A} mouse, genetic GFP labelling can be used to conclusively assess the role of this cell type in the motor cortex circuit and resolve the question of whether the protein or cell is altered.

Such an approach may also prove useful for investigating the innately differential responses of bipolar and multipolar interneurons to the SOD1^{G93A} mutation in Chapter 4. If the innate responses of these two populations are determined by their different embryonic origins, caudal/lateral or medial ganglionic eminence, this may be investigated by following the development of these cells with genetic fete mapping studies in ALS mouse models (Miyoshi et al 2007, Miyoshi et al 2010). However, more directly in the context of inhibitory dysfunction, it would be interesting to conduct further electrophysiological examination to assess if inhibitory post-synaptic potentials generated by these cells are altered. Additionally, it would be interesting to explore if synaptic scaling occurs in these cells, as this represents a homeostatic regulatory mechanism which allows neurons to altering synaptic strength to respond to prolonged changes in the cells intrinsic electrical activity (Turrigiano 2012). Without homeostatic synaptic scaling, neuronal networks can become unstable. Interestingly this mechanism is thought to activity-dependent process modified by glia (Stellwagen & Malenka 2006), therefore it may be of interest to explore this firstly due to the altered intrinsic excitability demonstrated in Chapter 4, but also due to the suspected involvement of microglia in the onset of the disease (Boillee et al 2006b, Casas et al 2016).

Another consideration for future studies may be the investigation of the expression of GABA receptors profiles on interneuron populations, as the formation and function of the inhibitory circuit rely on excitatory and inhibitory synapse formation, including the GABA receptor profile of interneurons. As previously described in Chapter 1 and 3, there is evidence of reduced $GABA_A$ receptor expression and binding in ALS patients (Lloyd et al 2000, Petri et al 2003). Given the differential involvement of interneuron populations described in Chapters 2, 3 and 4, it would be

interesting to see if the receptor composition is differentially affected in these different interneuron subtypes at varied stages of disease.

A receptor-based approach may also allow for further insight into the role of NPY in the disease. As a potential neuroprotective compound it will be interesting to assess brain levels of NPY receptors in ALS patients, as this may predict the efficacy of a therapeutic strategy centred around harnessing it's endogenous therapeutic potential. The use of specific radioligands to determine the distribution and kinetics of NPY receptor binding has been previously demonstrated in both *in vitro* and *in vivo* receptor-autoradiography studies in Alzheimer's disease (Martel et al 1990) and epilepsy (Furtinger et al 2001). This may be an interesting avenue for future research due to the increase in NPY demonstrated throughout the motor cortex in Chapter 2 and 3. Investigation in other mouse models would also build a more holistic picture of the potential role of NPY in the disease and should be considered for future studies (Leitner et al 2009). In particular, it would be of interest to determine if NPY administration may preserve motor circuitry, further investigating the correlation of NPY, with CR and pyramidal cell pathology identified in ALS cases, but not explored in the $SOD1^{G93A}$ mouse model. Nonetheless, in line with the broader pathogenesis of the disease, it is notable that more recent studies suggest that the neuroprotective properties of NPY may also extend to the suppression of excitotoxicity and regulation of calcium homeostasis (Duarte-Neves et al 2016). Therefore, the role of NPY-interneurons and the NPY peptide warrant further investigation.

Collectively this thesis has highlighted that interneuron involvement in ALS may be considerably more complex than previously appreciated, with multiple inhibitory compensatory mechanisms and innate susceptibilities most likely occurring over the disease course. Further characterisation of cortical interneuron vulnerability and the impact these cells have on the function of the cortical motor circuit needs to be made a priority, as it has the potential to lead to important therapeutic strategies for the treatment and prevention of ALS.

5.5 CONCLUSIONS

Altered excitability and the processes leading to loss of motor neuron function in ALS are complex and multifactorial. This thesis provides significant evidence to suggest that cortical interneuron dysfunction has an important and potentially evolving role in this process. It also supports an increasing cortical and non-cell autonomous nature of the disease, providing a novel perspective on the cellular basis for inhibitory dysfunction in the motor cortex of the $SOD1^{G93A}$ mouse model and in ALS patients. In summary, the findings of this thesis indicate that cortical interneuron populations may have a complex and evolving role in the disease, which may be initiated early during development and culminate in the failure of specific interneuron populations to compensate for dysfunction later in life. However, there is potential for inhibitory compensatory mechanisms, with future evaluation of inhibitory-based therapeutic strategies recommended as these compounds may be of great therapeutic benefit for the amelioration and normalisation of excitability in ALS.

6 REFERENCES

Al-Chalabi A, Jones A, Troakes C, King A, Al-Sarraj S, van den Berg LH. 2012. The genetics and neuropathology of amyotrophic lateral sclerosis. *Acta Neuropathol* 124: 339-52

Al-Chalabi A, Calvo A, Chio A, Colville S, Ellis CM, et al. 2014. Analysis of amyotrophic lateral sclerosis as a multistep process: a population-based modelling study. *Lancet neurology* 13: 1108-13

Alexianu ME, Ho BK, Mohamed AH, La Bella V, Smith RG, Appel SH. 1994. The role of calcium-binding proteins in selective motoneuron vulnerability in amyotrophic lateral sclerosis. *Ann Neurol* 36: 846-58

Alvarez FJ, Fyffe REW. 2007. The continuing case for the Renshaw cell. *The Journal of physiology* 584: 31-45

Andersen PM, Forsgren L, Binzer M, Nilsson P, Ala-Hurula V, et al. 1996. Autosomal recessive adult-onset amyotrophic lateral sclerosis associated with homozygosity for Asp90Ala CuZn-superoxide dismutase mutation. *Brain* 119: 1153-72

Arundine M, Tymianski M. 2003. Molecular mechanisms of calcium-dependent neurodegeneration in excitotoxicity. *Cell Calcium* 34: 325-37

Ascoli GA, Alonso-Nanclares L, Anderson SA, Barrionuevo G, Benavides-Piccione R, et al. 2008. Petilla terminology: nomenclature of features of GABAergic interneurons of the cerebral cortex. *Nat Rev Neurosci* 9: 557-68

Azzouz M, Leclerc N, Gurney M, Warter J-M, Poindron P, Borg J. 1997. Progressive motor neuron impairment in an animal model of familial amyotrophic lateral sclerosis In *Neurochemistry*, pp. 485-90: Springer

Bae JS, Simon NG, Menon P, Vucic S, Kiernan MC. 2013. The puzzling case of hyperexcitability in amyotrophic lateral sclerosis. *J Clin Neurol* 9: 65-74

Baglietto-Vargas D, Moreno-Gonzalez I, Sanchez-Varo R, Jimenez S, Trujillo-Estrada L, et al. 2010. Calretinin interneurons are early targets of extracellular amyloid-beta pathology in PS1/AbetaPP Alzheimer mice hippocampus. *Journal of Alzheimer's disease* 21: 119-32

Bar-Peled O, O'Brien RJ, Morrison JH, Rothstein JD. 1999. Cultured motor neurons possess calcium-permeable AMPA/kainate receptors. *Neuroreport* 10: 855-9

Baraban SC, Hollopeter G, Erickson JC, Schwartzkroin PA, Palmiter RD. 1997. Knock-out mice reveal a critical antiepileptic role for neuropeptide Y. *J Neurosci* 17: 8927-36

Barinka F, Druga R. 2010. Calretinin expression in the mammalian neocortex: a review. *Physiol Res* 59: 665-77

Beers DR, Henkel JS, Xiao Q, Zhao W, Wang J, et al. 2006. Wild-type microglia extend survival in PU.1 knockout mice with familial amyotrophic lateral sclerosis. *Proceedings of the National Academy of Sciences* 103: 16021-26

Beirowski B, Berek L, Adalbert R, Wagner D, Grumme DS, et al. 2004. Quantitative and qualitative analysis of Wallerian degeneration using restricted axonal labelling in YFP-H mice. *Journal of neuroscience methods* 134: 23-35

Ben-Ari Y. 2002. Excitatory actions of gaba during development: the nature of the nurture. *Nat Rev Neurosci* 3: 728-39

Benatar M, Boylan K, Jeromin A, Rutkove SB, Berry J, et al. 2016. ALS biomarkers for therapy development: State of the field and future directions. *Muscle Nerve* 53: 169-82

Bendotti C, Calvaresi N, Chiveri L, Prelle A, Moggio M, et al. 2001. Early vacuolization and mitochondrial damage in motor neurons of FALS mice are not associated with apoptosis or with changes in cytochrome oxidase histochemical reactivity. *J Neurol Sci* 191: 25-33

Bendotti C, Carri MT. 2004. Lessons from models of SOD1-linked familial ALS. *Trends in molecular medicine* 10: 393-400

Blizzard CA, Chuckowree JA, King AE, Hosie KA, McCormack GH, et al. 2011. Focal damage to the adult rat neocortex induces wound healing accompanied by axonal sprouting and dendritic structural plasticity. *Cerebral cortex* 21: 281-91

Blizzard CA, Southam KA, Dawkins E, Lewis KE, King AE, et al. 2015. Identifying the primary site of pathogenesis in amyotrophic lateral sclerosis - vulnerability of lower motor neurons to proximal excitotoxicity. *Disease models & mechanisms* 8: 215-24

Blizzard CA, Lee KM, Dickson TC. 2016. Inducing Chronic Excitotoxicity in the Mouse Spinal Cord to Investigate Lower Motor Neuron Degeneration. *Frontiers in neuroscience* 10: 76

Boillee S, Vande Velde C, Cleveland Don W. 2006a. ALS: A Disease of Motor Neurons and Their Nonneuronal Neighbors. *Neuron* 52: 39-59

Boillee S, Yamanaka K, Lobsiger CS, Copeland NG, Jenkins NA, et al. 2006b. Onset and Progression in Inherited ALS Determined by Motor Neurons and Microglia. *Science* 312: 1389-92

Bouilleret V, Schwaller B, Schurmans S, Celio MR, Fritschy JM. 2000. Neurodegenerative and morphogenic changes in a mouse model of temporal lobe epilepsy do not depend on the expression of the calcium-binding proteins parvalbumin, calbindin, or calretinin. *Neuroscience* 97: 47-58

Brecht M, Hatsopoulos NG, Kaneko T, Shepherd GM. 2013. Motor cortex microcircuits. *Frontiers in neural circuits* 7: 196

Brettschneider J, Del Tredici K, Toledo JB, Robinson JL, Irwin DJ, et al. 2013. Stages of pTDP-43 pathology in amyotrophic lateral sclerosis. *Ann Neurol* 74: 20-38

Brewer GJ. 1995. Serum-free B27/neurobasal medium supports differentiated growth of neurons from the striatum, substantia nigra, septum, cerebral cortex, cerebellum, and dentate gyrus. *J Neurosci Res* 42: 674-83

Brizuela M, Blizzard CA, Chuckowree JA, Dawkins E, Gasperini RJ, et al. 2015. The microtubule-stabilizing drug Epothilone D increases axonal sprouting following transection injury in vitro. *Mol Cell Neurosci* 66: 129-40

Brockington A, Ning K, Heath PR, Wood E, Kirby J, et al. 2013. Unravelling the enigma of selective vulnerability in neurodegeneration: motor neurons resistant to degeneration in ALS show distinct gene expression characteristics and decreased susceptibility to excitotoxicity. *Acta Neuropathol* 125: 95-109

Brownell B, Oppenheimer DR, Hughes JT. 1970. The central nervous system in motor neurone disease. *Journal of neurology, neurosurgery, and psychiatry* 33: 338-57

Bruijn LI, Miller TM, Cleveland DW. 2004. Unraveling the mechanisms involved in motor neuron degeneration in ALS. *Annual review of neuroscience* 27: 723-49

Burnashev N, Monyer H, Seeburg PH, Sakmann B. 1992. Divalent ion permeability of AMPA receptor channels is dominated by the edited form of a single subunit. *Neuron* 8: 189-98

Buzsaki G, Geisler C, Henze DA, Wang X-J. 2004. Interneuron Diversity series: Circuit complexity and axon wiring economy of cortical interneurons. *Trends Neurosci* 27: 186-93

Byrne S, Elamin M, Bede P, Shatunov A, Walsh C, et al. 2012. Cognitive and clinical characteristics of patients with amyotrophic lateral sclerosis carrying a C9orf72 repeat expansion: a population-based cohort study. *Lancet neurology* 11: 232-40

Campbell MJ, Morrison JH. 1989. Monoclonal antibody to neurofilament protein (SMI-32) labels a subpopulation of pyramidal neurons in the human and monkey neocortex. *J Comp Neurol* 282: 191-205

Cancedda L, Fiumelli H, Chen K, Poo MM. 2007. Excitatory GABA action is essential for morphological maturation of cortical neurons in vivo. *J Neurosci* 27: 5224-35

Cantello R, Gianelli M, Civardi C, Mutani R. 1992. Magnetic brain stimulation: the silent period after the motor evoked potential. *Neurology* 42: 1951-9

Caramia MD, Cicinelli P, Paradiso C, Mariorenzi R, Zarola F, et al. 1991. 'Excitability changes of muscular responses to magnetic brain stimulation in patients with central motor disorders. *Electroencephalography and clinical neurophysiology* 81: 243-50

Caramia MD, Palmieri MG, Desiato MT, Iani C, Scalise A, et al. 2000. Pharmacologic reversal of cortical hyperexcitability in patients with ALS. *Neurology* 54: 58-64

Carrì MT, D'Ambrosi N, Cozzolino M. 2016. Pathways to mitochondrial dysfunction in ALS pathogenesis. *Biochemical and Biophysical Research Communications*

Carunchio I, Curcio L, Pieri M, Pica F, Caioli S, et al. 2010. Increased levels of p70S6 phosphorylation in the G93A mouse model of Amyotrophic Lateral Sclerosis and in valine-exposed cortical neurons in culture. *Exp Neurol* 226: 218-30

Casas C, Manzano R, Vaz R, Osta R, Brites D. 2016. Synaptic Failure: Focus in an Integrative View of ALS. *Brain Plasticity* 1: 159-75

Cauli B, Zhou X, Tricoire L, Toussay X, Staiger JF. 2014. Revisiting enigmatic cortical calretinin-expressing interneurons. *Frontiers in neuroanatomy* 8: 52

Chang Q, Martin LJ. 2009. Glycinergic Innervation of Motoneurons Is Deficient in Amyotrophic Lateral Sclerosis Mice: A Quantitative Confocal Analysis. *The American journal of pathology* 174: 574-85

Charcot J, Joffroy A. 1869. Deux cas d'a trophie musculaire progressive avec lesion de la substance grise et des faisceaux antero-lateraux de la moelle epiniere. *Arch Physiol Neurol Pathol* 2: 744-54

Chaudhry FA, Reimer RJ, Bellocchio EE, Danbolt NC, Osen KK, et al. 1998. The vesicular GABA transporter, VGAT, localizes to synaptic vesicles in sets of glycinergic as well as GABAergic neurons. *J Neurosci* 18: 9733-50

Cheah BC, Vucic S, Krishnan AV, Kiernan MC. 2010. Riluzole, Neuroprotection and Amyotrophic Lateral Sclerosis. *Current Medicinal Chemistry* 17: 1942-59

Chen R, Lozano AM, Ashby P. 1999. Mechanism of the silent period following transcranial magnetic stimulation. Evidence from epidural recordings. *Experimental brain research* 128: 539-42

Chio A, Calvo A, Moglia C, Mazzini L, Mora G, group Ps. 2011. Phenotypic heterogeneity of amyotrophic lateral sclerosis: a population based study. *Journal of neurology, neurosurgery, and psychiatry* 82: 740-6

Chio A, Logroscino G, Traynor BJ, Collins J, Simeone JC, et al. 2013. Global epidemiology of amyotrophic lateral sclerosis: a systematic review of the published literature. *Neuroepidemiology* 41: 118-30

Chung YH, Joo KM, Nam RH, Cho MH, Kim DJ, et al. 2005. Decreased expression of calretinin in the cerebral cortex and hippocampus of SOD1G93A transgenic mice. *Brain Res* 1035: 105-9

Clark JA, Southam KA, Blizzard CA, King AE, Dickson TC. 2016a. Axonal degeneration, distal collateral branching and neuromuscular junction architecture alterations occur prior to symptom onset in the SOD1G93A mouse model of amyotrophic lateral sclerosis. *Journal of chemical neuroanatomy*

Clark JA, Yeaman EJ, Blizzard CA, Chuckowree JA, Dickson TC. 2016b. A Case for Microtubule Vulnerability in Amyotrophic Lateral Sclerosis: Altered Dynamics During Disease. *Frontiers in cellular neuroscience* 10

Clarke LE, Young KM, Hamilton NB, Li H, Richardson WD, Attwell D. 2012. Properties and fate of oligodendrocyte progenitor cells in the corpus callosum, motor cortex, and piriform cortex of the mouse. *J Neurosci* 32: 8173-85

Clement AM, Nguyen MD, Roberts EA, Garcia ML, Boillee S, et al. 2003. Wild-Type Nonneuronal Cells Extend Survival of SOD1 Mutant Motor Neurons in ALS Mice. *Science* 302: 113-17

Cleveland DW, Rothstein JD. 2001. From charcot to lou gehrig: deciphering selective motor neuron death in als. *Nat Rev Neurosci* 2: 806-19

Colasante G, Sessa A. 2010. Last but not least: cortical interneurons from caudal ganglionic eminence. *J Neurosci* 30: 7449-50

Danbolt NC. 2001. Glutamate uptake. *Prog Neurobiol* 65: 1-105

Darian-Smith C, Gilbert CD. 1994. Axonal sprouting accompanies functional reorganization in adult cat striate cortex. *Nature* 368: 737-40

De Carvalho M, Swash M. 1998. Fasciculation potentials: a study of amyotrophic lateral sclerosis and other neurogenic disorders. *Muscle Nerve* 21: 336-44

De Carvalho M, Eisen A, Krieger C, Swash M. 2014. Motoneuron firing in amyotrophic lateral sclerosis (ALS). *Frontiers in human neuroscience* 8: 719

De Lanerolle NC, Kim JH, Robbins RJ, Spencer DD. 1989. Hippocampal interneuron loss and plasticity in human temporal lobe epilepsy. *Brain Res* 495: 387-95

De Marco Garcia NV, Karayannis T, Fishell G. 2011. Neuronal activity is required for the development of specific cortical interneuron subtypes. *Nature* 472: 351-5

DeFelipe J. 1997. Types of neurons, synaptic connections and chemical characteristics of cells immunoreactive for calbindin-D28K, parvalbumin and calretinin in the neocortex. *Journal of chemical neuroanatomy* 14: 1-19

DeFelipe J. 2002. Cortical interneurons: from Cajal to 2001. *Progress in brain research* 136: 215-38

DeFelipe J. 2011. The evolution of the brain, the human nature of cortical circuits and intellectual creativity. *Frontiers in neuroanatomy* 5

DeJesus-Hernandez M, Mackenzie IR, Boeve BF, Boxer AL, Baker M, et al. 2011. Expanded GGGGCC hexanucleotide repeat in noncoding region of C9ORF72 causes chromosome 9p-linked FTD and ALS. *Neuron* 72: 245-56

Del Rio MR, DeFelipe J. 1994. A study of SMI 32-stained pyramidal cells, parvalbumin-immunoreactive chandelier cells, and presumptive thalamocortical axons in the human temporal neocortex. *J Comp Neurol* 342: 389-408

Del Rio MR, DeFelipe J. 1997. Synaptic connections of calretinin-immunoreactive neurons in the human neocortex. *J Neurosci* 17: 5143-54

Delestree N, Manuel M, Iglesias C, Elbasiouny SM, Heckman CJ, Zytnicki D. 2014. Adult spinal motoneurones are not hyperexcitable in a mouse model of inherited amyotrophic lateral sclerosis. *The Journal of physiology* 592: 1687-703

Desiato MT, Bernardi G, Hagi HA, Boffa L, Caramia MD. 2002. Transcranial magnetic stimulation of motor pathways directed to muscles supplied by cranial nerves in amyotrophic lateral sclerosis. *Clinical neurophysiology : official journal of the International Federation of Clinical Neurophysiology* 113: 132-40

Devlin AC, Burr K, Borooah S, Foster JD, Cleary EM, et al. 2015. Human iPSC-derived motoneurons harbouring TARDBP or C9ORF72 ALS mutations are dysfunctional despite maintaining viability. *Nature communications* 6: 5999

DiBernardo AB, Cudkowicz ME. 2006. Translating preclinical insights into effective human trials in ALS. *Biochimica et biophysica acta* 1762: 1139-49

Douglas R, Markram H, Martin K. 2004. *"Neocortex," in The Synaptic Organization of the Brain*. pp. 499–558. New York, NY, USA: Oxford University Press.

Drexel M, Kirchmair E, Wieselthaler-Holzl A, Preidt AP, Sperk G. 2012. Somatostatin and neuropeptide Y neurons undergo different plasticity in parahippocampal regions in kainic acid-induced epilepsy. *J Neuropathol Exp Neurol* 71: 312-29

Drory VE, Kovach I, Groozman GB. 2001. Electrophysiologic evaluation of upper motor neuron involvement in amyotrophic lateral sclerosis. *Amyotrophic lateral sclerosis and other motor neuron disorders : official publication of the World Federation of Neurology, Research Group on Motor Neuron Diseases* 2: 147-52

Duarte-Neves J, Pereira de Almeida L, Cavadas C. 2016. Neuropeptide Y (NPY) as a therapeutic target for neurodegenerative diseases. *Neurobiol Dis* 95: 210-24

Dzaja D, Hladnik A, Bicanic I, Bakovic M, Petanjek Z. 2014. Neocortical calretinin neurons in primates: increase in proportion and microcircuitry structure. *Frontiers in neuroanatomy* 8: 103

Eccles J, Fatt P, Koketsu K. 1954. Cholinergic and inhibitory synapses in a pathway from motor-axon collaterals to motoneurones. *The Journal of physiology* 126: 524-62

Eisen A, Kim S, Pant B. 1992. Amyotrophic lateral sclerosis (ALS): a phylogenetic disease of the corticomotoneuron? *Muscle Nerve* 15: 219-24

Eisen A, Pant B, Stewart H. 1993. Cortical excitability in amyotrophic lateral sclerosis: a clue to pathogenesis. *The Canadian journal of neurological sciences. Le journal canadien des sciences neurologiques* 20: 11-6

Eisen A, Weber M. 2001. The motor cortex and amyotrophic lateral sclerosis. *Muscle Nerve* 24: 564-73

Eisen A, Kiernan M, Mitsumoto H, Swash M. 2014. Amyotrophic lateral sclerosis: a long preclinical period? *Journal of neurology, neurosurgery, and psychiatry* 85: 1232-8

Ellis CM, Suckling J, Amaro E, Jr., Bullmore ET, Simmons A, et al. 2001. Volumetric analysis reveals corticospinal tract degeneration and extramotor involvement in ALS. *Neurology* 57: 1571-8

Erickson JC, Clegg KE, Palmiter RD. 1996. Sensitivity to leptin and susceptibility to seizures of mice lacking neuropeptide Y. *Nature* 381: 415-21

Ernst A, Frisen J. 2015. Adult neurogenesis in humans- common and unique traits in mammals. *PLoS biology* 13: e1002045

Fatima M, Tan R, Halliday GM, Kril JJ. 2015. Spread of pathology in amyotrophic lateral sclerosis: assessment of phosphorylated TDP-43 along axonal pathways. *Acta Neuropathol Commun* 3: 47

Ferrari R, Kapogiannis D, Huey ED, Momeni P. 2011. FTD and ALS: a tale of two diseases. *Current Alzheimer research* 8: 273-94

Figueroa-Romero C, Hur J, Bender DE, Delaney CE, Cataldo MD, et al. 2012. Identification of epigenetically altered genes in sporadic amyotrophic lateral sclerosis. *PLoS One* 7: e52672

Fisher RS, van Emde Boas W, Blume W, Elger C, Genton P, et al. 2005. Epileptic seizures and epilepsy: definitions proposed by the International League Against Epilepsy (ILAE) and the International Bureau for Epilepsy (IBE). *Epilepsia* 46: 470-2

Foerster BR, Callaghan BC, Petrou M, Edden RA, Chenevert TL, Feldman EL. 2012. Decreased motor cortex gamma-aminobutyric acid in amyotrophic lateral sclerosis. *Neurology* 78: 1596-600

Foerster BR, Pomper MG, Callaghan BC, Petrou M, Edden RA, et al. 2013. An imbalance between excitatory and inhibitory neurotransmitters in amyotrophic lateral sclerosis revealed by use of 3-T proton magnetic resonance spectroscopy. *JAMA neurology* 70: 1009-16

Fogarty M, Grist M, Gelman D, Marin O, Pachnis V, Kessaris N. 2007. Spatial genetic patterning of the embryonic neuroepithelium generates GABAergic interneuron diversity in the adult cortex. *J Neurosci* 27: 10935-46

Fogarty MJ, Noakes PG, Bellingham MC. 2015. Motor cortex layer V pyramidal neurons exhibit dendritic regression, spine loss, and increased synaptic excitation in the presymptomatic hSOD1(G93A) mouse model of amyotrophic lateral sclerosis. *J Neurosci* 35: 643-7

Foster V, Oakley AE, Slade JY, Hall R, Polvikoski TM, et al. 2014. Pyramidal neurons of the prefrontal cortex in post-stroke, vascular and other ageing-related dementias. *Brain* 137: 2509-21

Freund TF, Buzsaki G. 1996. Interneurons of the hippocampus. *Hippocampus* 6: 347-470

Fuchs A, Kutterer S, Muhling T, Duda J, Schutz B, et al. 2013. Selective mitochondrial Ca2+ uptake deficit in disease endstage vulnerable motoneurons of the SOD1G93A mouse model of amyotrophic lateral sclerosis. *The Journal of physiology* 591: 2723-45

Furtinger S, Pirker S, Czech T, Baumgartner C, Ransmayr G, Sperk G. 2001. Plasticity of Y1 and Y2 receptors and neuropeptide Y fibers in patients with temporal lobe epilepsy. *J Neurosci* 21: 5804-12

Gall D, Roussel C, Susa I, D'Angelo E, Rossi P, et al. 2003. Altered neuronal excitability in cerebellar granule cells of mice lacking calretinin. *J Neurosci* 23: 9320-7

Geevasinga N, Menon P, Nicholson GA, Ng K, Howells J, et al. 2015. Cortical Function in Asymptomatic Carriers and Patients With C9orf72 Amyotrophic Lateral Sclerosis. *JAMA neurology* 72: 1268-74

Goodall EF, Morrison KE. 2006. Amyotrophic lateral sclerosis (motor neuron disease): proposed mechanisms and pathways to treatment. *Expert Reviews in Molecular Medicine* 8: 1-22

Gruber B, Greber S, Rupp E, Sperk G. 1994. Differential NPY mRNA expression in granule cells and interneurons of the rat dentate gyrus after kainic acid injection. *Hippocampus* 4: 474-82

Guerreiro R, Bras J, Hardy J. 2015. SnapShot: Genetics of ALS and FTD. *Cell* 160: 798 e1

Gulyas AI, Hajos N, Freund TF. 1996. Interneurons containing calretinin are specialized to control other interneurons in the rat hippocampus. *J Neurosci* 16: 3397-411

Gurney M, Pu H, Chiu A, Dal Canto M, Polchow C, et al. 1994. Motor neuron degeneration in mice that express a human Cu, Zn superoxide dismutase mutation. *Science* 264: 1772-75

Hanajima R, Ugawa Y, Terao Y, Ogata K, Kanazawa I. 1996. Ipsilateral cortico-cortical inhibition of the motor cortex in various neurological disorders. *J Neurol Sci* 140: 109-16

Handley EE, Pitman KA, Dawkins E, Young KM, Clark RM, et al. 2016. Synapse Dysfunction of Layer V Pyramidal Neurons Precedes Neurodegeneration in a Mouse Model of TDP-43 Proteinopathies. *Cerebral cortex*

Hardiman O, Van Den Berg LH, Kiernan MC. 2011. Clinical diagnosis and management of amyotrophic lateral sclerosis. *Nature Reviews Neurology* 7: 639-49

Hideyama T, Yamashita T, Suzuki T, Tsuji S, Higuchi M, et al. 2010. Induced Loss of ADAR2 Engenders Slow Death of Motor Neurons from Q/R Site-Unedited GluR2. *The Journal of Neuroscience* 30: 11917-25

Hinoi E, Takarada T, Tsuchihashi Y, Yoneda Y. 2005. Glutamate Transporters as Drug Targets. *Current Drug Targets - CNS & Neurological Disorders* 4: 211-20

Holt GR, Koch C. 1997. Shunting inhibition does not have a divisive effect on firing rates. *Neural computation* 9: 1001-13

Hooks BM, Mao T, Gutnisky DA, Yamawaki N, Svoboda K, Shepherd GM. 2013. Organization of cortical and thalamic input to pyramidal neurons in mouse motor cortex. *J Neurosci* 33: 748-60

Hooten KG, Beers DR, Zhao W, Appel SH. 2015. Protective and toxic neuroinflammation in amyotrophic lateral sclerosis. *Neurotherapeutics : the journal of the American Society for Experimental NeuroTherapeutics* 12: 364-75

Hsu SM, Soban E. 1982. Color modification of diaminobenzidine (DAB) precipitation by metallic ions and its application for double immunohistochemistry. *The journal of histochemistry and cytochemistry : official journal of the Histochemistry Society* 30: 1079-82

Ilieva H, Polymenidou M, Cleveland DW. 2009. Non–cell autonomous toxicity in neurodegenerative disorders: ALS and beyond. *J Cell Biol* 187: 761-72

Ince P, Stout N, Shaw P, Slade J, Hunziker W, et al. 1993. Parvalbumin and calbindin D-28k in the human motor system and in motor neuron disease. *Neuropathol Appl Neurobiol* 19: 291-99

Inghilleri M, Berardelli A, Cruccu G, Manfredi M. 1993. Silent period evoked by transcranial stimulation of the human cortex and cervicomedullary junction. *The Journal of physiology* 466: 521-34

Isaac JTR, Ashby M, McBain CJ. 2007. The role of the GluR2 subunit in AMPA receptor function and synaptic plasticity. *Neuron* 54: 859-71

Ittner LM, Halliday GM, Kril JJ, Gotz J, Hodges JR, Kiernan MC. 2015. FTD and ALS--translating mouse studies into clinical trials. *Nat Rev Neurol* 11: 360-6

Jara JH, Villa SR, Khan NA, Bohn MC, Ozdinler PH. 2012. AAV2 mediated retrograde transduction of corticospinal motor neurons reveals initial and selective apical dendrite degeneration in ALS. *Neurobiol Dis* 47: 174-83

Jara JH, Genc B, Klessner JL, Ozdinler PH. 2014. Retrograde labeling, transduction, and genetic targeting allow cellular analysis of corticospinal motor neurons: implications in health and disease. *Frontiers in neuroanatomy* 8: 16

Jones EG. 1993. GABAergic neurons and their role in cortical plasticity in primates. *Cerebral cortex* 3: 361-72

Justice MJ, Dhillon P. 2016. Using the mouse to model human disease: increasing validity and reproducibility. *Disease models & mechanisms* 9: 101-3

Kaas JH, Krubitzer LA, Chino YM, Langston AL, Polley EH, Blair N. 1990. Reorganization of retinotopic cortical maps in adult mammals after lesions of the retina. *Science* 248: 229-31

Kanai K, Kuwabara S, Misawa S, Tamura N, Ogawara K, et al. 2006. Altered axonal excitability properties in amyotrophic lateral sclerosis: impaired potassium channel function related to disease stage. *Brain* 129: 953-62

Karademir B, Corek C, Ozer NK. 2015. Endoplasmic reticulum stress and proteasomal system in amyotrophic lateral sclerosis. *Free Radical Biology and Medicine* 88: 42-50

Karayannis T, De Marco Garcia NV, Fishell GJ. 2012. Functional adaptation of cortical interneurons to attenuated activity is subtype-specific. *Frontiers in neural circuits* 6: 66

Kaufman L, Rousseeuw PJ. 1990. *Finding groups in data: an introduction to cluster analysis*. New York: John Wiley and Sons.

Kaur SJ, McKeown SR, Rashid S. 2016. Mutant SOD1 mediated pathogenesis of amyotrophic lateral sclerosis. *Gene* 577: 109-18

Kawahara Y, Ito K, Sun H, Aizawa H, Kanazawa I, Kwak S. 2004. Glutamate receptors: RNA editing and death of motor neurons. *Nature* 427: 801-01

Kepecs A, Fishell G. 2014. Interneuron cell types are fit to function. *Nature* 505: 318-26

Kharlamov EA, Kharlamov A, Kelly KM. 2007. Changes in neuropeptide Y protein expression following photothrombotic brain infarction and epileptogenesis. *Brain Res* 1127: 151-62

Kim EH, Thu DC, Tippett LJ, Oorschot DE, Hogg VM, et al. 2014a. Cortical interneuron loss and symptom heterogeneity in Huntington disease. *Ann Neurol* 75: 717-27

Kim EH, Thu DCV, Tippett LJ, Oorschot DE, Hogg VM, et al. 2014b. Cortical interneuron loss and symptom heterogeneity in Huntington disease. *Ann Neurol* 75: 717-27

King AE, Dickson TC, Blizzard CA, Foster SS, Chung RS, et al. 2007. Excitotoxicity mediated by non-NMDA receptors causes distal axonopathy in long-term cultured spinal motor neurons. *The European journal of neuroscience* 26: 2151-9

Kiskinis E, Sandoe J, Williams LA, Boulting GL, Moccia R, et al. 2014. Pathways disrupted in human ALS motor neurons identified through genetic correction of mutant SOD1. *Cell stem cell* 14: 781-95

Kleine BU, Stegeman DF, Schelhaas HJ, Zwarts MJ. 2008. Firing pattern of fasciculations in ALS: evidence for axonal and neuronal origin. *Neurology* 70: 353-9

Kovac S, Walker MC. 2013. Neuropeptides in epilepsy. *Neuropeptides* 47: 467-75

Kowall NW, Ferrante RJ, Martin JB. 1987. Patterns of cell loss in Huntington's disease. *Trends Neurosci* 10: 24-29

Kubota Y. 2014. Untangling GABAergic wiring in the cortical microcircuit. *Current opinion in neurobiology* 26: 7-14

Kuo JJ, Schonewille M, Siddique T, Schults AN, Fu R, et al. 2004. Hyperexcitability of cultured spinal motoneurons from presymptomatic ALS mice. *Journal of Neurophysiology* 91: 571-75

Kuo JJ, Siddique T, Fu R, Heckman CJ. 2005. Increased persistent Na+ current and its effect on excitability in motoneurones cultured from mutant SOD1 mice. *The Journal of physiology* 563: 843-54

Labrakakis C, Rudolph U, De Koninck Y. 2014. The heterogeneity in GABAA receptor-mediated IPSC kinetics reflects heterogeneity of subunit composition among inhibitory and excitatory interneurons in spinal lamina II. *Frontiers in cellular neuroscience* 8: 424

Lasiene J, Yamanaka K. 2011. Glial cells in amyotrophic lateral sclerosis. *Neurology research international* 2011: 718987

Le Magueresse C, Monyer H. 2013. GABAergic interneurons shape the functional maturation of the cortex. *Neuron* 77: 388-405

Lee S, Kim HJ. 2015. Prion-like Mechanism in Amyotrophic Lateral Sclerosis: are Protein Aggregates the Key? *Exp Neurobiol* 24: 1-7

Lee W-CA, Chen JL, Huang H, Leslie JH, Amitai Y, et al. 2008. A dynamic zone defines interneuron remodeling in the adult neocortex. *Proceedings of the National Academy of Sciences* 105: 19968-73

Lehmann K, Steinecke A, Bolz J. 2012. GABA through the ages: regulation of cortical function and plasticity by inhibitory interneurons. *Neural Plast* 2012: 892784

Leitner M, Menzies S, Lutz C. 2009. Working with ALS mice: Guidelines for Preclinical Testing & Colony Management., ME: Prize4Life and The Jackson Laboratory, Bar Harbor

Leroy F, Lamotte d'Incamps B, Imhoff-Manuel RD, Zytnicki D. 2014. Early intrinsic hyperexcitability does not contribute to motoneuron degeneration in amyotrophic lateral sclerosis. *eLife* 3

Lewis DA, Curley AA, Glausier JR, Volk DW. 2012. Cortical parvalbumin interneurons and cognitive dysfunction in schizophrenia. *Trends Neurosci* 35: 57-67

Lin CL, Bristol LA, Jin L, Dykes-Hoberg M, Crawford T, et al. 1998. Aberrant RNA processing in a neurodegenerative disease: the cause for absent EAAT2, a glutamate transporter, in amyotrophic lateral sclerosis. *Neuron* 20: 589-602

Ling SC, Polymenidou M, Cleveland DW. 2013. Converging mechanisms in ALS and FTD: disrupted RNA and protein homeostasis. *Neuron* 79: 416-38

Liu CQ, Shan L, Balesar R, Luchetti S, Van Heerikhuize JJ, et al. 2010. A quantitative in situ hybridization protocol for formalin-fixed paraffin-embedded archival post-mortem human brain tissue. *Methods* 52: 359-66

Liu J, Liu B, Zhang X, Yu B, Guan W, et al. 2014. Calretinin-positive L5a pyramidal neurons in the development of the paralemniscal pathway in the barrel cortex. *Molecular brain* 7: 84

Lloyd CM, Richardson MP, Brooks DJ, Al-Chalabi A, Leigh PN. 2000. Extramotor involvement in ALS: PET studies with the GABAA ligand [11C]flumazenil. *Brain* 123: 2289-96

Lomeli H, Mosbacher J, Melcher T, Hoger T, Geiger, et al. 1994. Control of kinetic properties of AMPA receptor channels by nuclear RNA editing. *Science* 266: 1709-13

Lorenzo L-E, Barbe A, Portalier P, Fritschy J-M, Bras H. 2006. Differential expression of GABAA and glycine receptors in ALS-resistant vs. ALS-vulnerable motoneurons: possible implications for selective vulnerability of motoneurons. *European Journal of Neuroscience* 23: 3161-70

Maekawa S, Al,ÄêSarraj S, Kibble M, Landau S, Parnavelas J, et al. 2004. Cortical selective vulnerability in motor neuron disease: a morphometric study. *Brain* 127: 1237-51

Majounie E, Renton AE, Mok K, Dopper EG, Waite A, et al. 2012. Frequency of the C9orf72 hexanucleotide repeat expansion in patients with amyotrophic lateral sclerosis and frontotemporal dementia: a cross-sectional study. *Lancet neurology* 11: 323-30

Maniecka Z, Polymenidou M. 2015. From nucleation to widespread propagation: A prion-like concept for ALS. *Virus Res* 207: 94-105

Mannen T, Iwata M, Toyokura Y, Nagashima K. 1977. Preservation of a certain motoneurone group of the sacral cord in amyotrophic lateral sclerosis: its clinical significance. *Journal of neurology, neurosurgery, and psychiatry* 40: 464-9

Marin B, Couratier P, Arcuti S, Copetti M, Fontana A, et al. 2016. Stratification of ALS patients' survival: a population-based study. *Journal of neurology* 263: 100-11

Markram H, Toledo-Rodriguez M, Wang Y, Gupta A, Silberberg G, Wu C. 2004. Interneurons of the neocortical inhibitory system. *Nat Rev Neurosci* 5: 793-807

Marksteiner J, Ortler M, Bellmann R, Sperk G. 1990. Neuropeptide Y biosynthesis is markedly induced in mossy fibers during temporal lobe epilepsy of the rat. *Neuroscience letters* 112: 143-8

Martel JC, Alagar R, Robitaille Y, Quirion R. 1990. Neuropeptide Y receptor binding sites in human brain. Possible alteration in Alzheimer's disease. *Brain Res* 519: 228-35

Martin E, Cazenave W, Cattaert D, Branchereau P. 2013. Embryonic alteration of motoneuronal morphology induces hyperexcitability in the mouse model of amyotrophic lateral sclerosis. *Neurobiol Dis* 54: 116-26

Martin L, Chang Q. 2012. Inhibitory Synaptic Regulation of Motoneurons: A New Target of Disease Mechanisms in Amyotrophic Lateral Sclerosis. *Molecular neurobiology* 45: 30-42

Martin LJ, Brambrink AM, Lehmann C, Portera-Cailliau C, Koehler R, et al. 1997. Hypoxia—ischemia causes abnormalities in glutamate transporters and death of astroglia and neurons in newborn striatum. *Ann Neurol* 42: 335-48

Martin LJ, Liu Z, Chen K, Price AC, Pan Y, et al. 2007. Motor neuron degeneration in amyotrophic lateral sclerosis mutant superoxide dismutase-1 transgenic mice: mechanisms of mitochondriopathy and cell death. *J Comp Neurol* 500: 20-46

Mathern GW, Babb TL, Pretorius JK, Leite JP. 1995. Reactive synaptogenesis and neuron densities for neuropeptide Y, somatostatin, and glutamate

decarboxylase immunoreactivity in the epileptogenic human fascia dentata. *J Neurosci* 15: 3990-4004

Matus S, Valenzuela V, Medinas DB, Hetz C. 2013. ER dysfunction and protein folding stress in ALS. *International journal of cell biology* 2013

McBain CJ, Fisahn A. 2001. Interneurons unbound. *Nat Rev Neurosci* 2: 11-23

Mendez P, Bacci A. 2011. Assortment of GABAergic plasticity in the cortical interneuron melting pot. *Neural Plast* 2011: 976856

Menon P, Kiernan MC, Vucic S. 2014. Cortical hyperexcitability precedes lower motor neuron dysfunction in ALS. *Clinical neurophysiology : official journal of the International Federation of Clinical Neurophysiology*

Mills KR, Nithi KA. 1998. Peripheral and central motor conduction in amyotrophic lateral sclerosis. *J Neurol Sci* 159: 82-7

Minciacchi D, Kassa RM, Del Tongo C, Mariotti R, Bentivoglio M. 2009. Voronoi-based spatial analysis reveals selective interneuron changes in the cortex of FALS mice. *Exp Neurol* 215: 77-86

Miri A, Azim E, Jessell TM. 2013. Edging toward entelechy in motor control. *Neuron* 80: 827-34

Mitra NK, Goh TE, Bala Krishnan T, Nadarajah VD, Vasavaraj AK, Soga T. 2013. Effect of intra-cisternal application of kainic acid on the spinal cord and locomotor activity in rats. *Int J Clin Exp Pathol* 6: 1505-15

Miyoshi G, Butt SJ, Takebayashi H, Fishell G. 2007. Physiologically distinct temporal cohorts of cortical interneurons arise from telencephalic Olig2-expressing precursors. *J Neurosci* 27: 7786-98

Miyoshi G, Hjerling-Leffler J, Karayannis T, Sousa VH, Butt SJ, et al. 2010. Genetic fate mapping reveals that the caudal ganglionic eminence produces a large and diverse population of superficial cortical interneurons. *J Neurosci* 30: 1582-94

Miyoshi G, Fishell G. 2011. GABAergic Interneuron Lineages Selectively Sort into Specific Cortical Layers during Early Postnatal Development. *Cerebral cortex* 21: 845-52

Mohammadi B, Kollewe K, Samii A, Dengler R, Munte TF. 2011. Functional neuroimaging at different disease stages reveals distinct phases of neuroplastic changes in amyotrophic lateral sclerosis. *Human brain mapping* 32: 750-8

Morrison BM, Gordon JW, Ripps ME, Morrison JH. 1996. Quantitative immunocytochemical analysis of the spinal cord in G86R superoxide dismutase transgenic mice: neurochemical correlates of selective vulnerability. *J Comp Neurol* 373: 619-31

Morrison BM, Janssen WG, Gordon JW, Morrison JH. 1998. Time course of neuropathology in the spinal cord of G86R superoxide dismutase transgenic mice. *J Comp Neurol* 391: 64-77

Morrison JH, Lewis DA, Campbell MJ, Huntley GW, Benson DL, Bouras C. 1987. A monoclonal antibody to non-phosphorylated neurofilament protein marks the vulnerable cortical neurons in Alzheimer's disease. *Brain Res* 416: 331-6

Nagy D, Kato T, Kushner PD. 1994. Reactive astrocytes are widespread in the cortical gray matter of amyotrophic lateral sclerosis. *J Neurosci Res* 38: 336-47

Neumann E, Nachmansohn D. 1975. Nerve excitability toward an integrating concept. *Biomembranes* 7: 99-166

Neumann M, Sampathu DM, Kwong LK, Truax AC, Micsenyi MC, et al. 2006. Ubiquitinated TDP-43 in frontotemporal lobar degeneration and amyotrophic lateral sclerosis. *Science* 314: 130-3

Nihei K, Kowall NW. 1993. Involvement of NPY-immunoreactive neurons in the cerebral cortex of amyotrophic lateral sclerosis patients. *Neuroscience letters* 159: 67-70

Nihei K, McKee AC, Kowall NW. 1993. Patterns of neuronal degeneration in the motor cortex of amyotrophic lateral sclerosis patients. *Acta Neuropathol* 86: 55-64

Nikonenko I, Boda B, Steen S, Knott G, Welker E, Muller D. 2008. PSD-95 promotes synaptogenesis and multiinnervated spine formation through nitric oxide signaling. *J Cell Biol* 183: 1115-27

Nonneman A, Robberecht W, Van Den Bosch L. 2014. The role of oligodendroglial dysfunction in amyotrophic lateral sclerosis. *Neurodegenerative disease management* 4: 223-39

Ozdinler PH, Benn S, Yamamoto TH, Guzel M, Brown RH, Jr., Macklis JD. 2011. Corticospinal motor neurons and related subcerebral projection neurons undergo early and specific neurodegeneration in hSOD1G(9)(3)A transgenic ALS mice. *J Neurosci* 31: 4166-77

Pambo-Pambo A, Durand J, Gueritaud J-P. 2009. Early Excitability Changes in Lumbar Motoneurons of Transgenic SOD1G85R and SOD1G93A-Low Mice. *Journal of Neurophysiology* 102: 3627-42

Pamphlett R, Kril J, Hng TM. 1995. Motor neuron disease: a primary disorder of corticomotoneurons? *Muscle Nerve* 18: 314-8

Pardo AC, Wong V, Benson LM, Dykes M, Tanaka K, et al. 2006. Loss of the astrocyte glutamate transporter GLT1 modifies disease in SOD1(G93A) mice. *Exp Neurol* 201: 120-30

Patrylo PR, van den Pol AN, Spencer DD, Williamson A. 1999. NPY inhibits glutamatergic excitation in the epileptic human dentate gyrus. *J Neurophysiol* 82: 478-83

Paxinos G, Franklin K. 2007. *The Mouse Brain in Stereotaxic Coordinates*. New York, NY: Academic Press.

Peters S. 2010. *A practical guide to frozen section technique*. pp. 117-122. Springer.

Petri S, Krampfl K, Hashemi F, Grothe C, Hori A, et al. 2003. Distribution of GABAA Receptor mRNA in the Motor Cortex of ALS Patients. *Journal of Neuropathology & Experimental Neurology* 62: 1041-51

Pieri M, Albo F, Gaetti C, Spalloni A, Bengtson CP, et al. 2003. Altered excitability of motor neurons in a transgenic mouse model of familial amyotrophic lateral sclerosis. *Neuroscience letters* 351: 153-56

Pieri M, Carunchio I, Curcio L, Mercuri NB, Zona C. 2009. Increased persistent sodium current determines cortical hyperexcitability in a genetic model of amyotrophic lateral sclerosis. *Exp Neurol* 215: 368-79

Poujois A, Schneider FC, Faillenot I, Camdessanche JP, Vandenberghe N, et al. 2013. Brain plasticity in the motor network is correlated with disease progression in amyotrophic lateral sclerosis. *Human brain mapping* 34: 2391-401

Powers R, Binder M. 2001. Input-output functions of mammalian motoneurons. *Rev Physiol Biochem Pharmacol* 143: 137-263

Prout AJ, Eisen AA. 1994. The cortical silent period and amyotrophic lateral sclerosis. *Muscle Nerve* 17: 217-23

Quinlan KA, Schuster JE, Fu R, Siddique T, Heckman CJ. 2011. Altered postnatal maturation of electrical properties in spinal motoneurons in a mouse model of amyotrophic lateral sclerosis. *The Journal of physiology* 589: 2245-60

Ravits J, Laurie P, Fan Y, Moore DH. 2007. Implications of ALS focality: rostral-caudal distribution of lower motor neuron loss postmortem. *Neurology* 68: 1576-82

Ravits JM, La Spada AR. 2009. ALS motor phenotype heterogeneity, focality, and spread: deconstructing motor neuron degeneration. *Neurology* 73: 805-11

Raynor EM, Shefner JM. 1994. Recurrent inhibition is decreased in patients with amyotrophic lateral sclerosis. *Neurology* 44: 2148

Renshaw B. 1941. Influence of discharge of motoneurons upon excitation of neighbouring motoneurons. *J Neurophysiol* 4: 167-83

Renton AE, Majounie E, Waite A, Simon-Sanchez J, Rollinson S, et al. 2011. A hexanucleotide repeat expansion in C9ORF72 is the cause of chromosome 9p21-linked ALS-FTD. *Neuron* 72: 257-68

Renton AE, Chio A, Traynor BJ. 2014. State of play in amyotrophic lateral sclerosis genetics. *Nature neuroscience* 17: 17-23

Rizzi M, Monno A, Samanin R, Sperk G, Vezzani A. 1993. Electrical kindling of the hippocampus is associated with functional activation of neuropeptide Y-containing neurons. *The European journal of neuroscience* 5: 1534-8

Rosen DR, Siddique T, Patterson D, Figlewicz DA, Sapp P, et al. 1993. Mutations in Cu/Zn superoxide dismutase gene are associated with familial amyotrophic lateral sclerosis. *Nature* 362: 59-62

Roshan L, Paradiso GO, Chen R. 2003. Two phases of short-interval intracortical inhibition. *Experimental brain research* 151: 330-7

Rothstein JD, Tsai G, Kuncl RW, Clawson L, Cornblath DR, et al. 1990. Abnormal excitatory amino acid metabolism in amyotrophic lateral sclerosis. *Ann Neurol* 28: 18-25

Rothstein JD, Patel S, Regan MR, Haenggeli C, Huang YH, et al. 2005. Beta-lactam antibiotics offer neuroprotection by increasing glutamate transporter expression. *Nature* 433: 73-7

Rothstein JD. 2009. Current hypotheses for the underlying biology of amyotrophic lateral sclerosis. *Ann Neurol* 65: S3-S9

Saba L, Viscomi MT, Caioli S, Pignataro A, Bisicchia E, et al. 2015. Altered Functionality, Morphology, and Vesicular Glutamate Transporter Expression of Cortical Motor Neurons from a Presymptomatic Mouse Model of Amyotrophic Lateral Sclerosis. *Cerebral cortex*

Sanger TD, Garg RR, Chen R. 2001. Interactions between two different inhibitory systems in the human motor cortex. *The Journal of physiology* 530: 307-17

Sareen D, O'Rourke JG, Meera P, Muhammad AK, Grant S, et al. 2013. Targeting RNA foci in iPSC-derived motor neurons from ALS patients with a C9ORF72 repeat expansion. *Science translational medicine* 5: 208ra149

Saxena S, Roselli F, Singh K, Leptien K, Julien JP, et al. 2013. Neuroprotection through excitability and mTOR required in ALS motoneurons to delay disease and extend survival. *Neuron* 80: 80-96

Schwaller B, Meyer M, Schiffmann S. 2002. 'New' functions for 'old' proteins: the role of the calcium-binding proteins calbindin D-28k, calretinin and parvalbumin, in cerebellar physiology. Studies with knockout mice. *Cerebellum* 1: 241-58

Schwarzer C, Sperk G, Samanin R, Rizzi M, Gariboldi M, Vezzani A. 1996. Neuropeptides-immunoreactivity and their mRNA expression in kindling: functional implications for limbic epileptogenesis. *Brain research. Brain research reviews* 22: 27-50

Seeburg PH. 1993. The TINS/TiPS Lecture. The molecular biology of mammalian glutamate receptor channels. *Trends Neurosci* 16: 359-65

Shibuya K, Park SB, Geevasinga N, Menon P, Howells J, et al. 2016. Motor cortical function determines prognosis in sporadic ALS. *Neurology* 87: 513-20

Sieghart W, Sperk G. 2002. Subunit composition, distribution and function of GABA(A) receptor subtypes. *Current topics in medicinal chemistry* 2: 795-816

Sigel E, Steinmann ME. 2012. Structure, function, and modulation of GABA(A) receptors. *J Biol Chem* 287: 40224-31

Silver RA. 2010. Neuronal arithmetic. *Nat Rev Neurosci* 11: 474-89

Sommer M, Tergau F, Wischer S, Reimers C, Beuche W, Paulus W. 1999. Riluzole does not have an acute effect on motor thresholds and the intracortical excitability in amyotrophic lateral sclerosis. *Journal of neurology* 246: III22-III26

Somogyi P, Tamás G, Lujan R, Buhl EH. 1998. Salient features of synaptic organisation in the cerebral cortex. *Brain Res Rev.* 26: 113-35

Southwell DG, Paredes MF, Galvao RP, Jones DL, Froemke RC, et al. 2012. Intrinsically determined cell death of developing cortical interneurons. *Nature* 491: 109-13

Spreux-Varoquaux O, Bensimon G, Lacomblez L, Salachas F, Pradat PF, et al. 2002. Glutamate levels in cerebrospinal fluid in amyotrophic lateral sclerosis: a reappraisal using a new HPLC method with coulometric detection in a large cohort of patients. *J Neurol Sci* 193: 73-78

Sreedharan J, Blair IP, Tripathi VB, Hu X, Vance C, et al. 2008. TDP-43 mutations in familial and sporadic amyotrophic lateral sclerosis. *Science* 319: 1668-72

Stafstrom CE. 2007. Persistent sodium current and its role in epilepsy. *Epilepsy currents / American Epilepsy Society* 7: 15-22

Stellwagen D, Malenka RC. 2006. Synaptic scaling mediated by glial TNF-alpha. *Nature* 440: 1054-9

Stephens B, Navarrete R, Guiloff RJ. 2001. Ubiquitin immunoreactivity in presumed spinal interneurones in motor neurone disease. *Neuropathol Appl Neurobiol* 27: 352-61

Stephens B, Guiloff RJ, Navarrete R, Newman P, Nikhar N, Lewis P. 2006. Widespread loss of neuronal populations in the spinal ventral horn in sporadic motor neuron disease. A morphometric study. *J Neurol Sci* 244: 41-58

Strong MJ, Grace GM, Freedman M, Lomen-Hoerth C, Woolley S, et al. 2009. Consensus criteria for the diagnosis of frontotemporal cognitive and behavioural syndromes in amyotrophic lateral sclerosis. *Amyotrophic lateral sclerosis : official publication of the World Federation of Neurology Research Group on Motor Neuron Diseases* 10: 131-46

Sun H, Kawahara Y, Ito K, Kanazawa I, Kwak S. 2006. Slow and selective death of spinal motor neurons in vivo by intrathecal infusion of kainic acid: implications for AMPA receptor-mediated excitotoxicity in ALS. *J Neurochem* 98: 782-91

Suzuki N, Bekkers JM. 2010a. Distinctive classes of GABAergic interneurons provide layer-specific phasic inhibition in the anterior piriform cortex. *Cerebral cortex* 20: 2971-84

Suzuki N, Bekkers JM. 2010b. Inhibitory neurons in the anterior piriform cortex of the mouse: Classification using molecular markers. *J Comp Neurol* 518: 1670-87

Swash M, Fox KP. 1974. The pathology of the human muscle spindle: effect of denervation. *J Neurol Sci* 22: 1-24

Swash M, Leader M, Brown A, Swettenham KW. 1986. Focal loss of anterior horn cells in the cervical cord in motor neuron disease. *Brain* 109 (Pt 5): 939-52

Swash M, Scholtz CL, Vowles G, Ingram DA. 1988. Selective and asymmetric vulnerability of corticospinal and spinocerebellar tracts in motor neuron disease. *Journal of neurology, neurosurgery, and psychiatry* 51: 785-9

Swash M. 2012. Why are upper motor neuron signs difficult to elicit in amyotrophic lateral sclerosis? *Journal of neurology, neurosurgery, and psychiatry* 83: 659-62

Swinnen B, Robberecht W. 2014. The phenotypic variability of amyotrophic lateral sclerosis. *Nat Rev Neurol* 10: 661-70

Talbot K. 2014. Amyotrophic lateral sclerosis: cell vulnerability or system vulnerability? *Journal of anatomy* 224: 45-51

Tallent MK, Siggins GR. 1999. Somatostatin acts in CA1 and CA3 to reduce hippocampal epileptiform activity. *J Neurophysiol* 81: 1626-35

Tallent MK, Qiu C. 2008. Somatostatin: an endogenous antiepileptic. *Mol Cell Endocrinol* 286: 96-103

Tamamaki N, Yanagawa Y, Tomioka R, Miyazaki J, Obata K, Kaneko T. 2003. Green fluorescent protein expression and colocalization with calretinin, parvalbumin, and somatostatin in the GAD67-GFP knock-in mouse. *J Comp Neurol* 467: 60-79

Tan RH, Kril JJ, Fatima M, McGeachie A, McCann H, et al. 2015. TDP-43 proteinopathies: pathological identification of brain regions differentiating clinical phenotypes. *Brain* 138: 3110-22

Tanaka YH, Tanaka YR, Fujiyama F, Furuta T, Yanagawa Y, Kaneko T. 2011. Local connections of layer 5 GABAergic interneurons to corticospinal neurons. *Frontiers in neural circuits* 5: 12

Taniguchi H, He M, Wu P, Kim S, Paik R, et al. 2011. A resource of Cre driver lines for genetic targeting of GABAergic neurons in cerebral cortex. *Neuron* 71: 995-1013

Thiel G. 1993. Synapsin I, synapsin II, and synaptophysin: marker proteins of synaptic vesicles. *Brain Pathol* 3: 87-95

Thomson AM, Lamy C. 2007. Functional maps of neocortical local circuitry. *Frontiers in neuroscience* 1: 19-42

Toth K, Eross L, Vajda J, Halasz P, Freund TF, Magloczky Z. 2010. Loss and reorganization of calretinin-containing interneurons in the epileptic human hippocampus. *Brain* 133: 2763-77

Toth K, Magloczky Z. 2014. The vulnerability of calretinin-containing hippocampal interneurons to temporal lobe epilepsy. *Frontiers in neuroanatomy* 8: 100

Trotti D, Rolfs A, Danbolt NC, Brown RH, Jr., Hediger MA. 1999. SOD1 mutants linked to amyotrophic lateral sclerosis selectively inactivate a glial glutamate transporter. *Nature neuroscience* 2: 848

Turner MR, Osei-Lah AD, Hammers A, Al-Chalabi A, Shaw CE, et al. 2005. Abnormal cortical excitability in sporadic but not homozygous D90A SOD1 ALS. *Journal of Neurology, Neurosurgery & Psychiatry* 76: 1279-85

Turner MR, Kiernan MC, Leigh PN, Talbot K. 2009. Biomarkers in amyotrophic lateral sclerosis. *Lancet neurology* 8: 94-109

Turner MR, Kiernan MC. 2012. Does interneuronal dysfunction contribute to neurodegeneration in amyotrophic lateral sclerosis? *Amyotroph Lateral Sc* 13: 245-50

Turner MR, Bowser R, Bruijn L, Dupuis L, Ludolph A, et al. 2013. Mechanisms, models and biomarkers in amyotrophic lateral sclerosis. *Amyotrophic lateral sclerosis & frontotemporal degeneration* 14 Suppl 1: 19-32

Turner MR, Swash M. 2015. The expanding syndrome of amyotrophic lateral sclerosis: a clinical and molecular odyssey. *Journal of neurology, neurosurgery, and psychiatry* 86: 667-73

Turrigiano G. 2012. Homeostatic synaptic plasticity: local and global mechanisms for stabilizing neuronal function. *Cold Spring Harbor perspectives in biology* 4: a005736

Udaka F, Kameyama M, Tomonaga M. 1986. Degeneration of Betz cells in motor neuron disease. A Golgi study. *Acta Neuropathol* 70: 289-95

Van Damme P, Van den Bosch L, Van Houtte E, Callewaert G, Robberecht W. 2002. GluR2-Dependent Properties of AMPA Receptors Determine the Selective Vulnerability of Motor Neurons to Excitotoxicity. *Journal of Neurophysiology* 88: 1279-87

Van Den Bosch L, Van Damme P, Bogaert E, Robberecht W. 2006. The role of excitotoxicity in the pathogenesis of amyotrophic lateral sclerosis. *Biochimica et Biophysica Acta (BBA)-Molecular Basis of Disease* 1762: 1068-82

van Zundert B, Peuscher MH, Hynynen M, Chen A, Neve RL, et al. 2008. Neonatal Neuronal Circuitry Shows Hyperexcitable Disturbance in a Mouse Model of the Adult-Onset Neurodegenerative Disease Amyotrophic Lateral Sclerosis. *The Journal of Neuroscience* 28: 10864-74

Vance C, Rogelj B, Hortobagyi T, De Vos KJ, Nishimura AL, et al. 2009. Mutations in FUS, an RNA processing protein, cause familial amyotrophic lateral sclerosis type 6. *Science* 323: 1208-11

Vandenberg RJ. 1998. Molecular pharmacology and physiology of glutamate transporters in the central nervous system. *Clinical and experimental pharmacology & physiology* 25: 393-400

Verstraete E, Veldink JH, van den Berg LH, van den Heuvel MP. 2014. Structural brain network imaging shows expanding disconnection of the motor system in amyotrophic lateral sclerosis. *Human brain mapping* 35: 1351-61

Vezzani A, Schwarzer C, Lothman EW, Williamson J, Sperk G. 1996. Functional changes in somatostatin and neuropeptide Y containing neurons in the rat hippocampus in chronic models of limbic seizures. *Epilepsy research* 26: 267-79

Vezzani A, Hoyer D. 1999. Brain somatostatin: a candidate inhibitory role in seizures and epileptogenesis. *The European journal of neuroscience* 11: 3767-76

Vezzani A, Sperk G. 2004. Overexpression of NPY and Y2 receptors in epileptic brain tissue: an endogenous neuroprotective mechanism in temporal lobe epilepsy? *Neuropeptides* 38: 245-52

Vinsant S, Mansfield C, Jimenez-Moreno R, Del Gaizo Moore V, Yoshikawa M, et al. 2013. Characterization of early pathogenesis in the SOD1(G93A) mouse model of ALS: part II, results and discussion. *Brain Behav* 3: 431-57

Vucic S, Kiernan MC. 2006a. Axonal excitability properties in amyotrophic lateral sclerosis. *Clinical neurophysiology : official journal of the International Federation of Clinical Neurophysiology* 117: 1458-66

Vucic S, Kiernan MC. 2006b. Novel threshold tracking techniques suggest that cortical hyperexcitability is an early feature of motor neuron disease. *Brain* 129: 2436-46

Vucic S, Nicholson GA, Kiernan MC. 2008. Cortical hyperexcitability may precede the onset of familial amyotrophic lateral sclerosis. *Brain* 131: 1540-50

Vucic S, Kiernan MC. 2010. Upregulation of persistent sodium conductances in familial ALS. *Journal of Neurology, Neurosurgery & Psychiatry* 81: 222-27

Vucic S, Cheah BC, Yiannikas C, Kiernan MC. 2011. Cortical excitability distinguishes ALS from mimic disorders. *Clinical neurophysiology : official journal of the International Federation of Clinical Neurophysiology* 122: 1860-6

Vucic S, Ziemann U, Eisen A, Hallett M, Kiernan MC. 2013. Transcranial magnetic stimulation and amyotrophic lateral sclerosis: pathophysiological insights. *Journal of neurology, neurosurgery, and psychiatry* 84: 1161-70

Wainger BJ, Kiskinis E, Mellin C, Wiskow O, Han SS, et al. 2014. Intrinsic membrane hyperexcitability of amyotrophic lateral sclerosis patient-derived motor neurons. *Cell reports* 7: 1-11

Wang L, Sharma K, Grisotti G, Roos RP. 2009. The effect of mutant SOD1 dismutase activity on non-cell autonomous degeneration in familial amyotrophic lateral sclerosis. *Neurobiol Dis* 35: 234-40

Ward JH. 1963. Hierarchical Grouping to Optimize an Objective Function. *Journal of the American Statistical Association* 58: 236-44

Weber M, Eisen A, Stewart HG, Andersen PM. 2000. Preserved slow conducting corticomotoneuronal projections in amyotrophic lateral sclerosis with autosomal recessive D90A CuZn-superoxide dismutase mutation. *Brain* 123 (Pt 7): 1505-15

Werhahn KJ, Kunesch E, Noachtar S, Benecke R, Classen J. 1999. Differential effects on motorcortical inhibition induced by blockade of GABA uptake in humans. *The Journal of physiology* 517 (Pt 2): 591-7

Wijesekera L, Leigh PN. 2009. Amyotrophic lateral sclerosis. *Orphanet Journal of Rare Diseases* 4: 3

Williams TL, Day NC, Ince PG, Kamboj RK, Shaw PJ. 1997. Calcium-permeable alpha-amino-3-hydroxy-5-methyl-4-isoxazole propionic acid receptors: a molecular determinant of selective vulnerability in amyotrophic lateral sclerosis. *Ann Neurol* 42: 200-7

Wonders CP, Anderson SA. 2006. The origin and specification of cortical interneurons. *Nat Rev Neurosci* 7: 687-96

Wooley CM, Sher RB, Kale A, Frankel WN, Cox GA, Seburn KL. 2005. Gait analysis detects early changes in transgenic SOD1(G93A) mice. *Muscle Nerve* 32: 43-50

Yamashita T, Kwak S. 2014. The molecular link between inefficient GluA2 Q/R site-RNA editing and TDP-43 pathology in motor neurons of sporadic amyotrophic lateral sclerosis patients. *Brain Res* 1584: 28-38

Yin H, Cheng SH, Zhang J, Ma L, Gao Y, et al. 2008. Corticospinal tract degeneration in amyotrophic lateral sclerosis: a diffusion tensor imaging and fibre tractography study. *Annals of the Academy of Medicine, Singapore* 37: 411-5

Yokota T, Yoshino A, Inaba A, Saito Y. 1996. Double cortical stimulation in amyotrophic lateral sclerosis. *Journal of Neurology, Neurosurgery & Psychiatry* 61: 596-600

Yu J, Anderson CT, Kiritani T, Sheets PL, Wokosin DL, et al. 2008. Local-Circuit Phenotypes of Layer 5 Neurons in Motor-Frontal Cortex of YFP-H Mice. *Frontiers in neural circuits* 2: 6

Zach N, Kueffner R, Atassi N, Chio A, Cudkowicz M, et al. 2016. The ALS Stratification Prize-Using the Power of Big Data and Crowdsourcing for Catalyzing Breakthroughs in Amyotrophic Lateral Sclerosis (ALS)(P5. 102). *Neurology* 86: P5. 102

Zanette G, Tamburin S, Manganotti P, Refatti N, Forgione A, Rizzuto N. 2002a. Changes in motor cortex inhibition over time in patients with amyotrophic lateral sclerosis. *Journal of neurology* 249: 1723-8

Zanette G, Tamburin S, Manganotti P, Refatti N, Forgione A, Rizzuto N. 2002b. Different mechanisms contribute to motor cortex hyperexcitability in amyotrophic lateral sclerosis. *Clinical neurophysiology : official journal of the International Federation of Clinical Neurophysiology* 113: 1688-97

Zeman S, Lloyd C, Meldrum B, Leigh PN. 1994. Excitatory amino acids, free radicals and the pathogenesis of motor neuron disease. *Neuropathol Appl Neurobiol* 20: 219-31

Zhang W, Zhang L, Liang B, Schroeder D, Zhang ZW, et al. 2016. Hyperactive somatostatin interneurons contribute to excitotoxicity in neurodegenerative disorders. *Nature neuroscience* 19: 557-9

Ziemann U, Lonnecker S, Steinhoff BJ, Paulus W. 1996. The effect of lorazepam on the motor cortical excitability in man. *Experimental brain research* 109: 127-35

Ziemann U, Winter M, Reimers CD, Reimers K, Tergau F, Paulus W. 1997. Impaired motor cortex inhibition in patients with amyotrophic lateral sclerosis. Evidence from paired transcranial magnetic stimulation. *Neurology* 49: 1292-8

Ziemann U. 2004. TMS and drugs. *Clinical neurophysiology : official journal of the International Federation of Clinical Neurophysiology* 115: 1717-29